



TRABALHO FINAL

MESTRADO INTEGRADO EM MEDICINA

Instituto de Microbiologia

**A new method based on depolarization
detection, for quantification of HbSS
erythrocytes**

Sheila Correia Joosab

Orientado por:

Prof. Dr. Thomas Hänscheid

MAIO'2023

Acknowledgments

My sincere acknowledgments to Prof. Doctor Thomas Hänscheid, for being a great source of admiration and for truly guiding this work and sharing his vast wisdom with enormous availability, and for all the support, motivation and confidence that has transmitted during the realization of this project.

I also want to thank the technician Ana Lúcia from the *Serviço de Patologia Clínica* of the *Centro Hospitalar Universitário de Lisboa Norte* (CHULN), for providing the blood samples and the sodium metabisulphite reagent that I used in this project, and for her availability to introduce me to the laboratory methods carried out in that facility. And would also like to acknowledge Prof. Doctor José Melo Cristino, director of the *Serviço de Patologia Clínica* of the CHULN, and Dr. Ana Miranda, coordinator of the *Laboratório de Hematologia* of the *Serviço de Patologia Clínica* of the CHULN, for authorizing the realization of this project, making all this possible.

I want to thank my family, especially to my mother and father, for giving me and my sisters every opportunity to follow our dreams. To my sisters who have always supported me. And to my grandmother who I want to make proud everyday as a good student and a good person.

I thank my friends and classmates for their constant companionship and support, not only in college, but also in life.

And finally, I want to thank my boyfriend, for all the motivation, patience and understanding he has shown, that was especially important during this journey.

The conclusion of the *Trabalho Final de Mestrado* represents an important milestone in my life, so I leave here my sincere appreciation and recognition to those that in some way contributed to my personal and professional evolution and accompanied me until the accomplishment of this goal.

Thank you very much.

Abstract

Introduction: Sickle-cell-disease (SCD) is a hemoglobin disorder (HbS) with significant morbidity and mortality. Simple screening-tests depend on the detection of polymerized HbS (i.e., sickled Red-Blood-Cells, solubility of HbS), while definitive diagnosis and monitoring depend on electrophoretic (or High-Performance-Liquid-Chromatography) detection and quantification of HbS. Polymerized HbS depolarizes light and is easily identified inside Red-Blood-cells (RBCs) by microscopic observation using crossed polarizers.

Objective: To investigate if depolarization would allow the identification of HbS containing RBCs and any correlation with HbS.

Methods: EDTA-anticoagulated blood from 51 SCD patients were observed after 24h incubation, using the standard metabisulfite sickling test. Photographic images of light and polarization microscopy (1000x) of at least 100 RBCs were manually counted using Image J software. A preliminary experiment investigated if the anti-sickling effect of voxelated could be detected using depolarization.

Results: Light microscopy detected typical sickle cells and other deformed cells in all samples but showed only a weak correlation with HbS levels. Depolarizing polymerized HbS could be easily identified in RBCs. All depolarizing RBCs but also depolarizing deformed RBCs showed a high correlation with HbS: Pearson's coefficient of $R=0,85$ ($P<0,001$) and $R=0,84$ ($P<0,001$), respectively. Samples processed within two days showed the best correlation ($R=0,94$) which decreased with delays in processing. The drug effect of voxelator was easily assessed with depolarization using an automated image analysis.

Conclusion: This new method could be a possible screening tool to identify SCD as it detects depolarizing HbS not only in deformed, but also in non-deformed RBCs. Most importantly, counting depolarizing cells may allow to approximately determine the concentration of HbS (%) quantitatively. The observed results are likely even more convincing when fresh samples (same day) are used. This novel method could be a simple and easy POC-test to screen for SCD and monitor the amount of HbS, especially in resource-limited areas.

Resumo

Introdução: A drepanocitose é uma hemoglobinopatia com significativa morbimortalidade. Métodos de rastreio simples permitem a detecção da HbS polimerizada (visualização de eritrócitos falciformes, solubilidade da HbS), enquanto o diagnóstico definitivo e a monitorização dependem da detecção e quantificação da HbS por eletroforese (ou Cromatografia Líquida de Alta Performance). A HbS forma polímeros birrefringentes que despolarizam a luz, sendo facilmente identificada por microscopia polarizada.

Objetivo: Investigar se a despolarização permite a identificação de eritrócitos com HbS e se possui correlação com a HbS.

Métodos: Sangue anticoagulado com EDTA de 51 pacientes com drepanocitose foi observado após 24h de incubação, usando a prova de falciformação com metabissulfito. Fotografias de microscopia ótica e polarizada (1000x) de pelo menos 100 eritrócitos foram contadas manualmente usando o software Image J. Uma experiência preliminar investigou se o efeito anti-falciforme do voxelotor poderia ser detetado avaliando a despolarização.

Resultados: A microscopia ótica confirmou a presença de células falciformes típicas e outras células deformadas em todas as amostras, que demonstraram fraca correlação com os níveis de HbS. Todos os eventos de despolarização e os eritrócitos deformados despolarizantes mostraram uma alta correlação com a HbS: coeficiente de Pearson de $R=0,85$ ($P<0,001$) e $R=0,84$ ($P<0,001$), respetivamente. As amostras processadas em dois dias apresentaram a melhor correlação ($R=0,94$), que diminuiu com os atrasos no processamento. O efeito do voxelotor foi facilmente avaliado com a despolarização através de análise de imagem automatizada.

Conclusão: Este novo método deteta HbS despolarizante tanto em eritrócitos deformados como em não deformados, sendo uma ferramenta útil de rastreio. A contagem de células despolarizantes pode permitir determinar aproximadamente a concentração de HbS (%) quantitativamente. Quanto mais recentes as amostras, maior a credibilidade dos resultados. Poderá ser um método simples e fácil, útil em áreas com recursos limitados, para rastreio da drepanocitose e monitorização da HbS.

Keywords:

Sickle cell disease • Hemoglobin S • Polymerization • Depolarization • Diagnosis

Palavras-chave:

Drepanocitose • Hemoglobina S • Polimerização • Despolarização • Diagnóstico

The Final Work is from the sole responsibility of its author, and FMUL assumes no responsibility for the contents presented therein.

O Trabalho Final é da exclusiva responsabilidade do seu autor, não cabendo qualquer responsabilidade à FMUL pelos conteúdos nele apresentados.

Contents

Acknowledgments	1
Abstract.....	2
Resumo	3
Keywords Palavras-chave	4
List of Figures.....	8
List of Tables	9
List of Abbreviations	10
1. Introduction.....	13
1.1. Blood diseases.....	13
1.2. Basic physiology of RBCs and hemoglobin	13
1.2.1. The erythrocyte	14
1.2.2. Hemoglobin (Hb)	16
1.3. Hemoglobinopathies.....	21
1.4. Sickle Cell Anemia	25
1.4.1. Pathophysiology – The sickling process.....	25
1.4.2. Pathophysiology – Inflammation and damage.....	28
1.4.3. Pathophysiology – Vasoocclusion and hemolytic anemia.....	29
1.5. The role of HbF in SCD	30
1.6. Clinical manifestations and management	32
1.7. Treatment approaches – Current strategies and new therapeutic agents	35
1.8. Diagnosis and diagnostic methods for SCD	38
1.8.1. Routine laboratory (hematology/biochemistry) parameters.....	39
1.8.2. Simple (screening) tests for SCD.....	41
1.8.3. Tests for definitive diagnosis of SCD.....	47
1.8.4. Other tests/methods in development.....	51
1.8.5. Neonatal and prenatal screening techniques.....	52
1.8.6. Comparison of the different diagnostic methods for SCD	53
1.9. A novel and simple method based on depolarization	57
1.10. The idea for the research project	58

2. Aims and objectives	59
3. Methods.....	60
3.1. Study populations and samples	60
3.2. Reagents and equipment	60
3.3. Procedures	61
3.4. Image analysis	63
3.5. Data analysis and statistics	67
3.6. Ethics	67
4. Results.....	68
4.1. Sample characteristics	68
4.2. Sickling and depolarization at two different time points (1h and 24h).....	69
4.3. Optical microscopy observations.....	70
4.4. Polarization microscopy observations.....	72
4.4.1. Correlation of polarizing events versus deformed RBCs	73
4.4.2. Correlation of polarizing events versus HbS levels (%)	74
4.4.3. Possible effect of delayed sample processing	75
4.5. Drug (voxelotor) experiment	77
4.5.1. Automated analysis of images of control and drug-treated RBCs	78
4.5.2. Statistical analysis of image data comparing control to drug treated sample	79
5. Discussion	81
6. Conclusions	88
7. References	89

List of Figures

Figure 1: Erythrocyte differentiation and stages of erythropoiesis	14
Figure 2: Shape and dimensions of the erythrocyte	15
Figure 3: The globin genes.....	16
Figure 4: Physiological profile of Hbs during development	17
Figure 5: Quaternary structure of human HbA	18
Figure 6: OxyHb dissociation curve	19
Figure 7: Structure of R state (magenta) superimposed on the structure of T state (blue) hemoglobin.....	20
Figure 8: The pathophysiology of sickle cell disease	25
Figure 9: Sick cells after 24h of incubation (37°C) upon realization of the sickling test	26
Figure 10: SCA pathophysiology and potential therapeutic targets	35
Figure 11: Paper-based hemoglobin solubility test.....	42
Figure 12: Blood stains produced on paper by samples with various %HbS	43
Figure 13: Schematic representation of the four most important outcomes of a density based rapid low-cost test for SCD	44
Figure 14: The Sick SCAN based on lateral flow immunoassay to detect SCD	45
Figure 15: HemoTypeSC based on lateral flow immunoassay to detect SCD	45
Figure 16: Synchronous fluorescence excitation spectra (SXS) of plasma from different subjects.....	46
Figure 17: Schematic presentation of cellulose acetate electrophoresis	48
Figure 18: Relative mobilities of normal and variant hemoglobins measured by electrophoresis	48
Figure 19: Ion-exchange high-performance liquid chromatography (HPLC) separation of hemoglobins	50
Figure 20: Microscopic images of sickled HbSS-RBC	57
Figure 21: Principles of polarized microscopy	61
Figure 22 Procedure of the sickle cell test	62
Figure 23: Settings for image acquisitions (bright-field and crossed polarizers)	63
Figure 24: Steps and settings in Fiji/ImageJ for automatic analysis	66
Figure 25: Distribution of the percentage of HbS in each sample (HbS %).....	68
Figure 26: Distribution of time-intervals (days) from collection to processing	68

Figure 27: Sick cell test after 1h (top) and 24h (bottom) of incubation	69
Figure 28: Cell types observed with optical microscopy	70
Figure 29: Correlation between HbS (%) and deformed RBCs in optical microscopy	71
Figure 30: Representation of all cell categories identified in each sample with polarizing microscopy.....	72
Figure 31: Correlation between depolarizing events versus deformed RBCs.....	73
Figure 32: Correlation between HbS (%) and different depolarizing events (%)	74
Figure 33: Influence of delayed sample processing on correlation of HbS – depolarizing events	76
Figure 34: Images of brightfield and depolarizing RBCs after voxelotor treatment	77
Figure 35: Automated analysis of depolarizing images.....	78
Figure 36: Difference in distribution of area and brightness between control and drug	79
Figure 37: Representative images of two samples using polarizing microscopy	83
Figure 38: Sample of SCD patient that possibly undergone a blood transfusion	85
Figure 39: Different types of depolarization patterns in sickled RBCs	86

List of Tables

Table 1: Characteristics of the main Hb disorders	22
Table 2: Manifestations and complications of sickle cell anemia	32
Table 3: Upstream and downstream therapies for SCD.....	35
Table 4: Pertinent diagnostic laboratory tests for hemolysis	40
Table 5: Comparison of the principal diagnostic methods for SCD.....	55
Table 6: Categories for the different cell shapes with respective code number	64
Table 7: Representative images for RBC classification.....	65
Table 8: Summary of parameters comparing control to drug treated sample	80
Table 9: Low proportion of sickled RBC in two studied samples	82

List of Abbreviations

2,3-BPG	2,3-bisphosphoglycerate
5-HMF	5-hydroxymethyl-2-furfural
ABO	ABO blood group system
ACS	Acute chest syndrome
AMPSs	Aqueous multiphase systems
ARMS	Amplification refractory mutation system
ASS	Acute splenic sequestration
CAC	Cellulose acetate electrophoresis
CAG	Citrate agar electrophoresis
CAML	<i>Centro Académico de Medicina de Lisboa</i>
CE	Capillary electrophoresis
CHULN	<i>Centro Hospitalar Universitário de Lisboa Norte</i>
CO ₂	Carbon dioxide
DMSO	Dimethyl sulfoxide
DALYs	Disability-adjusted life years
DNA	Deoxyribonucleic acid
EDTA	Ethylenediaminetetraacetic acid
FAD	Flavin adenine dinucleotide
FDA	Food and Drug Administration
FMUL	<i>Faculdade de Medicina da Universidade de Lisboa</i>
Hb	Hemoglobin
HbA	Adult hemoglobin
HbF	Fetal hemoglobin
HbS	Sickle hemoglobin
HPFH	Hereditary persistence of fetal hemoglobin
HPLC	High-performance liquid chromatography
HU	Hydroxyurea
IEF	Isoelectric focusing
ISC	Irreversibly sickled cell

MCHC	Mean corpuscular hemoglobin concentration
MCV	Mean corpuscular volume
NAD1	Nicotinamide adenine dinucleotide (oxidized form)
NADH	Nicotinamide adenine dinucleotide (reduced form)
NADPH	Nicotinamide adenine dinucleotide phosphate (reduced form)
NO	Nitric oxide
O2	Oxygen
ODC	Oxyhemoglobin dissociation curve
OP	Optical microscopy
PBS	Peripheral blood smear
PBS	Phosphate-buffered saline
PCR	Polymerase chain reaction
POC	Point of care
POL	Polarization microscopy
RBC	Red blood cell
RDW	Red blood cell distribution width
RNA	Ribonucleic acid
SCA	Sickle cell anemia
SCD	Sickle cell disease
SCT	Sickle cell trait
SXS	Synchronous fluorescence excitation spectra
TALENs	Transcription activator-like effector nucleases
TLR4	Toll-like receptor 4
VOC	Vaso-occlusive crisis
YLDs	Years lived with disability
YLLs	Years of life lost
ZFNs	Zinc-finger nucleases

1. Introduction

1.1. Blood diseases

Blood diseases are an important and timely topic, not only for the hematologist, but also for all clinicians and researchers since multidisciplinary team caring is essential for the diagnosis and medical management of this increasing patient population (1). Although all hematologic conditions can be seen in any population, their management depends on the human and material resources available, which vary widely (2). In resource-rich nations, the management usually involves advanced diagnostic tools and therapies, whereas in resource-poor environments the priorities are often focused on more basic needs (2,3).

Red-Blood-Cell (RBC) disorders are arguably the most frequent blood diseases, especially anemia, which affects a third of the global population and is an important contributing factor to increased morbidity and mortality worldwide (4). Anemia is defined as a disorder in which Hb concentration is lower than normal, reference range is defined as 13.5 to 18 grams (g) of hemoglobin per deciliter (dL) of blood for men and 12 to 16 g/dL for women, although lower values are often seen in areas like Africa, likely due to other factors, such as helminths infections, malaria, or malnutrition (5).

Inherited genetic disorders of Hb, such as sickle cell disease (SCD) are important diseases affecting RBCs. Globally 330,000 children are estimated to be born each year with a serious inherited Hb disorder (83% with sickle cell anemia or one of its variants; 17% with a form of thalassemia) (4). Over the next 20 years, more babies with Hb disorders will survive, because of reduction in childhood mortality due to infection and malnutrition. However, many may be dying due to a lack of appropriate medical care later on (6).

1.2. Basic physiology of RBCs and hemoglobin

The physiological function of RBCs is the transport of oxygen and carbon dioxide between lungs and tissues, whereby the blood (within the blood stream) itself is the transport vehicle (7).

1.2.1. The erythrocyte

Erythrocytes or red blood cells (RBCs) are produced in the red bone marrow, in a process called erythropoiesis, where erythroblasts (RBCs precursors) undergo a series of morphological changes to mature into erythrocytes (figure 1). Mature erythrocytes have no nucleus (DNA/RNA) or any of the other typical intracellular organelles (i.e., mitochondria) and thus, also very little metabolic pathways. They metabolize glucose through the Embden-Meyerhof-Parnas anaerobic pathway. In addition of ATP production, this process also contributes to generate NADH and NADPH, important for the antioxidant defense function of RBCs (8,9).

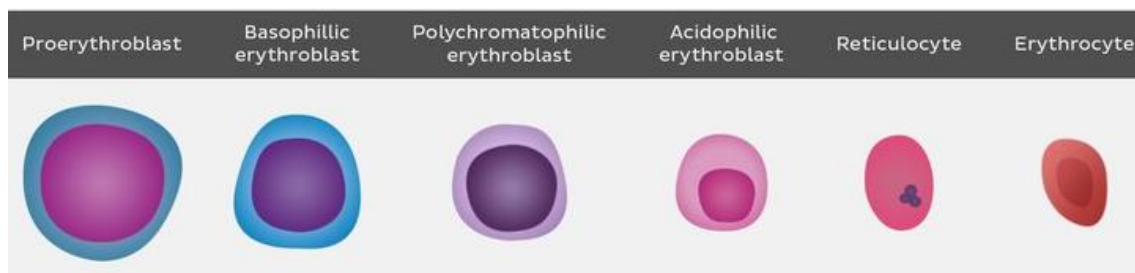


Figure 1: Erythrocyte differentiation and stages of erythropoiesis.

Note that each new cell type histologically resembles the “final” erythrocyte more closely. Reticulocytes are nonnucleated direct precursors of RBCs, they contain little amounts of RNA and are rich in polyribosomes. The reticulocyte count reflects the erythropoietic activity of the bone marrow, normal values in the circulating blood are about 1%. Adapted from (10) and (11).

A unique feature of mammalian erythrocytes is the lack of protein synthesis, meaning the functional proteins in erythrocytes are gradually denaturing during their lifespan (12). The life span of erythrocytes is approximately 120 days, after which most of them are phagocytosed by macrophages who recognize cell membrane damage of senescent erythrocytes, with the spleen being the primary site of erythrocyte clearance. This process is called eryptosis which occurs in balance with erythropoiesis in a healthy being, ensuring physiological amounts of RBCs (7,13). Giving their physiological function for oxygen transport only two major structures of RBCs are truly important: (i) the surrounding cell membrane, and (ii) the cytoplasm filled with Hb, a protein specialized for the transport of oxygen and carbon dioxide.

The cell membrane of an erythrocyte is the typical lipid bilayer, containing integral and peripheral membrane proteins. The integral membrane proteins serve as anchor points for the cytoskeletal network to the cell membrane and express the erythrocyte surface antigens that determine the ABO blood groups, which are important for blood transfusions (14). The peripheral membrane proteins contribute to the characteristic biconcave disk shape of RBCs (figure 2), meaning that their periphery is larger/thicker than their central part. This feature is essential to maximize the total surface of the cell membrane, facilitating gas exchange and transport, because more Hb molecules are closer to the plasma membrane than they would be in a spherical cell (7).

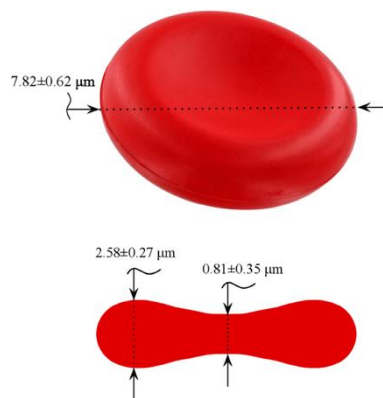


Figure 2: Shape and dimensions of an erythrocyte.

Note the biconcave disk shape. Adapted from (15).

This disk shape also plays a role in elasticity and strength of the erythrocytes, allowing them to easily pass through even the smallest capillaries by being able to undergo deformations, preventing them from breaking (7,13). The three major factors for cellular deformability are: (i) the cell shape, (ii) the intracellular viscosity and (iii) the membrane flexibility; this is the field of study of hemorheology (12).

Hb is the most abundant protein inside the erythrocytes and thus, the concentration of Hb (represented by mean corpuscular Hb concentration = MCHC, reference range: 32 - 36g/dL) reflects their intracellular viscosity (16) which is essential in determining the rheological properties of erythrocytes (12).

1.2.2. Hemoglobin (Hb)

Normal Hb consists of a heterotetramer that comprises two pairs of different polypeptide subunits called globin chains. Four physiological types of globin chains (α , β , γ , δ) give rise to three main Hb classes called HbA ($\alpha_2\beta_2$), HbA₂ ($\alpha_2\delta_2$) and HbF ($\alpha_2\gamma_2$) (6). Human alpha cluster and beta cluster globin genes are present on chromosomes 16 and 11, respectively (figure 3).

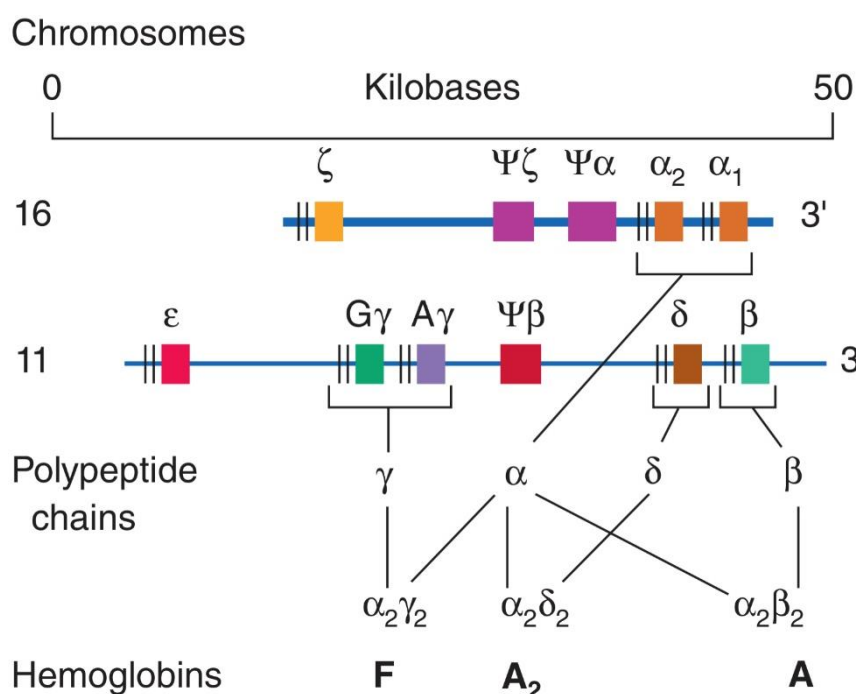


Figure 3: The globin genes.

The α -like genes (α , ζ) are encoded on chromosome 16; the β -like genes (β , γ , δ , ϵ) are encoded on chromosome 11. The ζ and ϵ genes encode embryonic globins. Adapted from (17).

Different types of Hbs are present at the various stages of development (figure 4). Red cells first appear at about 6 weeks after conception and contain the embryonic Hbs until the yolk sac stage of development. Then, at 10-11 weeks these are replaced by fetal Hb that becomes predominant during most of gestation (reaching 75-80% at birth). After birth, HbF is then replaced by HbA and HbA₂ over the first year of life (HbF falls to <1% levels in adults) (18). This switch from predominant expression of fetal Hb to adult Hb is mediated by a transcriptional switch in definitive erythroid progenitors from γ to β -globin (19).

By far, the most prevalent Hb in adults is HbA (97%) while HbA2 represents only 2,5% (18). However, HbF can also be produced in small amounts during postnatal life by a few red cell clones called F cells. These cells retain this ability and are recruited during profound erythroid stress, such as severe hemolytic anemias, with a consequent rise in HbF levels. This phenomenon may help to explain the ability of some agents, like hydroxyurea, to increase levels of HbF in adults (17).

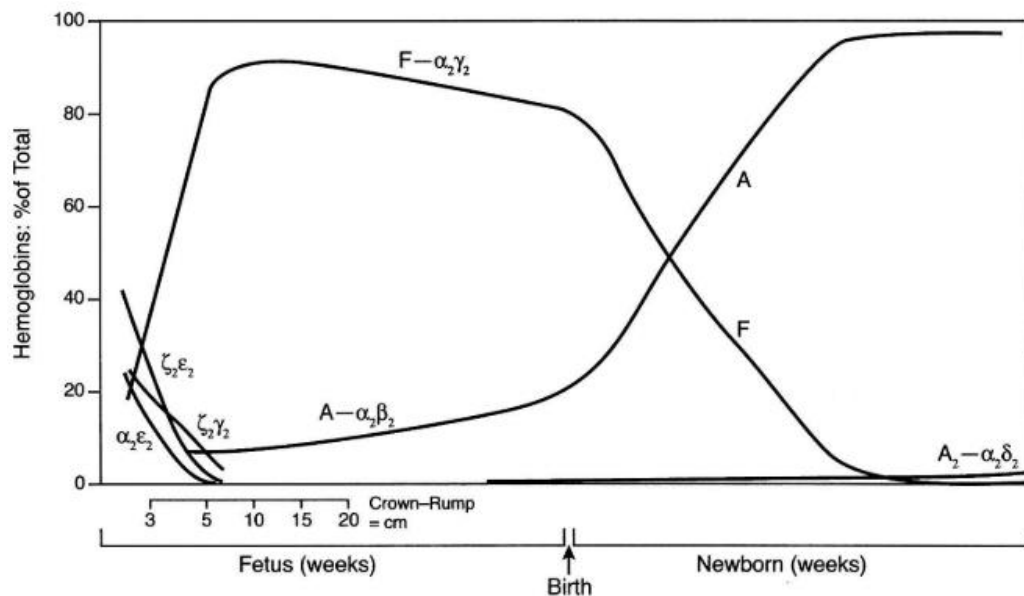


Figure 4: Physiological profile of HbS during development.

The names of the normal embryonic Hbs are Gower-1 (z2e2), Gower-2 (a2e2), and Portland-1 (z2g2). Hb Portland-2 (z2b2) is not usually found. Adapted from (20).

Although all physiological Hbs have very similar structures, interactions between their subunits are very different. The consequences are differences in O₂ affinity and interactions with allosteric effectors (20). This is important for optimal physiological properties of each type of Hb. For example, HbF has increased oxygen affinity, which allows the developing fetus to retrieve oxygen from the mother's bloodstream (HbA) in the placenta (21).

The Hb tetramer is highly soluble although, interestingly, individual globin chains are insoluble. Unpaired globin may precipitate and cause cell damage with triggering of apoptosis. The exterior surface of Hb is rich in polar (hydrophilic) amino acids that enhance solubility. Contrary to this, the interior forms a hydrophobic pocket into which a heme moiety is inserted, consisting of a protoporphyrin IX ring complexed with a single

iron atom in its ferrous state (Fe^{2+}), (figure 5). Each heme moiety can bind reversibly to a single oxygen molecule and therefore, each Hb can transport up to four molecules of oxygen (17). Each RBC contains approximately 260 million Hb molecules, being able to transport about 1 billion O_2 molecules (22).

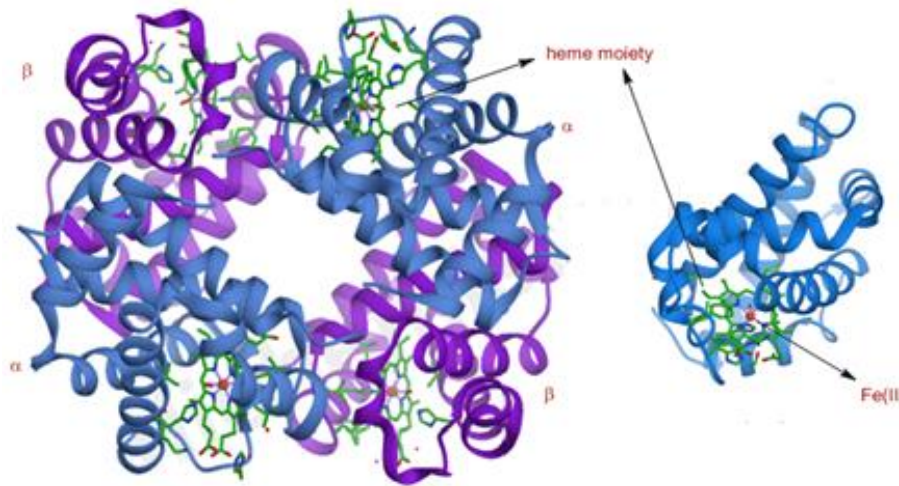


Figure 5: Quaternary structure of human HbA.

Note the four Hb subunits arranged around a central water cavity. Heme moieties are shown in green color and Fe^{2+} ion is shown in red. Adapted from (23).

The reversible binding of oxygen by Hb and the sigmoid shape of the oxyHb dissociation curve (ODC) (figure 6) is of significant relevance in multiple areas, such as biochemistry, physiology, physical chemistry, and clinical medicine. The early work on the Hb oxygen equilibrium begun in the 19th century when Stokes associated the “reduction and oxidation” of Hb with changes in the visible spectrum, and showed these processes were reversible (24).

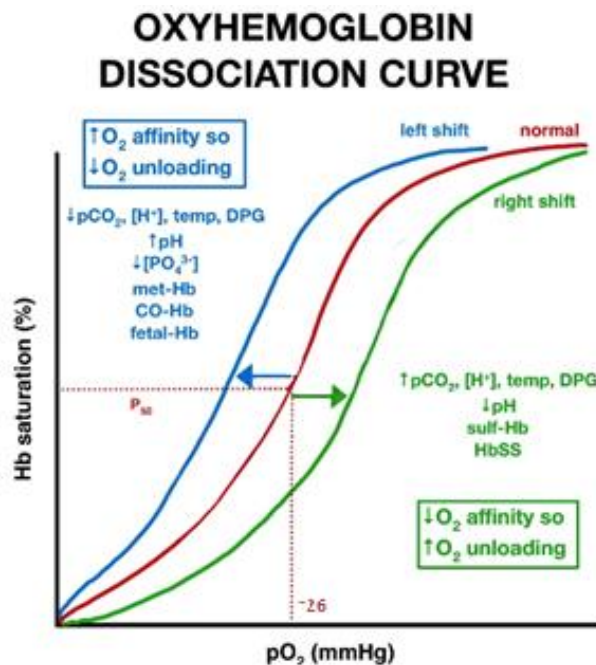


Figure 6: OxyHb dissociation curve.

The pO_2 at 50% O_2 saturation (P_{50}) measures the O_2 -affinity for Hb (26 mmHg for HbA). (25) Rightward shift (green arrow and curve): $\uparrow pO_2$ to achieve 50% O_2 saturation. 2,3-biphosphoglycerate (2,3-BPG) binds to deoxyHb and is central for Hb allostery: \downarrow affinity for oxygen for efficient tissue oxygenation. (25) HbF- O_2 complex (\downarrow affinity for 2,3-BPG) provides access to oxygen from maternal blood (26). RBCs with abnormal Hb may have abnormal ODC because of: (i) an intrinsic abnormality of Hb- O_2 dissociation, (ii) an altered interaction of Hb with 2,3-BPG, and (iii) an altered Bohr effect (27). Adapted from (28).

The Hb-oxygen dissociation curve consists in a graphical representation of the relationship between oxygen saturation and oxygen partial pressure, which is a very useful tool to understand some of the principles underpinning this process (figure 6). The overarching idea is that Hb should easily bind O_2 in the lungs (where oxygen partial pressure is high) and release it more easily in the tissues (where oxygen partial pressure is low). In fact, Hb undergoes conformational changes to increase its affinity for oxygen (29), meaning that the binding of one oxygen molecule induces H^+ protons dissociation which progressively increases Hb's affinity for oxygen until all four of its binding sites are occupied (30). This process occurs in lung capillaries and leads to a high-affinity form of Hb, called relaxed form (R). This characterizes oxyHb which is also responsible for the bright red color of the arterial blood. As the RBCs reach the tissue capillaries, Hb enters an acidic environment as the result of carbon dioxide production within the tissues, inducing a configuration shift to the taut form (T). Hb releases oxygen in favor of the attachment of H^+ protons, leading to a low-affinity Hb that characterizes deoxyHb which gives venous blood, a purple blue color (figure 7) (25,29–31).

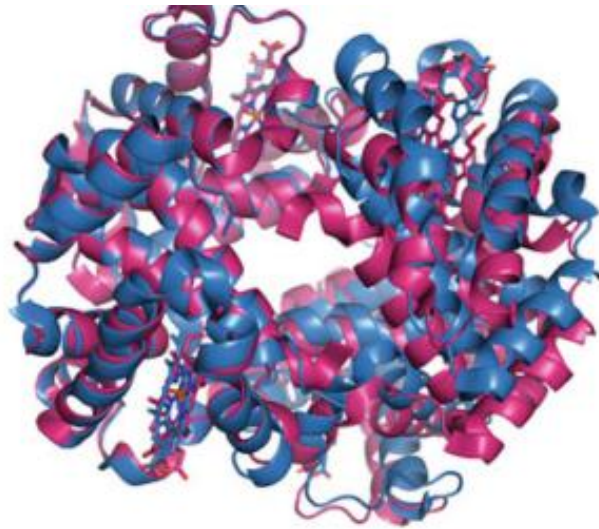


Figure 7: Structure of R state (magenta) superimposed on T state (blue) hemoglobin.

Upon the allosteric transition from the T state to the R state, a sliding motion occurs between the $\beta 2$ -subunit and the opposite $\alpha 1$ -subunit (first reported by Baldwin and Chotia, 1979). The T \rightarrow R transition leads to the narrowing of the central water cavity and the α - and β - clefts, as well as an increase in $\alpha 1\beta 2$ iron–iron distance and a decrease in the $\beta 1\beta 2$ iron–iron-distance. (25) Note the larger central water cavity in the T structure. Adapted from reference (25).

A variety of allosteric modulators (effector molecules that regulate the properties of proteins) such as 2,3-bisphosphoglycerate (2,3-BGP), protons (H^+), carbon dioxide (CO_2), or chloride (Cl^-) affect the equilibrium between the T and R states of Hb, modulating Hb- O_2 affinity either by stabilizing the R state Hb (left-shift of the ODC) or stabilizing the T state Hb (right-shift of the ODC) (figure 6) (25).

Hb has a lower affinity for oxygen in environments with increased partial pressure of CO_2 or low blood pH. This effect, known as the Bohr effect, describes the increased likelihood of O_2 dissociation under such conditions. In the oxygen-dissociation-curve, this is represented as a rightward shift of the curve (figure 6), which translates into a better unloading of oxygen to meet the tissue demands (where CO_2 is high, and pH is low). Thus, the Bohr effect is essential in maximizing oxygen transport capabilities of Hb (29).

Based on these findings it appears very likely that alterations of the Hb, either in structure (Hb-chain amino-acid changes) or in composition (different tetramer composition), may have a profound effect on the physiological functions of RBCs.

1.3. Hemoglobinopathies

Inherited Hb disorders are among the commonest genetic conditions, some with serious clinical expression. The term “Hemoglobinopathy” includes all genetic Hb disorders. In general, they fall into two main groups: (i) those in which a mutation leads to decreased globin chain production (thalassemias), and (ii) those that result from mutations that alter the sequence of a globin chain (structural Hb variants) (32). The first group consists in quantitative alterations, whereas the second group refers to qualitative changes in the Hb.

(i) The thalassemia syndromes are autosomal, recessive, hereditary disorders caused by mutations in the genes related to the α globin (alpha thalassemia) or in the genes related to the β globin (beta thalassemia). This results in disruption of the balanced production of the globin chains, essential for the reciprocal pairing into the normal tetramers. Consequently, an accumulation of the normally produced chain within the developing red cell occurs, leading to impaired erythropoiesis, and therefore, premature destruction of RBCs. The degree of chain imbalance determines the severity of the disease (33).

(ii) The structural Hb variants mostly result from single amino-acid substitutions in the α or β chains, affecting Hb synthesis and function by altering its structure and biochemical properties. (34) The most common β globin variants include HbS, HbC, HbD, HbE, and HbG (18).

HbS is caused by a single point mutation (adenine \rightarrow thymine) in the sixth codon of the β -globin gene that changes the sixth amino acid position of the β chain from glutamic acid to valine, given rise to HbS ($\alpha_2\beta_2^{6 \text{ Glu} \rightarrow \text{Val}}$). Several sickle syndromes occur as the result of the inheritance of HbS from one parent and another hemoglobinopathy, such as β thalassemia or HbC ($\alpha_2\beta_2^{6 \text{ Glu} \rightarrow \text{Lys}}$), from the other parent (17). The homozygous state for HbS (SS) causes the prototypical disease, called sickle cell anemia, in which the abnormal HbS damages and deforms the red blood cell. The abnormal RBCs are removed from circulation, causing anemia. The less deformable, sickled RBCs can cause obstruction of blood vessels, leading to recurrent episodes of severe pain and ultimately multi-organ ischemic damage (18).

The combination of the variant HbS and normal Hb denotes the heterozygote state, also known as sickle cell trait (AS), which is often clinically asymptomatic, although a mild anemia may exist (17). Although many Hb variants (affecting either α -globin or β -globin) are clinically silent, some produce clinically significant symptoms, ranging from serious severity to life-threatening conditions (table 1).

Table 1: Characteristics of the main Hb disorders.

Gene type	Hemoglobin pattern ¹	Comments
HbSS	HbS = 55 to 90% HbA2 > 3.5% HbF = 5 to 20%	Most common genotype. Sickle-cell crises/pain crises. Acute organ syndromes. Chronic hemolytic anemia.
HbAS	HbS = 35 to 40% HbA2 \geq 3.5%	No apparent illness. Anemia and painful crises are rare. Rare painless hematuria due to papillary necrosis. May be a risk factor for sudden death during physical training. Also carries some anesthetic risks.
HbS β^+ -thalassemia	HbS > 55% HbF > 20% HbA2 > 3.5%	Variable, mild sickle-cell disease.
HbS β^0 - thalassemia	HbS > 80% HbF < 20% HbA2 > 3.5%	Severe sickle-cell disease.
HbSC	HbS \approx 50% HbC \approx 50% HbF < 5%	Weak symptoms of sickle-cell disease. Chronic hemolytic anemia. Interacts with HbS.
HbCC	HbC > 95% HbA2 \approx 2.5% HbF \approx 0.5%	Pain crises. Organ events. Chronic hemolytic anemia.
HbAC	HbC \approx 50% HbA \approx 47% HbA2 = 3%	No apparent disease.
HbAE	HbE = 25 to 35%	Mild, hypochromic anemia.
HbEE	HbE > 95% HbA2 \approx 2.5% HbF < 3%	Mild anemia. Hemolysis caused by infections/medical drugs.
HbSE	HbS \approx 70% HbF \approx 2%	Mild disease.

HbE β +-thalassemia	HbE + HbA2 = 25 to 80% HbF = 6 to 50% HbA = 5 to 60%	Variable, intermediate, hypochromic anemia.
HbE β 0-thalassemia	HbE up to 85% HbA2 < 5% HbF = 15 to 25%	As for β -thalassemia major.
HbS/HPFH	HbS \approx 70% HbF \approx 30%	Pancellular distribution of HbF.

¹ Average percent hemoglobin present in various genotypes of the main Hb disorders. Brief description of each hemoglobinopathy. The most severe forms of SCD are HbSS and HbS β 0, whereas HbSC and HbS β + are considered the less severe forms (35). Adapted from references (17), (32), (36) and (37).

Sickle cell anemia is by far the most common form of sickle cell disease, accounting for 65-70% of SCD cases occurring in populations of African ethnic origin, followed by hemoglobin SC disease with 30-35% of the cases, and the most remainder having HbS β thalassemia. (38)

A strong geographical correspondence between the highest HbS allele frequencies and high malaria endemicity reflects a balancing selection referred to as the “malaria hypothesis” that results from the advantage conferred by such a disorder in protecting against severe malaria (39). These hypotheses have led to maps that show the geographical distribution of the sickle gene, which matches the geographical distribution of malaria (40). It is important to emphasize that this selective advantage does not mean that individuals with the trait are less likely to develop malaria, but rather seem to translate into a lower death rate. Epidemiology observations in Africa show that children with sickle cell trait are less likely to die from malaria than children without the trait (41). The estimates of prevalence of HbAS in Africa range from 10 to 40% across equatorial Africa reflecting the selection pressure due to malaria in areas of high transmission (42). Contrary to this, individuals with sickle cell anemia (HbSS) seem to have some protection against infection, however, when they have malaria, these patients tend to develop severe disease and have a high death rate from malaria (41). A common notion is that “they pay the price for the HbAS advantage survival for malaria”.

Globally, the sickle cell gene occurs at the highest frequency in five geographic areas: sub-Saharan Africa, Arab-India, the Americas, Eurasia, and Southeast Asia (43). Sub-Saharan Africa accounts for the highest frequency where approximately 230,00 babies

are born each year with sickle cell disease (HbSS). Contrasting with North America and Europe, where approximately 2600 babies and 1300, respectively, are born each year with sickle cell disease (43).

Although the sickle mutation of the HbB gene first reached high population frequencies mostly in tropical regions (6), population migrations, either by slavery routes or by the globalization process, have led to their wide-spread distribution in many countries (44). Worldwide, more than 100 million individuals have HbAS (45).

SCD carries a high burden of morbidity and mortality worldwide (3). In 2010 it was estimated that sickle cell disorders accounted for 0.42 deaths per 100,000; 28.69 years of life lost (YLLs) per 100,000 and 53.21 years lived with disability (YLDs) per 100,000, adding up to 81.9 disability-adjusted life years (DALYs) per 100,000 (44). However, it is Africa which carries the highest burden of SCD in the world, with most African patients being homozygous. With increasing population growth from increasing birth rates, it is estimated that, globally, 14 million babies will be born with SCA between 2010 and 2050, with 80 % of these births being in sub-Saharan Africa (40). SCD is a major public health concern that has great impact on both individuals and society.

1.4. Sickle Cell Anemia

1.4.1. Pathophysiology – The sickling process

The fundamental pathological mechanism of this disease is the intracellular polymerization of HbS, rather than sickling or morphologic deformation of erythrocytes (figure 8, a) (46).

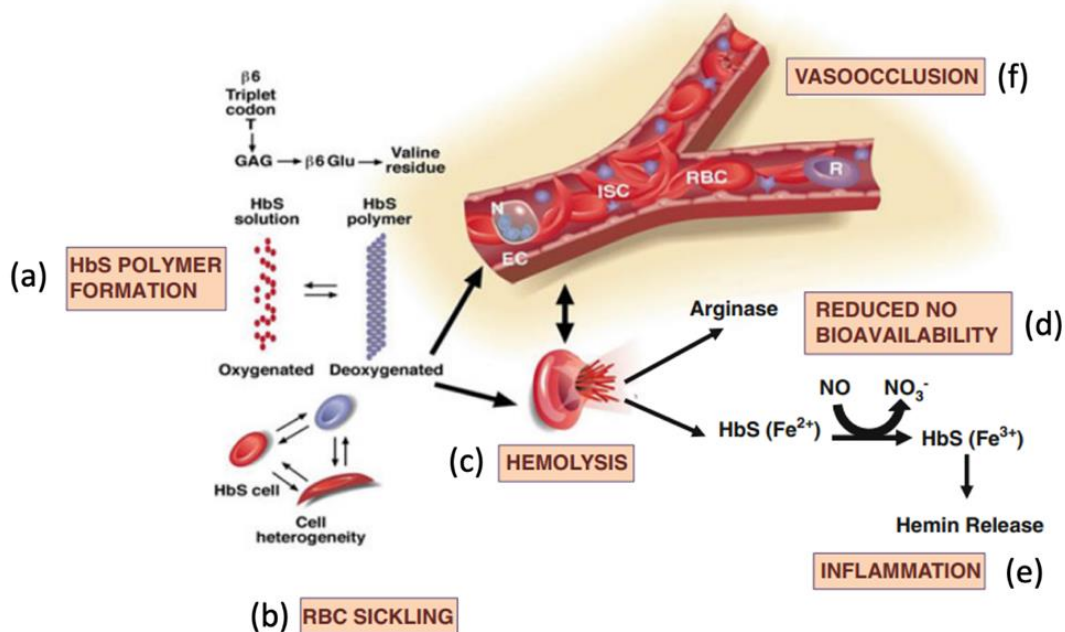


Figure 8: The pathophysiology of sickle cell disease.

The intracellular polymerization of HbS (a) leads to: (b) RBC sickling, (c) hemolysis, (d) reduced NO, (e) inflammation, (f) vaso-occlusion. See text for detailed description. Adapted from (37).

The amino acid substitution from glutamic acid (polar) to valine (non-polar) affects the way Hb molecules interact with one another within the erythrocyte. The β chain folds in a way that glutamic acid extends outward to bind water, contributing for hemoglobin solubility. Because valine is placed in the position that the glutamic acid once held, this hydrophobic amino acid is extended outward but instead of binding water, it seeks a hydrophobic niche to bind (43).

Under low oxygen saturation, the natural allosteric changes that occur create a hydrophobic pocket that allows the valine from an adjacent hemoglobin molecule to bind, forming a double strand that becomes the seed for HbS polymer formation (43). According to the double nucleation model, the nucleation of a single fiber at random locations in the solution is called homogeneous nucleation, which then triggers an

exponential growth of the polymer via nucleation of additional fibers on the surface of pre-existing ones (47). This second process is called heterogeneous nucleation, in which valine residues on the polymer surface (hydrophobic receptor) provide the stability for the nucleation of new fibers (37). A gelatinous network of fibrous polymers is formed, filling the erythrocyte and growing in length beyond its diameter, which causes disruption of its architecture leading to sickling (figure 8, b and figure 9) (48). Frequently, upon reoxygenation, the polymers disassemble and the cells usually resume their normal biconcave disk shape, although irreversibly sickled cells (ISCs) are an exception (49).

In heterozygotes (HbAS), sickling does not occur unless the oxygen saturation of hemoglobin is reduced to less than 40%. In contrast with homozygotes (HbSS), in which the sickling process begins when oxygen saturation decreases to less than 85% (43).

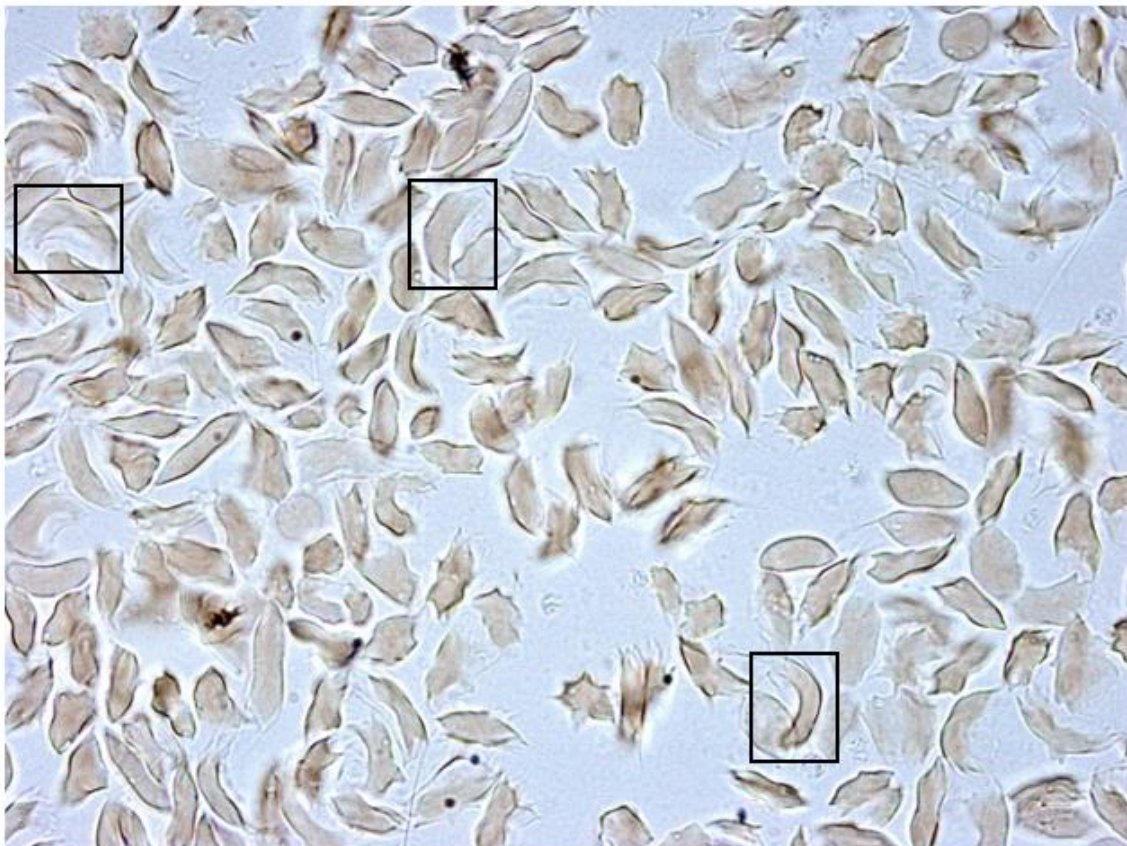


Figure 9: Sickie RBCs after 24h of incubation (37°C) upon realization of the sickling test. Notice that the typical sickle shape is elongated with a point at each end, similarly to a crescent moon or a hand sickle weapon. Image was acquired with an optical microscope using a 100x oil-immersion objective. The sample was prepared for analysis 2 days after blood collection and possessed 90,4% of HbS. No stain was applied in the sample.

The rate and extent of HbS polymerization, as well as the distribution of polymerized HbS, seems to depend on two crucial factors: (i) speed and duration of hemoglobin deoxygenation, and (ii) the intracellular HbS concentration (47,48). The kinetics of polymerization is characterized by a marked delay period before any polymer fibers can be detected, the duration is determined by two factors mentioned above (47). When a red cell is traveling within the microcirculation, it transits from the arteriole to the venous circulation, where it can either (i) deform and pass through the capillary, escaping into the large vessels without intracellular polymerization, because the transit time is shorter than the delay time, or (ii) it undergoes intracellular polymerization within the capillary, because the delay time is shorter than the capillary transit time, thus polymer fiber domains distort the cell and decrease the flexibility necessary for its passage through the narrow vessels, with the possibility of blocking the circulation (47). Microvascular factors, which could lead to variable hypoxia, depending on the microvascular site and wall shear rate, sickle RBC's factors and rates of HbS polymerization might be significant contributors for the occurrence of vaso-occlusive episodes (50).

The erythrocytes in SCA possess a decreased oxygen affinity compared to healthy individuals, because of an unusually high intracellular concentration of 2,3-DPG in the sickle RBC. This is believed to be a compensatory adaptation, which is generally observed in all forms of anemia to facilitate oxygen release to the tissues (51). However, more elevated levels of 2,3-DPG lead to a right shift of the hemoglobin-oxygen dissociation curve (figure 6), which may be counter-adaptive in sickle cell anemia, due to its promotion of the T-state of HbS and the decreased solubility of HbS, which promotes sickling (51).

The process of sickling leads to changes in various rheological properties which are responsible for the clinical course of this disease. Sickle polymers increase RBCs stiffness and the reduced flexibility inhibits their passage through the microvasculature (52). Blood flow in the microcirculation is highly dependent on the deformability of erythrocytes, which itself, also affects the blood flow, since a loss in deformability causes a rise in blood viscosity (53). Red cell volume and density are determinants of the cell flexibility and the ability to deform, they are physiologically closely controlled to permit

adequate flow through the microcirculation (37). Several transport channels that regulate cation content in the RBC may have altered activity in the sickle erythrocyte promoting cell dehydration due to potassium leakage and calcium influx (17,37). Loss of water content affects cell volume and density and leads to an increased mean corpuscular HbS concentration (MC[HbS]C) which is a dominant factor for deoxyHbS tendency for polymerization (37).

1.4.2. Pathophysiology – Inflammation and damage

About 10% - 30% of hemolysis occurs intravascularly (37) releasing hemoglobin and heme into the plasma, stimulating the production of inflammatory, pro-coagulant and vasoactive molecules that contribute to the activation and recruitment of leukocytes and platelets. (54) Extracellular heme can induce the expression of adhesion molecules on endothelial cells, thus enhancing leukocyte recruitment and adhesion (55). It also activates an innate inflammatory response by stimulating toll-like receptor-4 (TLR4) (54). And finally, plasma free heme levels also lead to a shift in the hemostatic balance towards a prothrombotic state and were shown to be independently associated with the risk of vaso-occlusive crisis (56). In addition, repeated cycles of RBC sickling and iron decompartmentalization in the erythrocyte produce higher amounts of oxygen radicals (37), further inducing changes in the surface membrane subjected to an increased oxidative stress, and thus promoting inflammation and tissue damage (figure 8, e) (55).

Damaged surface membranes enhance hemolysis, by facilitating erythrocyte recognition and removal by macrophages (37). The release of hemoglobin in the vasculature can exceed the capacity of endogenous hemoglobin sequestration and recycling mechanisms (54), leading to consumption and decreased bioavailability of nitric oxide (NO), which is a well-known regulator of endothelial homeostasis (56). Lysed erythrocytes also release arginase, which destroys L-arginine, the substrate for NO production, promoting further NO deficiency and loss of its regulation role. Therefore, depletion of NO further triggers inflammation and oxidative stress (figure 8, d) (55).

1.4.3. Pathophysiology – Vaso-occlusion and hemolytic anemia

Sickle erythrocytes also suffer an altered expression of red cell surface membrane proteins, becoming abnormally adherent to the vascular endothelium and to other circulating cells. These rigid, adherent, poorly deformable erythrocytes can clog in the microvasculature leading to episodes of vaso-occlusion and hemolysis (17). Hemolytic anemia is always present (figure 8, c), regardless of whether acute vaso-occlusive events are taking place (37). The life expectancy of red cells in sickle cell anemia is about 7-14 days compared with the 120 days for normal erythrocytes (37).

Repetitive cycles of HbS polymerization and depolymerization and oxidant-induced damage to the cell membrane and contents ultimately injures the sickle erythrocyte membrane, resulting in permanent deformation of the spectrin-actin membrane skeleton. The RBC acquires a permanent sickle shape regardless of whether or not the HbS is polymerized; these damaged cells are called irreversibly sickled cells (ISCs) (37), which are the predominant form of sickled RBCs seen on typical blood smears as elongated curved sickle cells with “pointed ends” (figure 9) (57). ISCs tend to be very dense, viscous, and adherent, being recognized by the spleen as abnormal and removed from circulation, which contributes to the hemolytic rate, reducing the cells’s lifespan by $\geq 75\%$ (35). However, it is less clear whether the ISC count correlates with vaso-occlusive severity (54,57). In fact, vaso-occlusive events (figure 8, f) are thought to be due to reversible sickle cells since they are able to travel into the microvasculature in the biconcave disk conformation, only converting to the sickle form within the vessel (43).

Reduced oxygen carrying capacity of blood, cellular dehydration, altered adhesive properties of erythrocytes, increased viscosity and increased physical and oxidative cellular stress contribute to formation of ISCs and premature RBC destruction (48), causing episodic, progressive, and cumulative organ injury (54) that characterizes the pathophysiology of sickle cell anemia (figure 8).

1.5. The role of HbF in SCD

Fetal hemoglobin is a major determinant of the disease severity by leading to decreased intracellular HbS concentration. It also inhibits polymerization (58), as neither HbF nor its mixed hybrid tetramer ($\alpha_2\beta_S\gamma$) enters the deoxyHbS polymer phase, in contrast to HbA and HbC that are able to co-polymerize extensively with HbS (37). The phenotype of sickle cell disease becomes manifest within 6 months to 2 years of age as HbF levels and its polymerization-preventing effects decline (37). HbF levels are associated with haplotypes of the β -globin gene complex and unusual high levels occur as result of point mutations or gene deletions in this cluster. This phenotype is called hereditary persistence of fetal hemoglobin (HPFH) (59).

Enough HbF in each individual RBC can prevent deoxyHbS polymerization. The protective effects can be understood assuming a homogeneous HbF distribution in all RBCs, as seen in HbS/HPFH genotype (58), where each erythrocyte possess approximately 10pg of HbF ($1/3$ of the total hemoglobin) (37). It is assumed that this is the concentration of HbF needed to protect the cell from deoxyHbS polymer induced damage (60).

F-cells (RBCs) contain both HbF and HbA (or HbS instead of HbA in the case of SCA); with the lower limit of detection of around 6 pg ($\sim 20\%$) of HbF, as measured by flow cytometry, the standard clinical method of enumerating F-cells (61).

In sickle cell anemia total HbF levels rarely reach more than 30%, but most importantly, it is very heterogeneously distributed (60). In fact, electrophoresis, or High-Performance-Liquid-Chromatography (HPLC) only provide the percentage of HbF in a hemolysate of all erythrocytes. They do not allow to determine the percentage of HbF-containing cells (F-cells), nor the amount of HbF in individual RBCs (58). In fact, the total number of F-cell or the concentration (%) of HbF in the hemolysate are not ideal predictors for the likelihood of severe disease (61).

Several studies focused on new methods to accurately determine the HbF/F-cell (the ratio of HbF per F-cell) and the proportion of F-cells that have enough HbF to exert protective effects against HbS polymerization (61), as these confer critical influence on disease severity. In fact, it would also be a useful tool in characterizing the baseline

distributions of HbF per individual RBC for comparison in evaluation of therapeutic response to HbF inducers such as hydroxyurea (58).

In homozygotes (HbSS) stable levels of HbF are not reached until age 5 – 10 years and in most adults HbF levels are increased. However, only when the total HbF concentration is near 30%, the percentage of protected cells may approach 70%. (61) Nonetheless, even if HbF levels reach 20% (and a mean ratio of 8pg HbF/F-cell), the distribution may still vary greatly (61). Therefore, hydroxyurea does not cure sickle cell anemia, as nearly all patients with therapy-induced increases of HbF levels still may have illness. (61) Both HbF concentration and its distribution among erythrocytes are heritable, meaning gene therapeutic approaches could be more promising in achieving curative pan-cellular levels of sufficiently high ratios of HbF/F-cell, by incorporating editing elements that modulate HbF gene expression. (37,60)

The distribution on HbF concentrations among F-cells and the HbS content and extent of polymerization are the main modulators of clinical severity of sickle cell anemia, being crucial targets of patient management.

1.6. Clinical manifestations and management

Despite being a monogenic disorder primarily affecting the erythrocytes, SCA is a multisystem disease characterized by acute events and progression to chronic complications (table 2), culminating in a wide range of severe, and even life-threatening consequences, conferring the characteristic high morbidity and mortality of this disease (62,63).

Table 2: Manifestations and complications of sickle cell anemia.

	Complication	Characteristics
Acute	Acute pain episodes (vaso-occlusive events)	Most common complication / most common cause of hospital admission. Severity varies (manageable at home or requires hospitalization). Frequent episodes are risk factor for mortality.
	Acute chest syndrome	Chest pain, accompanied by fever, respiratory symptoms, (X-ray: new pulmonary opacity), hypoxemia in severe cases.
	Stroke	Ischemic and hemorrhagic strokes.
	Thrombosis	Especially adults (pregnancy and post-partum).
	Liver complications	Acute right-upper quadrant pain (jaundice): work-up for acute cholecystitis, acute viral hepatitis, hepatic sequestration, sickle cell intra-hepatic cholestasis.
	Infections	Pneumonia (frequent), osteomyelitis, and urinary infections; may progress quickly to sepsis.
	Priapism	Compartment syndrome of the penis (short-lived, intermittent, or prolonged >4 h). Painful penile erections.
	Aplastic crisis	Severe anemia (reticulocytopenia) - parvovirus B19 infection.
Chronic	Hemolytic anemia	Normocytic, normochromic (Hb: 6 and 10 g/dL) with reticulocytosis.
	Functional asplenia	Splenic dysfunction, autosplenectomy (splenic infarction) usually during childhood.
	Avascular necrosis	Hip(s) or Shoulder(s) - early osteoarthritis and chronic pain.
	Osteopenia and osteoporosis	Early reduction of bone mass density.
	Pulmonary arterial hypertension	Exertional dyspnea or fatigue with chronic oxygen desaturation; associated with poor prognosis.
	Gallstones / cholelithiasis	Augmented heme breakdown (hemolysis).
	Retinopathy	Proliferative retinopathy (frequent), may cause blindness.
	Nephropathy	Hyperfiltration, hyposthenuria (early), microalbuminuria increases with age, possible end-stage kidney disease.
	Heart disease	Diastolic dysfunction with increased mortality, overt heart failure, acute myocardial infarction.
	Leg ulcers	Malleolar and distal leg skin (recurring complication), painful disfiguring ulcers, difficult healing.
	Neurological complications	Neurocognitive impairment (frequent). Moya Moya syndrome (proliferation of intracerebral blood vessels with increased risk for acute cerebrovascular events).

Adapted from (62) and (40).

(i) The vaso-occlusive crisis (VOC), also known as acute pain crisis, is the most typical clinical manifestation of SCA. It is characterized as episodes of excruciating musculoskeletal pain that typically appears in early childhood, presenting as dactylitis, in which the hands or feet are swollen, tender and erythematous (64). Although VOC may occur without triggering event they often seemed provoked by infections (fever), hypoxia, dehydration, excessive exercise, trauma, high altitudes, abrupt changes in temperature, and emotional stress (52). The principles of management of VOC consist of (i) warmth and hydration, (ii) analgesia (usually requiring opiates), and (iii) treatment of the underlying precipitating factor (if it can be established). Suboptimal pain management is associated with increased morbidity and may contribute to mortality (65). Recurrent crises requiring hospitalization (>3 episodes per year) correlate with reduced survival in adult life due to the accumulation of chronic end-organ damage associated with this episodes (17).

(ii) The acute chest syndrome (ACS), a term used to describe an acute pulmonary process that occurs exclusively in patients with SCD, is an acute complication of SCA, which consists of a life-threatening pneumonia-like illness characterized by chest pain, tachypnea, fever, cough, and arterial oxygen desaturation (64). ACS is thought to be caused by sickling within the lung, producing pain and temporary pulmonary dysfunction, and is one of the most common causes of death in adults with SCD (16,53). The treatment is symptomatic with both analgesia and fluid therapy, but also oxygen supplementation, adequate antibiotic coverage and transfusion if indicated (62,65).

(iii) Another potentially life-threatening manifestation of SCA is the acute trapping of blood in the spleen (acute splenic sequestration - ASS), which usually occurs in infancy and early childhood (36). This condition may lead to severe life-threatening anemia with need of immediate management with urgent blood transfusion to prevent hypovolemic shock and cardiac decompensation (62,65). By age of 5 years, a process of splenic fibrosis and autosplenectomy is usually complete, reducing the risk of ASS (65).

(iv) Children with SCA possess an increased risk for infection from encapsulated organisms, particularly by pneumococci, due to splenic dysfunction and disordered humoral immunity (64). Prophylactic penicillin and adequate immunizations significantly reduces the risk of pneumococcal infection in pediatric SCD patients (65). They also

present unusual susceptibility to osteomyelitis that can be caused by organisms such as non-typhoid *Salmonella enterica* (17). Fever in patients with SCA is a medical emergency, which requires parenteral antibiotics to cover against *Streptococcus pneumoniae* and gram-negative enteric organisms, along with an adequate physical examination, a complete laboratory workup and indicated complementary diagnostic methods (laboratory workup and imaging methods) to find a focus of infection (65). In sub-Saharan Africa, children with SCD have a high mortality rate estimated at 50-80% by 5 years old. The most common cause of death is infection, including invasive pneumococcal disease and malaria (35). Children with SCA also face chronic issues including decreased growth that is likely due to chronic severe anemia, suboptimal nutrition, hypermetabolism, and possible endocrine dysfunction (64).

(v) Repeated microinfarction episodes lead to ischemia-reperfusion injury that progresses into multiorgan damage causing chronic complications including chronic kidney disease, heart failure, functional asplenia, retinopathy, pulmonary hypertension, cerebrovascular complications, among others (17,36).

(vi) Hemolysis results in a normocytic normochromic anemia with levels of Hb varying between 6 and 10g/dL and reticulocyte counts ranging around 5-20%. Clinical features secondary to chronic hemolytic anemia include pallor and jaundice (62). Chronic anemia is not usually a major source of morbidity for individuals with SCA but viral infections, such as Parvovirus B19, can cause a life-threatening anemia as a result of an aplastic crisis (33,54). Acute symptomatic anemia is an indication for considering blood transfusion, as well as refractory pain crises. To prevent iron overload due to chronic blood transfusions, iron chelation may be prescribed (62).

As in all chronic illnesses, patient education is a crucial aspect of treatment as they must be followed-up, ideally within a multidisciplinary care approach. Patients need to be knowledgeable of its acute and chronic complications and be taught to identify alarming signs to know when to seek medical help (65). Mortality due to sickle cell disease has decreased in recent years, primarily due to early diagnosis (via newborn screening), penicillin prophylaxis, better medical care, and education of family members, making possible for most patients with sickle cell disease to live well into adulthood (36).

1.7. Treatment approaches – Current strategies and new therapeutic agents

Based on the pathophysiological processes, multiple potential therapeutic targets exist (figure 10). This can be classified into two groups, (i) upstream targets, and (ii) downstream targets (table 3).

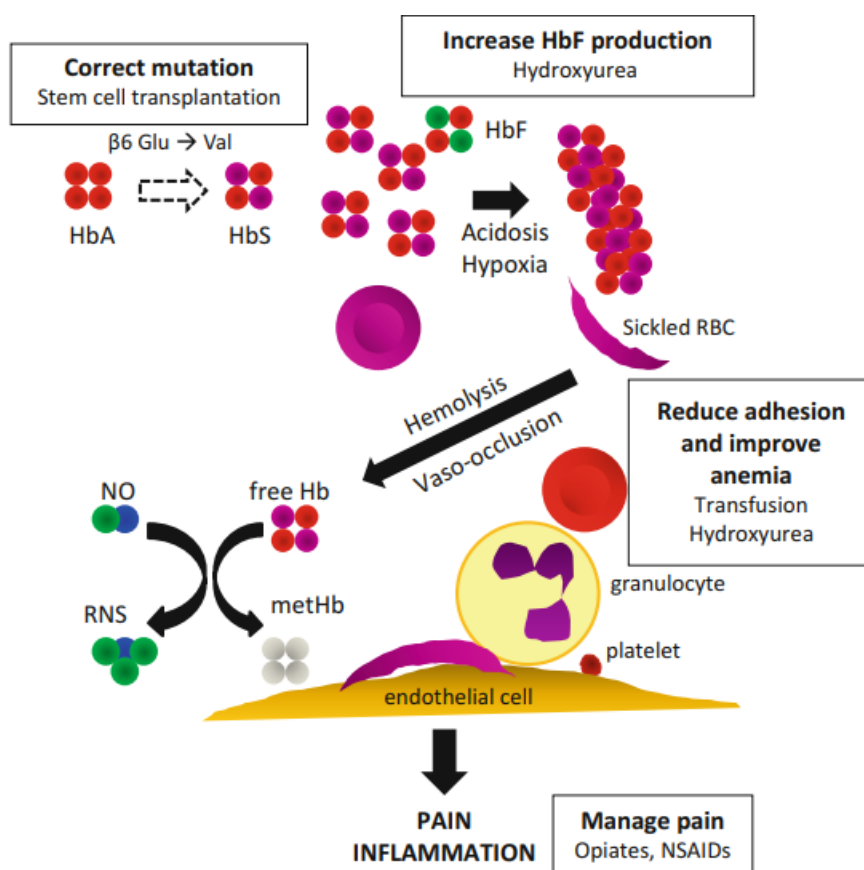


Figure 10: SCA pathophysiology and potential therapeutic targets.
Adapted from (62).

Table 3: Upstream and downstream therapies for SCD.

	Target/MOA	Therapy
Upstream	Correction of genetic defect	Hematopoietic stem cell transplantation
		Gene editing
	Hb switch: fetal \rightarrow adult	Gene editing
	Preventing HbS polymerization	\uparrow HbF production (Hydroxyurea)
		Altering Hb O ₂ affinity (Voxelotor)

Adapted from (61), MOA: Mode of Action.

Table 3: Upstream and downstream therapies for SCD (continued).

	Target/MOA	Therapy
Downstream	Control of pathophysiological effects	Antioxidants (L-glutamine)
		Anti-adhesive (Crizanlizumab)
		Anti-inflammatory (Statins, Vitamin D)
		Vasodilatory (Sildenafil, Arginine, inhaled nitric oxide)
		Anti-thrombotic and anti-platelet (Aspirin, Prasugrel, Rivaroxaban)
		Anti-RBC dehydration (Magnesium sulfate)
	Ameliorating symptoms	Pain relief (Opioids)
		Management and prevention of complications (Blood transfusions)

Adapted from (61), MOA: Mode of Action.

Allogeneic hematopoietic stem cell transplantation (HSCT), using matched sibling donors or HLA-matched unrelated donors (although the latter possesses high rates of graft-versus-host disease), is the only curative treatment for SCA. It is increasingly being used for young children with early complications, while older adults are considered less favorable candidates. However, the applicability of transplants remains limited by the availability of donors. Alternatives with curative intent include umbilical cord blood transplant, haploidentical donors, gene therapy targeting autologous stem cells for subsequent transplantation and genome editing (65). Genome editing focuses on correction of SCD mutation, downregulation of BCL11A (inhibitor of the γ -globin gene) or mimicking of hereditary persistence of fetal hemoglobin (HPFH) mutations. These strategies rely on technology such as CRISPR-Cas9 or engineered DNA-cleaving enzymes such as zinc-finger nucleases (ZFNs) or transcription activator-like effector nucleases (TALENs) (66). Some of this curative approaches have ongoing clinical trials with encouraging preliminary results, while some are still in preclinical stages (67).

The major FDA-approved drug therapies for the treatment of SCD are hydroxyurea (HU), L-glutamine, crizanlizumab, and voxelotor:

(i) Hydroxyurea was approved by the FDA in 1998 for adults with SCD and subsequently approved for children ≥ 2 years of age in 2017 to reduce the frequency of pain events and need for blood transfusions. HU is a HbF inducer, therefore it reduces the HbS polymerization. It also reduces inflammation by reducing the production of white blood cells and platelets, reduces adhesion molecule expression involved in vaso-occlusion, and is a nitric oxide donor. (66) It has been shown to decrease mortality in SCD (68).

(ii) L-glutamine is an essential amino acid required for the synthesis of glutathione, nicotinamide adenine dinucleotide (NAD⁺) and arginine, which are important for red blood cells protection against oxidative damage. It was approved by the FDA in 2017 for adults and children ≥ 5 years old to reduce sickle cell complications. (66,69)

(iii) Crizanlizumab was approved by the FDA in 2019 for adults and adolescents ≥ 16 years old to reduce the frequency of vaso-occlusive crises. Its mechanism of action consists in binding to P-selectin (expression is triggered by inflammation) and blocking its interaction with ligands. It plays a role in inhibiting adhesion of neutrophils, activated platelets and sickle RBCs to the endothelial surface and to each other, which promotes vaso-occlusion. (66)

(iv) Voxelotor (GBT440) was approved by the FDA in 2019 for adults and children ≥ 12 years old to increase the hemoglobin concentration. (66) It is an allosteric modifier of HbS that increases oxygen affinity and stabilizes the oxyHb state. Thus, it inhibits HbS polymerization, prevents sickling, extends RBCs half-life, reduces hemolysis, reduces reticulocyte counts, and may provide long term disease modification. (70)

(v) Another potential modulator of HbO₂ affinity for the treatment of SCD is 5-hydroxymethyl-2-furfural (5HMF) which has high-specificity for Hb and is able to restrict the transition to the T-state, inhibiting hypoxia-induced sickling in vitro. It has completed pre-clinical testing and has entered clinical trials. (51)

(vi) Other potential HbF inducers include: decitabine, lenalidomide and pomalidomide.

- Decitabine was FDA approved for treatment of myelodysplastic syndrome in 2006. Clinical trials in patients with SCD showed a marked increase in both HbF and F-cells. Its mechanism involves hypomethylation of the γ -globin gene promoter, which triggers its expression and induces γ -globin synthesis, increasing HbF production. It has also showed a concomitant decrease in other pathogenic mechanisms of SCD such as adhesion, endothelial activation and development of a procoagulant state (71,72).

- Lenalidomide and pomalidomide are structurally related to thalidomide and have immunomodulatory properties that have been shown to slow erythrocyte maturation, increased proliferation of immature cells and induction of HbF in vitro (71). These drugs are under investigation using in vitro erythropoiesis models derived from human CD34+ progenitor cells from normal and SCD donors (73).

A combination of upstream and downstream targets would be the ideal therapeutic regimen for maximum benefit, however there are still numerous challenges to implement these treatments. The potential curative therapies face significant limitations for widespread use in the developing world and some still remain largely experimental. Although significant scientific and clinical advances in these approaches have been made, there is still a need for investigation to develop improved therapies for this disease, which would be of paramount importance considering its important global health burden.

1.8. Diagnosis and diagnostic methods for SCD

The keystone of management is based on early diagnosis of SCD, which can help reduce mortality. Therefore, various techniques have been developed to detect sickle cell disease and the carrier states.

SCD may cause a serious of alterations in routinely performed laboratory blood tests, although they usually only confirm a hemolytic anemia and are non-diagnostic for SCD. Several simple tests exist, which are often used as a first economic approach to test for SCD and may be used for screening larger number of samples. Definitive diagnosis

requires either the demonstration of HbS by hemoglobin separation techniques such as electrophoresis or HPLC, or the identification of genetic changes (35).

Some of these tests may be used for prenatal screening. While most or all these tests are available in Europe, the limited resources in countries with lots of cases, like most of sub-Saharan-Africa, translates into different requirements for tests. Therefore, efforts are being made to provide low-cost, simple, and user-friendly methods for detecting SCD (74).

Finally, laboratory tests have been developed, usually based on complex flow cytometry protocols, with the aim to identify new drugs for treatment (35).

Some tests are used in the follow-up of these patients, like the determination of the percentage of HbS and HbF by electrophoresis or HPLC. However, tests which would be better predictors of vaso-occlusive crisis or for overall prognosis are still needed.

1.8.1. Routine laboratory (hematology/biochemistry) parameters

Routine blood tests are the cornerstone for screening for hemoglobinopathies, as illustrated in the Portuguese recommendations from the “*Direção Geral de Saúde*” for the prevention of severe hemoglobinopathies, stating that a complete blood count should be performed in all pregnant women and in fertile women particularly in preconception consultation, followed by a HbS analysis if alterations are encountered (75).

As all hemolytic anemias, SCD shows typical changes in routine laboratory parameters. It usually presents as a normocytic (mean corpuscular volume - MCV of 80 to 100 fL) normochromic anemia, although a marked reticulocytosis can lead to an elevated measurement of mean corpuscular volume, because the average mean corpuscular volume of a reticulocyte is 150 fL (62,76). An elevated MCV is usually seen in SCD patients receiving hydroxyurea (35). The counts of white blood cells and platelets are variably elevated (35). In addition to the complete blood count, testing should also include measurement of lactate dehydrogenase, haptoglobin and unconjugated bilirubin levels, as well as urinalysis which may be positive for hemoglobinuria (table 4).

The destruction of red blood cells is characterized by increased unconjugated bilirubin, increased lactate dehydrogenase, and decreased haptoglobin levels (77).

Review of the peripheral blood smear (PBS) is also a critical step in the evaluation of any anemia. It may show pathognomonic red blood cell morphologies, in this case, occasional sickled RBCs are often found (76). Other findings in the PBS include (i) moderate to severe anisopoikilocytosis (varying shapes and sizes of RBCs - represented by an elevated red cell distribution width – RDW), (ii) normoblasts, which represent the fourth stage of erythroid maturation, (iii) polychromasia, which indicate that RBCs are being released prematurely from the bone marrow, (iv) target cells, due to the abnormal Hb present in the RBCs, and (v) Howell-Jolly bodies, which are pathognomonic for splenic dysfunction (78,79).

However, none of these tests can establish a definitive diagnosis of SCD (35).

Table 4: Pertinent diagnostic laboratory tests for hemolysis.

Test	Findings in hemolysis	Additional information	Normal Range
Complete blood count	Normocytic normochromic anemia	Hb values between 6 to 10g/dL.	♂ 13.5-18 g/dL ♀ 12 to 16 g/dL
	Reticulocytosis	Reticulocyte count ranging around 5-20%.	0.5%–1.5%
Unconjugated bilirubin	Increased	Liberated Hb is converted into unconjugated bilirubin and its production exceeds elimination capability.	Unconjugated hyperbilirubinemia is present when the direct fraction is <15% of the total serum bilirubin. Total serum bilirubin concentrations are between 3.4 and 15.4 µmol/L.
Lactate Dehydrogenase (LDH)	Increased	Released from lysis of RBCs.	313–618 µg/dL
Serum haptoglobin	Decreased	It binds to free Hb and this complex is quickly cleared by the liver.	30–200 mg/dL
Urinalysis	Hemoglobinuria		
Peripheral blood smear	Occasional sickled erythrocytes, anisopoikilocytosis, polychromasia, normoblasts, target cells and Howell-Jolly bodies.		

Adapted from (5,17,43,62,76,77,80).

1.8.2. Simple (screening) tests for SCD

Several simple and low-cost tests are often used as a first approach to screen many samples of specific groups perceived at risk or in resource limited settings. Screening in the setting of hemoglobinopathies is directed at optimizing management of the disorder by early diagnosis; it may be preoperative, neonatal, preconceptual or premarital (81); aiming to provide patients prompt counselling about disease complications, informed reproductive choice and implementation of immunizations and antibiotic prophylaxis. These methods need to be very sensitive to avoid false-negative results (82). However, all these methods permit only a presumptive diagnosis and need further confirmation (81). These screening tests include (i) the sickling test, (ii) the solubility sickling test which are currently used techniques, and (iii) some novel approaches related to point of care (POC) SCD detection.

(i) Sickling test – As mentioned previously, it is possible to observe occasional sickle cells in the routine blood smear, thus, by adding a reducing agent to the blood, the number of sickle erythrocytes is increased, enabling quantification. Sodium metabisulfite is the reducing agent most widely employed speeding up the deoxygenation of HbS and thus the sickling process. Blood is usually mixed with this substance in 2 % solution and sealed between a glass slide and a coverslip by applying paraffin or nail polish to the border of a coverslip (avoiding contact with ambient air), and then placed in a 37°C incubator for several hours, to posteriorly observe under optical microscopy. However, a positive test does not distinguish the sickle cell trait from sickle cell disease (83).

(ii) Solubility sickling test – In this test, RBCs are lysed with saponin to release the hemoglobin and mixed with the reducing agent sodium dithionite in the presence of a concentrated phosphate buffer, where HbS is insoluble. Thus, deoxyHbS crystallizes in the presence of this agents forming tactoids (water crystals) which refract and deflect light rays and cause solution turbidity, enabling HbS quantification by light absorption and comparison with negative and positive controls (83). However, other conditions can also cause increased absorption and might interfere with this test, such as Heinz-bodies,

unstable Hb, hyperlipidemia, high serum viscosity or blood protein disorders. Furthermore, false-negative results can occur with other Hb variants and when utilized for children under the age of 6 months, due to the presence of HbF, and when the HbS is less than 10%. Moreover, the sickle solubility tests cannot differentiate between SCT and SCD, and misses other hemoglobin variants (35).

(iii) Novel Point-Of-Care rapid tests for sickle cell disease/hemoglobin variants – These tests have emerged as potential alternative to the gold standard approaches for SCD definitive diagnosis, that are neither rapid, nor applicable in resource-limited settings. Among these are:

(a) Paper-based hemoglobin solubility test

In this test, a drop of the blood sample is mixed with a hemoglobin solubility buffer composed by a hemolytic agent, a reducing agent, and a high-phosphate buffer, then, the mixture is deposited onto a chromatography paper, allowing a stain to develop. This technique depends on the filtration properties of the paper substrate and the insolubility of the HbS. While the soluble HbS can freely permeate through the paper, the insoluble polymerized HbS becomes entangled in the meshed network of paper fibers, resulting in blood stains. The stains are then used to visually distinguish between HbSS, HbAS and HbAA (figure 11) (35).

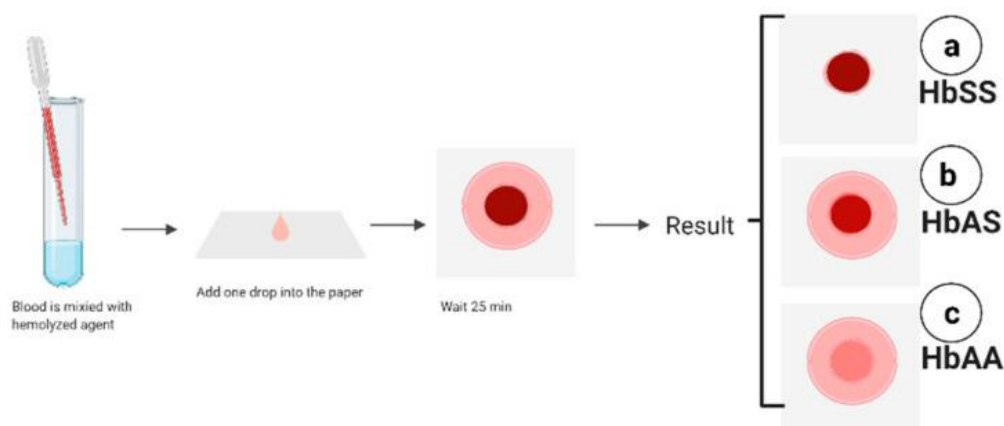


Figure 11: Paper-based hemoglobin solubility test.
Adapted from (35).

Moreover, this test's sensitivity can be increased when the stain is scanned and automatically analyzed with an image analysis algorithm, which is able to quantify the Hb in the sample based on the intensity of the color in the center spot (figure 12) (84).

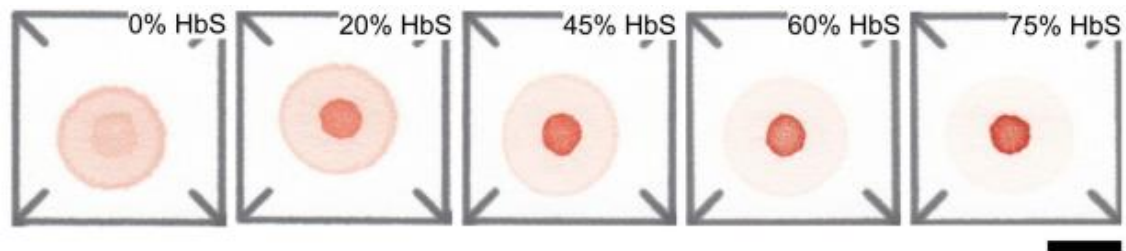


Figure 12: Blood stains produced on paper by samples with various %HbS.
Scale bar is 1 cm. Adapted from (84).

However, this test can be affected by blood clotting, does not differentiate between HbSC and HbAS and it is not reliable for newborns due to a high level of HbF (35).

(b) The density-based separation in aqueous multiphase system

This test allows the separation of RBCs by density upon centrifugation in capillary tubes through aqueous multiphase systems (AMPSs) which consist of mixtures of polymers in water that form immiscible liquid phases. An AMPS with three fluid phases provides enough interfaces to separate the three populations of erythrocytes required to distinguish the major subtypes of SCD (Hb SS and Hb SC), and allows to discriminate between HbAS and SCD. However, it does not distinguish between HbAA and HbAS. Dense red blood cells ($\rho > 1.120 \text{ g/cm}^3$) are characteristic of sickle cell disease, thus, the presence of red blood cells at the bottom of the tube indicates a positive test for SCD (figure 13) (35,85).

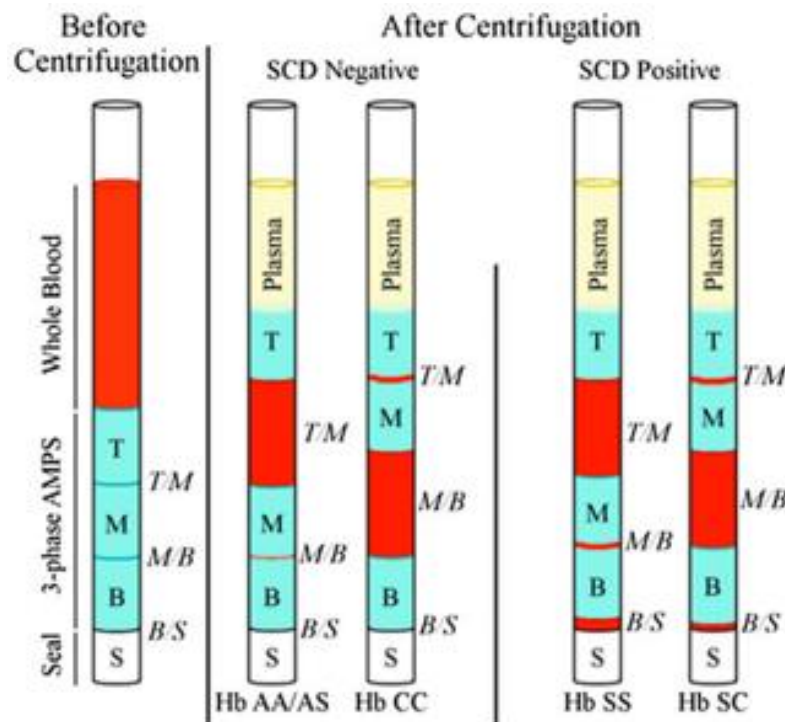


Figure 13: Schematic representation of the four most important outcomes of a density based rapid low-cost test for SCD.

Adapted from (85).

(c) The lateral flow immunoassay devices

Lateral flow assays are small devices useful in the POC settings, with potential large-scale screening utility in resource-limited settings. Among these, the Sickie SCAN from BioMedomix and the Hemotype SC from Silver Lake Research Corporation are commercially available (86). The Sickie SCAN uses polyclonal antibodies against HbS, HbC and HbA in the lateral flow chromatographic immunoassay. The sample migrates in the absorbent pads and the hemoglobin binds with the corresponding antibody attached on the test strip, producing blue lines (figure 14). It can detect normal hemoglobin (HbAA), the sickle cell trait (HbAS), the sickle cell anemia (HbSS), the hemoglobin C trait (HbAC) and the sickle cell-hemoglobin C disease (HbSC). It also demonstrated that it is not affected by the high concentration of HbF. It takes only a few minutes and costs a few dollars (35). The HemoTypeSC assay is based on competitive lateral flow immunochromatographic assay, which uses specific antibodies against Hb A, S and C in a test strip which collects 1.5 µl of blood. After the dried blood sample is diluted in a buffer is then placed in the test vial to migrate across the strip. The result is obtained in 20 minutes as red lines appear (figure 15). It can differentiate the normal Hb

AA, the sickle cell trait HbAS, the SCA HbSS, the C trait and the SC disease HbSC. However, it cannot detect HbF and HbA2, nor able to differentiate between HbSS and sickle- β 0-thalassemia; and it showed misinterpretation in patients who received blood transfusions recently (35).

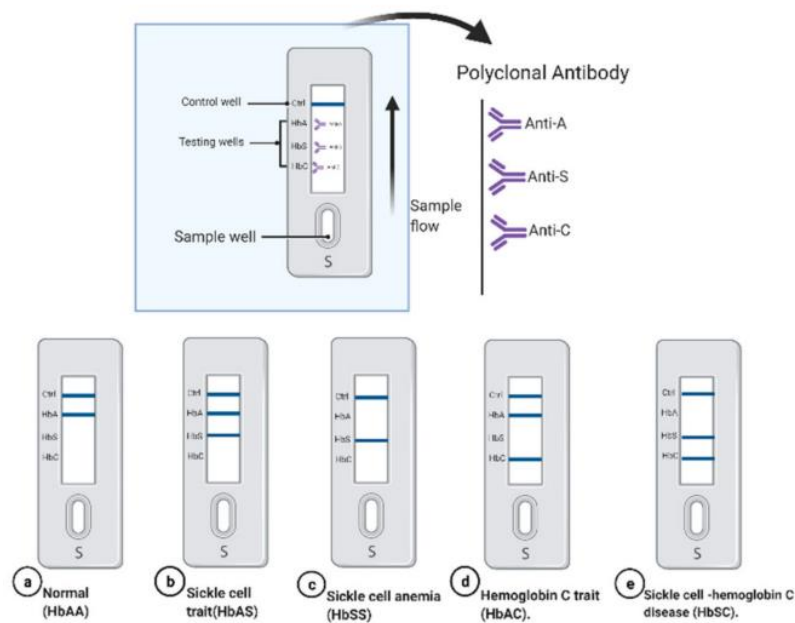


Figure 14: The Sickle SCAN based on lateral flow immunoassay to detect SCD.
Adapted from (35).

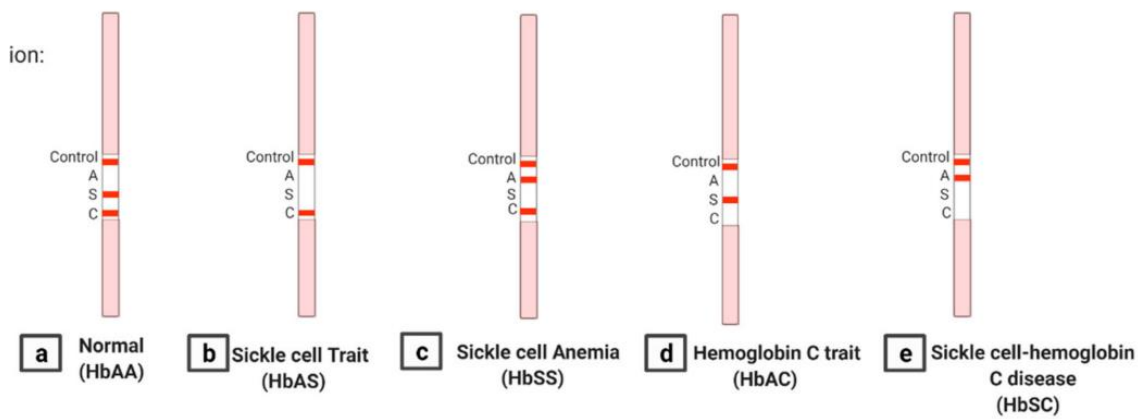


Figure 15: HemoTypeSC based on lateral flow immunoassay to detect SCD.
Adapted from (35).

(d) Spectral detection

This technique is based on the spectral analysis of biomolecular fluorescence of blood plasma and cellular components that have disproportionate concentration in SCA, functioning as indirect biomarkers of this disease. This include amino acids and coenzymes such as tyrosine, tryptophan, nicotinamide adenine dinucleotide (NADH), flavin adenine dinucleotide (FAD) and porphyrins (87). The lifetime of sickle RBC is reduced by 6-10 times compared to the normal, explaining the high concentration of bile pigments that lead to NADH consumption and FAD elevation (88). These can be identified and quantified by measuring the fluorescence emission peaks (figure 16) that function as fingerprints for each particular molecule (87). This innovative technique once made accurate and reliable could be applied to mass screening even in remote villages in the context of POC molecular-level diagnosis of SCA, since the instrumentation is compact (5kg), easily portable, and can be carried out with 5mL of blood in a time period of 10 minutes, conferring this method a simple and fast diagnostic protocol that processes an accuracy greater than 90% (87,88). However, more validation studies must be carried out to determine if this test is truly accurate enough to be applied in the field.

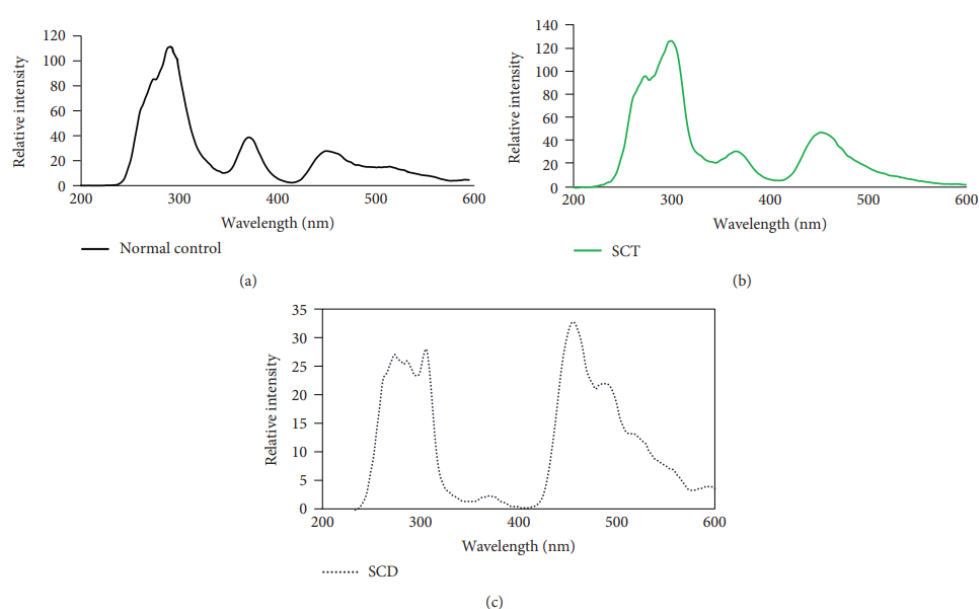


Figure 16: Synchronous fluorescence excitation spectra (SXS) of plasma from different subjects.

(a) The synchronous fluorescence excitation spectra (SXS) of normal plasma. The four peaks are at 275 nm due to tyrosine, at 290 nm due to tryptophan, at 360 nm due to NADH, and at 460 nm due to FAD. (b) The synchronous fluorescence excitation spectra (SXS) of SCT plasma. (c) The synchronous fluorescence excitation spectra of SCD plasma. Adapted from (87).

1.8.3. Tests for the definitive diagnosis of SCD

Currently, the gold standard approaches, validated for first-level neonatal screening and routine diagnosis include: (i) hemoglobin electrophoresis, (ii) high performance liquid chromatography (HPLC), (iii) isoelectric focusing (IEF) and (iv) genetic tests (86).

(i) Hemoglobin Electrophoresis

Electrophoresis is a chromatography technique based on the migration of electrically charged molecules under an applied electrical field. Different pH and mediums can be used to differentiate hemoglobin variants. Different hemoglobin types with different net charges migrate at different rates, resulting in stained bands with recognizable patterns unique to known hemoglobinopathies, which can be quantified by densitometric scanning. Cellulose acetate (CAC) electrophoresis at alkaline pH (8.4-8.6) is the standard method for the detection of the most common hemoglobin variants (35). At alkaline pH, Hb is a negatively charged protein which will migrate towards the anode (+) (figure 17). HbS has an additional positive charge compared to HbA, thus, it migrates more slowly. However, hemoglobins with same electrical charges show the same migration patterns, such as HbD and HbG which comigrate with HbS, whereas HbE has a similar migration to the HbC, enabling electrophoresis capacity to distinguish between these variants (35,89). Moreover, alkaline electrophoresis can be affected by the presence of large amounts of HbF in newborns, thus extra care should be taken to reliably detect HbS, making it necessary to use a more efficient test to overcome these limitations (35). Citrate agar (CAG) electrophoresis with an acidic pH (6.0-6.2) can effectively separate most hemoglobin variants that comigrate at alkaline pH and it is not affected by HbF in newborns (figure 18) (35). Capillary electrophoresis separates Hb fractions in an untreated fused-silica capillary support (35). It's capable of detecting HbA, HbF and separating the major hemoglobin variants, similarly to CAE at alkaline pH, but not identically because the pH is slightly different and the voltage is higher (89). Fully automated methods such as CAPILLARIS 2 system use capillaries in parallel, allowing multiple and simultaneous analysis, achieving fast separation and automation (35,90).

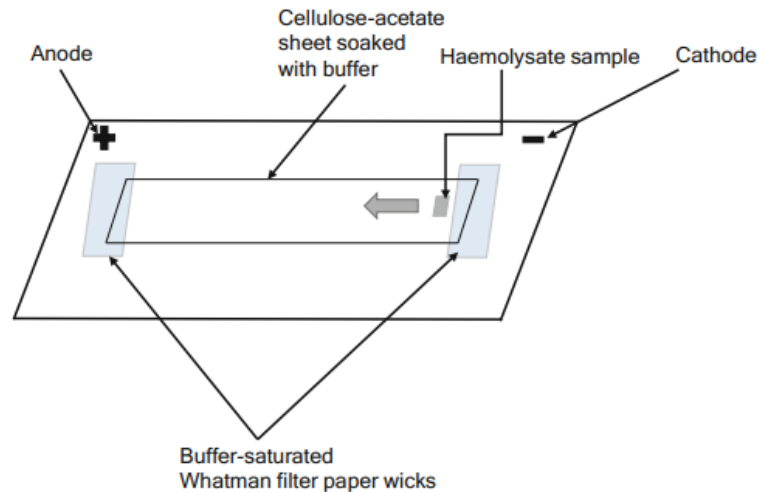


Figure 17: Schematic presentation of cellulose acetate electrophoresis.

The hemolysate is applied onto the marked area of strip on cathode (-) end and migrates towards the anode (+) end. Adapted from (91).

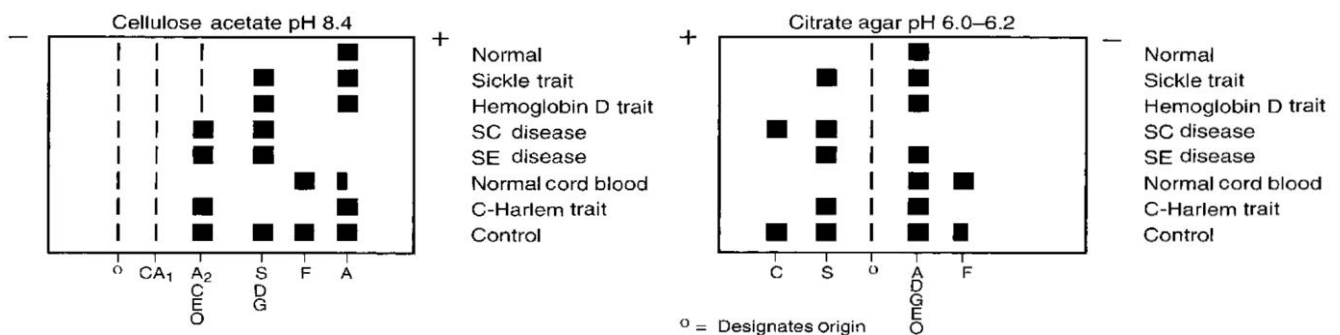


Figure 18: Relative mobilities of normal and variant Hbs measured by electrophoresis.

First panel is a cellulose acetate (CAC) electrophoresis at alkaline pH, second panel is a citrate agar (CAG) electrophoresis at acidic pH. Note that the relative amount of hemoglobins is not proportional to the size of the band; for example, in sickle cell trait (Hb AS), the bands may appear equal, but the amount of Hb A exceeds that of HbS. Adapted from (43).

(ii) High Performance Liquid Chromatography (HPLC)

Automated cation-exchange HPLC has been used for the analysis of globin and hemoglobin in research laboratories since the late 1970s and is increasingly being used as the initial diagnostic method in hemoglobinopathies (92). It is also used as the method of reference to quantitate HbA1c levels for monitoring of diabetic patients (43). This method separates hemoglobin types in a cation exchange column and only requires a very small amount of a blood sample (5µl), which is especially useful in pediatric work

(92). The hemolysate is introduced in a chromatography column containing negatively charged resin particles, thus, the hemoglobin molecules (positively charged) are adsorbed onto the resin and then eluted by passing prepared solutions with increasing concentrations of cations thorough the column (89). The elution rate, depends on the electrical affinity of the hemoglobin to the resin particles, allowing the separation of Hb molecules with different charges by ion exchange (89). The rate of elution is monitored with an ultraviolet/visible light detector and recorded on an integrating computer system, which analyzes the absorption peaks and gives the percentage of the fraction detected (89). HPLC detects different types of hemoglobin based on the retention time (elution time) and shape of the peak, which are compared with that of known Hbs. Since each Hb has a specific retention time (figure 19), it enables a highly accurate determination (35). It can detect and quantify HbF, HbA₂, HbS, HbC and other Hb variants, although, comigration of HbA and HbE occurs (43). It can differentiate between SCT and SCD giving a definitive SCD diagnostic, however, some Hb variants may co-elute with HbS leading to a misdiagnose of new variants that mimic HbS. Thus, a confirmatory test must be performed before giving a final diagnosis (35). In comparison with hemoglobin electrophoresis, it has fewer labor costs and the preparation and loading of samples can be undertaken by staff without scientific qualifications, nevertheless, the chromatogram must be always interpreted by experienced staff. Both capital and consumable costs are higher, but overall costs may be similar to those of Hb electrophoresis (89). It is also more reliable for monitoring patients under blood transfusion or hydroxyurea (35). Numerous automated HPLC systems are currently available which are useful in testing a large number of samples accurately, with better sensitivity in separation of Hb variants that electrophoresis (35).

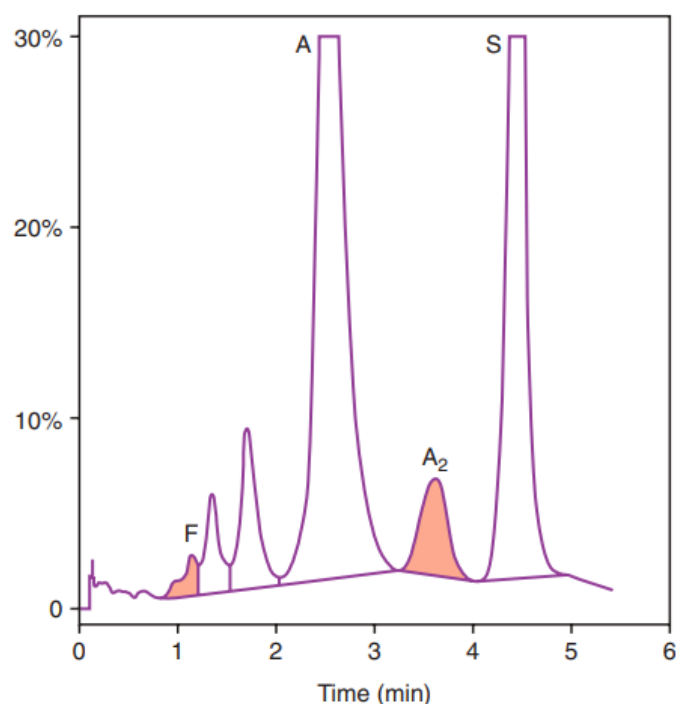


Figure 19: Ion-exchange high-performance liquid chromatography (HPLC) separation of hemoglobins.

Sample is from a patient with sickle cell trait demonstrating Hbs F, A, A₂, and an abnormal Hb in the S window. The retention time in minutes for each hemoglobin are 1.12, 2.48, 3.61 and 4.41, respectively (89). Adapted from (43).

(iii) Isoelectric focusing (IEF)

Isoelectric focusing (IEF) is a high-resolution electrophoretic technique that uses an electric current to push the hemoglobin molecules across a pH gradient until the migration stops and the hemoglobin molecules accumulate at their isoelectric position, where there is a net charge of zero (43). The precipitate of Hb molecules appears as sharp and narrow bands which allows a more precise and accurate quantification than electrophoresis. This technique can effectively separate molecules with isoelectric point differences of as little as 0.02 pH units (43). This sophisticated technique can detect HbS and HbA easily in a high concentration of HbF, in addition, it only requires a very small volume of sample and can be used with a dried blood spot, therefore, it is considered the standard test for newborn screening (35). It generally provides a result within 45 minutes. However, it is an expensive and complex technique that requires highly trained and experienced laboratory personnel to interpret the results (35).

It is also possible to combine the high resolution and specificity of identification of hemoglobins of the classical IEF, with the automation and quantification advantages of capillary electrophoresis instrumentation, naming this technique capillary isoelectric focusing (93).

(iv) Genetic tests

The precise detection of the various types of sickle cell disease requires a genetic study to detect the β -globin mutations involved. One of the most powerful diagnostic techniques is the polymerase chain reaction (PCR) which involves special enzymes for amplification of specific genetic materials. Several PCR-based techniques can detect β s mutations, such as the amplification-refractory mutation system (ARMS) which uses primers with specific sequences to allow the amplification of the DNA in the presence of the target allele, therefore, its detection is based on the presence of the PCR product. This technique has been used in prenatal diagnosis with fetal samples (35). Other existing methods are based on restriction enzymes which remove the recognition site at the β s mutated gene (35). DNA microarrays and sequencing techniques can also be carried out for whole-genome sequencing which allows identification of genetic modifications in the SCD severity. It even led to the creation of the Sickle Genome Project which is useful to study the association of SCD phenotypes with common genetic modifiers such as BCL11A, allowing the discovery of new treatments (35).

1.8.4. Other tests/methods in development

Innovative techniques which are mostly still in the research stage include:

(i) Image Processing Techniques that analyze different features of RBCs such as cell shape, with developed learning models being able to determine and categorize them in round shape (normal cells), elongated shape (sickle cells) and other blood shapes, as well as quantifying them. These techniques can even be combined with a smartphone microscope for the conception of an affordable, portable, and rapid screening test for the SCD. This automated interpretation of the blood cell images can minimize errors, providing more effectiveness of patient monitoring (35).

(ii) Flow Cytometry techniques can be used to detect sickle cells based on fluorescent markers or cell morphology. Imaging flow cytometry assays combined with an algorithm software to distinguish between sickle and normal cells based on their morphology can enhance the sensitivity of this method. Microfluidic flow cytometry can also be employed for the detection of changes in the electrical impedance resulting from the change in the cells' shape, measured with spectroscopy. However, this novel flow cytometry techniques are not yet validated to be used in monitorization of disease severity nor to distinguish between the SCT and SCD (35).

(iii) Mechanical differentiation of sickle cells which is based on the deformability of RBCs can be used to detect sickle cells which are mechanically fragile and poorly deformable, leading to impaired blood flow (35).

1.8.5. Neonatal and prenatal screening techniques

Neonatal screening requires a sophisticated approach with very sensitive and highly specific techniques such as high-performance liquid chromatography (HPLC), capillary electrophoresis (CE), and isoelectric focusing (IEF), which have been proven to be suitable methods. A multisystem approach is often needed to distinguish the various hemoglobin variants. Laboratories use two or more techniques to improve this identification. (43). An abnormal result with the first line method is repeated using a secondary method. The material used can be fresh cord blood spot or a dried blood spot from a heel prick. It is important to consider that newborn samples mainly contain HbF and a smaller amount of HbA, depending on gestational age, and thus reflecting the stage of hemoglobin switch. Therefore, premature babies, and babies who received blood transfusions might be a source for false negative and false positive results, respectively (94). To standardize quantitative interpretation of screening results, cut-offs and ratios (HbA/HbS, HbA/HbF) can be employed and often expressed as multiples of median (94).

The importance of newborn screening programs relies on the fact this disease can lead to life-threatening events on early childhood, making early diagnosis crucial for establish preventive measures such as prophylactic penicillin, vaccination, and parent education

(94). In Portugal, a pilot study to include the sickle cell disease in the *Programa Nacional de Rastreio Neonatal* (PNRN) begun in May 2021, in the districts of Setúbal and Lisboa, providing data that revealed a positive case per 944 newborns. In February 2022 this study was extended to the whole country with the goal of screening 100 000 newborns in a period of 2 years to assess the real necessity of including the sickle cell disease in the PNRN (95).

Newborn screening programs may also detect carriers of Hb variants providing reproductive information for those individuals. As this disease carries an important burden for individuals and families, preventive actions may be demanded. In this context, prenatal diagnosis also assumes a major role allowing an informed decision-making regarding hemoglobinopathies (94). In Portugal, a prenatal screening program is carried out in all women in fertile age, preferably in preconception consultation or the most precocial during pregnancy. This program targets areas with most prevalence in the country including the districts of Beja, Évora, Faro, Leiria, Lisboa, Santarém and Setúbal, as well as areas with most emigrants from regions with high prevalence such as African countries, India subcontinent, Timor, and Brazil. An Hb electrophoresis and quantification through HPLC is recommended. If a carrier state is identified, the partner must be studied as well. In case of both parents are carriers or one possesses the disease and the other possesses another hemoglobinopathy, they may be offered genetic counselling and/or proposed for a fetal study in case of pregnancy to provide the families with an informed decision (75).

1.8.6. Comparison of the different diagnostic methods for SCD

With multiple methods available for the diagnosis of SCD, the choice of methodology and equipment must be based on the framework for diagnosis, local availability, cost, ease of handling, required skilled personnel and volume of workload. All methods have advantages and disadvantages that must be considered (table 5).

The more definitive diagnostic laboratory methods include hemoglobin electrophoresis, capillary electrophoresis (CE), high-performance liquid chromatography (HPLC) and isoelectric focusing. These methods are very sensitive and highly specific, being even

suitable for neonatal screening programs. Universal screening programs or targeted to populations at risk are the headstone of prevention and early diagnosis of SCD. However, the aforementioned methods require a substantial financial investment, from the availability of electricity to the adherence to strict laboratory standards and requirement of trained technicians (86). Therefore, implementing these sophisticated techniques is not feasible in resource-limited settings, like most of sub-Saharan-Africa, with most of the cases of SCD worldwide. Lack of diagnosis and early intervention are the major factors contributing to high mortality. Thus, screening techniques in developing countries must be fast, inexpensive, reliable, and applicable for many samples. Multiple solutions have been developed for point-of-care settings, but these must be perfected to acquire better sensitivity and must be further distributed worldwide with potential to facilitate universal screening in resource-limited settings (74).

On the other hand, techniques for monitoring the disease, either for (i) prediction of vaso-occlusive crisis and evaluation of the disease severity, (ii) for evaluating the response of certain treatments and follow-up, or even to (iii) study new therapy approaches have different and more complex requirements compared to diagnosis. Some of these techniques are still highly experimental and lack validation of efficacy. However, this field of investigation is promising as it might become very useful in clinical trial designs of emerging therapies.

Lastly, it is important to reinforce that an ideal diagnostic method which fulfills all desired characteristics is still lacking. A test which would provide: a definitive diagnosis, be fast, be cost-effective, applicable for screening programs in POC settings, highly accurate and suitable for patient monitoring and prediction of crisis.

Table 5: Comparison of the principal diagnostic methods for SCD.

Technique	Sensitivity	Specificity	Advantages	Disadvantages
Sickling test	65,0%	95,6%	Simple preparation. Inexpensive. Fast results.	Relies on human interpretation. Does not differentiate between different types of SCD. Does not provide definitive diagnosis. Cannot be used for newborn screening.
Solubility sickling test	45,0%	90,0%	Easy to perform and interpret. Relatively fast. Requires minimal reagents cheaply prepared.	Short shelf-life of the reagents, requiring regular restocking and storage. Does not differentiate between different types of SCD. Does not provide definitive diagnosis. Cannot be used for newborn screening.
Paper-based Hb solubility test	94,2%	97,7%	Simple, rapid, inexpensive, does not need trained personal.	Difficult to distinguish HbAS (trait) from HbSC, humidity can affect the test result.
Sickle SCAN	90%	100%	Simple, rapid.	Relies on polyclonal antibody, low sensitivity and cross reactivity, qualitative test, the intensity of band shows inconsistency, does not identify hemoglobin F, limit of detection of Hb A is 2%.
HemoTypeSC	93,4%	99,9%	Cost-effective, rapid.	Cannot detect all hemoglobin variants, does not differentiate between HbSS and sickle- β 0-thalassemia, misinterpretation of the result in cases with recent blood transfusion.
Hemoglobin Electrophoresis	~100%	~100%	Simple to operate. Semi-quantitative.	Limited resolution. Difficulty of automation. Unresolved diagnosis. Inaccurate in the quantifications of low-concentration Hb variants.
Capillary electrophoresis	~100%	~100%	Reliable, ability to distinguish most types of sickle cell disease including heterozygous.	Expensive, requires skilled technicians.
High Performance Liquid Chromatography (HPLC)	~100%	~100%	Reliable, ability to distinguish most types of sickle cell disease including heterozygous. Fully automated, requires small volumes of sample. Ideal for a routine clinical laboratory with high work load.	Misdiagnoses the new variants that mimic HbS, Expensive and needs trained personnel. Not practical in limited resources areas.
Isoelectric focusing (IEF)	~100%	~100%	Detect HbS and HbA easily in a high concentration of HbF. Hb D-Punjab easily separated from HbS. Requires a small volume of the sample, able to use dried blood spot.	High cost and labor-intensive. Requires specialized reagents and highly trained staff to interpret the results.

Table 5: Comparison of the principal diagnostic methods for SCD (continued).

Technique	Result	Applicability	Turnaround time (TAT)	Cost
Sickling test	Detection of sickle cells.	Screening technique. Useful in an urgent need for diagnosis.	38 minutes.	\$0.33 per test.
Solubility sickling test	Detection of the sickling event.	Screening technique. May be employed in POC settings.	70 minutes.	\$0.60 per test.
Paper-based Hb solubility test	Diagnosis of HbSS.	POC settings.	20 minutes.	\$0.77 per test.
Sickle SCAN	Identification of HbC and HbS.	Large-scale screening utility.	2 minutes.	\$5–10 per test (commercial costs).
HemoTypeSC	Identification of HbAA, HbAS, HbAC, HbSC, and HbCC.	POC settings.	20 minutes.	\$0.25 for the materials used for the fabrication of this assay.
Hemoglobin Electrophoresis	Detection of the most common hemoglobin variants.	Definitive diagnosis in advanced laboratories.	70 minutes for CAC. 90 minutes for CAG.	Equipment cost of about \$2500 (\$5.76 for CAC plates and \$18 for CAG plates)
Capillary electrophoresis	Identification and quantification HbF, Hb A, Hb A2, Hb S, Hb C, Hb Barts and other.	Definitive diagnosis in advanced laboratories. Newborn screening programs.	Data not found.	Data not found.
High Performance Liquid Chromatography (HPLC)	Detect Hb F, Hb A2, Hb S, Hb C, Hb Barts, and other Hb variants.	Definitive diagnosis in advanced laboratories. Newborn screening programs.	3-4 minutes.	Equipment cost of about \$30000.
Isoelectric focusing (IEF)	Identification of Hb A, Hb F, Hb C, Hb S, Hb E and Hb O Arab	Definitive diagnosis in advanced laboratories. Newborn screening programs.	45 minutes	Equipment cost of about \$4000.

Adapted from (35), (74), (96) and (97).

1.9. A novel and simple method based on depolarization

Depolarization measurements may be used in several parts in the hematology laboratory, although they were mainly incorporated into the automated hematology analyzers (Abbott Cell Dyn© series) to distinguish eosinophils from other neutrophils due to their depolarizing granules (98). By chance it was observed that hemozoin-containing monocytes could also be detected in malaria patients, an observation later extended to hemozoin-containing Plasmodium-parasitized RBCs. In fact, depolarization microscopy had already been described as a method to detect these highly birefringent particles (99).

Interestingly, studies reported that some animal RBCs contain types of Hb which depolarizes light (100) as well as HbS in humans (47). These publications came accompanied by images of depolarizing HbS (figure 20, B). Observing a routine sickling test with a microscope with crossed polarizers showed that many RBCs, especially those in sickled shape showed clumps of highly depolarizing Hb (figure 20, D).

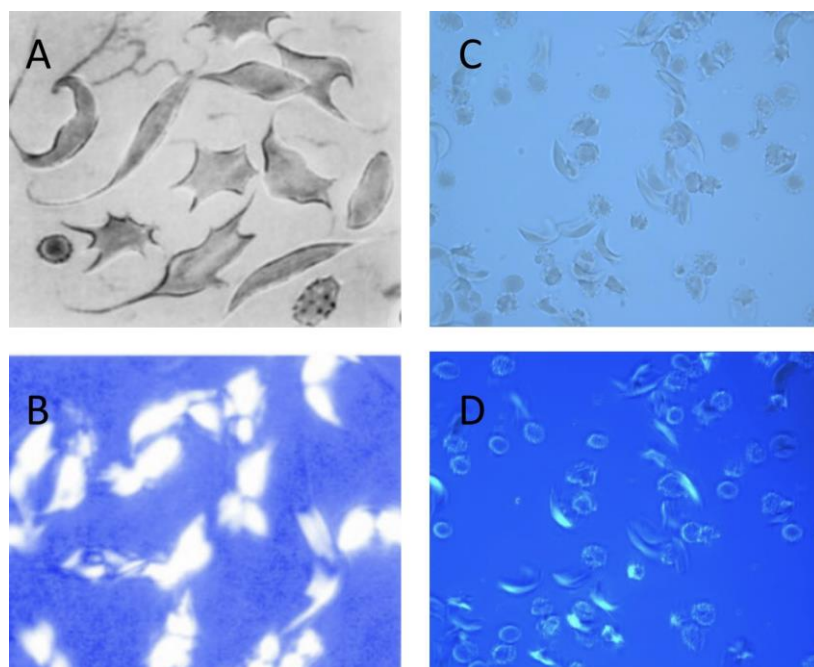


Figure 20: Microscopic images of sickled HbSS-RBCs.

Representative images of sickled RBCs from blood of a HbSS patient. Panels A and C show bright field microscopic images, panels B and D under crossed polarizers. The polymerized HbS depolarizes strongly in C and D. A and B from (47) 1000x, C and D images from the research laboratory (400x).

1.10. The idea for the research project

Previous reports suggested that not all RBCs containing polymerized HbS show a typical sickle form, but that several morphological forms might be observed (47). The closer observation of some sickle tests in the research laboratory also seemed to show that many more RBCs showed depolarization and not only those which had a sickle shape (figure 20, C and D). Apart from deoxygenation related factors, these observations also seemed to be in line with the fact that the HbS levels (measured by HPLC) correlate poorly with the percentage of sickled RBCs. A preliminary experiment also showed that depolarization became evident before RBCs would show a typical sickle shape.

Consequently, the idea was born to systematically investigate these findings and try to establish if measuring the effect of depolarization in RBC from SCD patients would be a possible indicator of this disease, might be closer related to the level of HbS, and perhaps quicker and easier to assess.

2. Aims and objectives

The aim of this study was to establish if depolarization measurements using a simple microscopic set-up could be an indicator for this disease, might be closer related to the level of HbS, and perhaps might be quicker and easier to assess.

To achieve this goal, this study had three objectives:

(i) Obtain blood samples from SCD patients with different levels of HbS and perform a sickle cell test to be observed by conventional microscopy and using crossed polarizers.

(ii) To establish time curves for the depolarization effect and compare quantitatively RBC populations observed by optical microscopy (using photographic images) and polarization microscopy, as well as their correlation to the known HbS levels (in %).

(iii) To ascertain if a drug effect on sickling, such as the inhibiting effect on polymerization by voxelotor, could be easily and better detected using depolarization measurements.

3. Methods

The study was carried out at the Centro Académico de Medicina de Lisboa. All experimental work was carried out in the Instituto de Microbiologia da FMUL.

3.1. Study populations and samples

EDTA-anticoagulated blood samples were obtained from HbSS SCD patients who had their Hb levels determined in the Serviço de Patologia Clínica do CHULN. Only “left-over” blood, which was about to be discarded, was used after all routine analysis had been successfully completed. A small sample of around 250-500 μL was kept at 4°C. All samples had been anonymized and only contained the information of the HbS level in (%). Samples were collected whenever available and used for research in this study. Ethical approval was obtained (see point 3.6.). Based on the number of weekly samples the objective was to obtain a total of around (n=50) samples.

3.2. Reagents and equipment

Reagents: Sodium metabisulfite ($\text{Na}_2\text{O}_5\text{S}_2$) was kindly provided by the Serviço de Patologia Clínica do CHULN. White solid paraffin used for histology was kindly provided by the Comparative Pathology Unit at IMM (CAML). Dimethyl sulfoxide (DMSO), Glucose and PBS were obtained from Sigma-Aldrich, Lisboa, Portugal. Voxelotor was purchased from Quimigen, Alverca, Portugal. Ultra-pure grade water from a MilliQ purifier was used. Common microscopic glass slides and 20x20mm coverslips were used.

Equipment: A *Leica* microscope (DM2800) was used, which was equipped with crossed polarizers (figure 21). Photographs were taken using the Leica DFC480 digital camera with the Leica FireCam 3.4.1 software (Leica Microsystems, Milton Keynes, United Kingdom).

Image-analysis: Images were manually analyzed by counting cells in the ImageJ program (Windows PC, IE 6.0, Microsoft Java 1.1.4.). Automatic image analysis was attempted for some images using opensource image software (Fiji/ImageJ2, version 2.9.0/1.53t).

Data-analysis: Data were entered into a spreadsheet and analyzed with Microsoft Excel (Office 16).

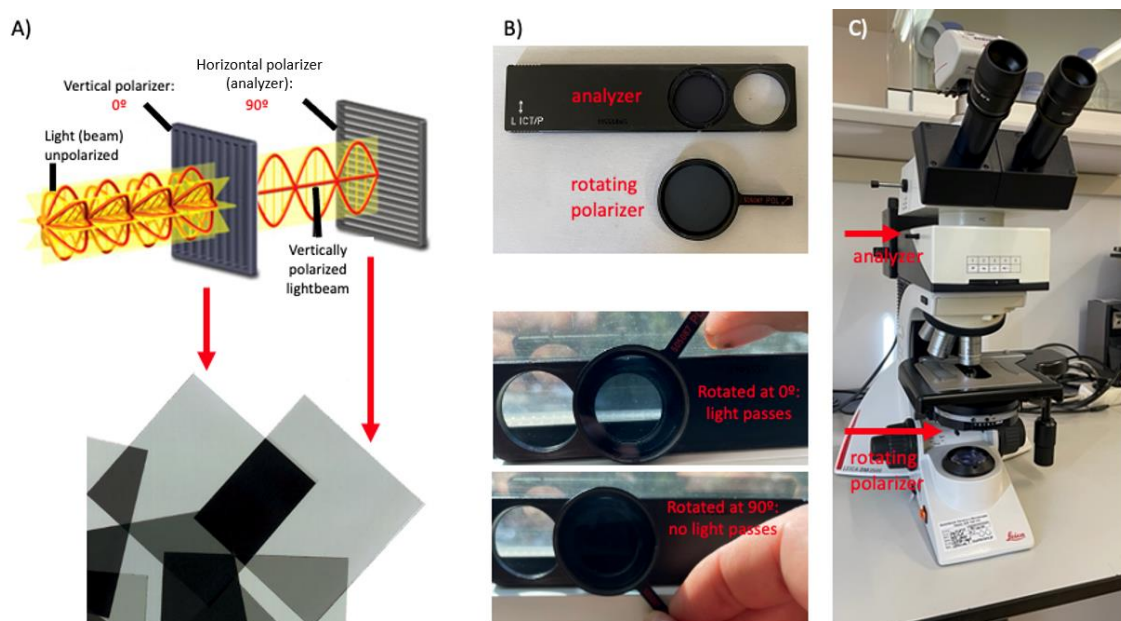


Figure 21: Principles of polarized microscopy.

Unpolarized light is polarized with a linear (rotating) polarizer at 0° (A). When a second polarizer (analyzer) is placed perpendicular at 90° the polarized light does not pass (A, B). Position of polarizer and analyzer in the microscope (C). If a substance in a sample, placed between both polarizers, turns the polarized light beam (depolarization) this substance becomes visible on a dark background (see figure 20).

3.3. Procedures

Sickle cell test (figure 22): For each test a fresh solution of Metabisulfite (200mg) in 10mL of ultra-pure water was prepared in order to achieve a concentration of 0,02 g/mL. A drop (μL) of EDTA-anticoagulated blood and a drop (20 μL) of metabisulfite were mixed on a microscopic glass slide and covered under a coverslip avoiding air-inclusions (bubbles). Molten paraffin (heated on a common laboratory electric hotplate at 100°C) was applied with a fine, flat brush to the edges of the coverslip, with the objective to seal the blood/metabisulfite sample airtight. The glass slides were then placed in a 37°C incubator. All samples were observed after an overnight incubation with the objective to produce maximum deoxygenation and consequently, maximum sickling. The time point for observation of all samples ($n=51$) was 24h. Of those, 6 samples were also observed after only 1h of incubation for comparison and establishment of a time evolution of events (sickling and depolarization) experiment with 2 time points (1h and 24h of incubation upon the sickling test).

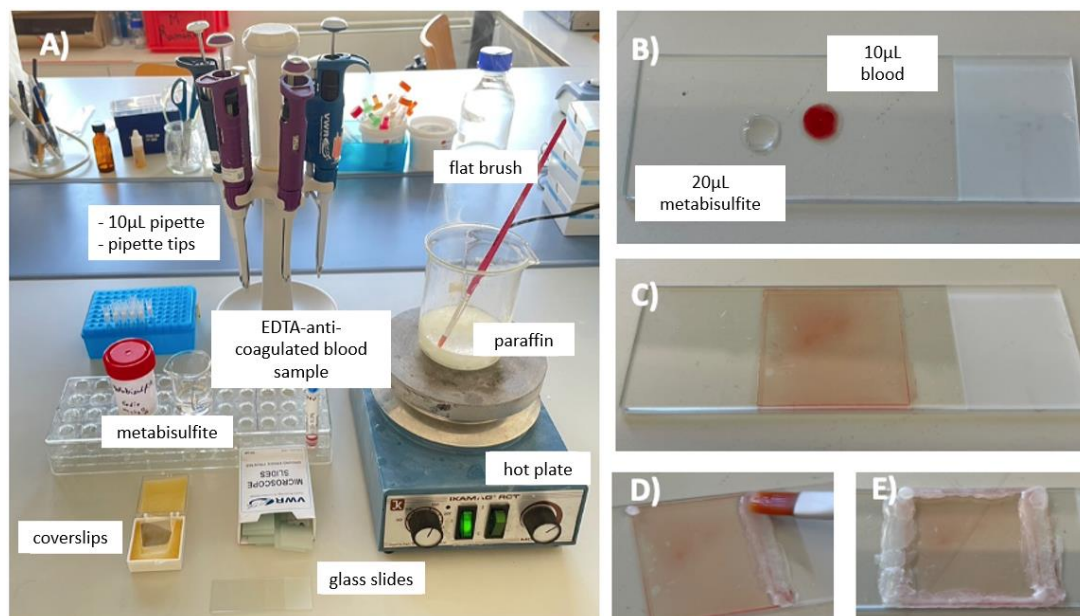


Figure 22: Procedure of the sickle cell test.

The 5 panels show the steps in the sickle cell test: (A) necessary materials; (B) blood is mixed with metabisulfite in a 1:2 ratio; (C) a coverslip is placed; (D) molten paraffin is used to seal the coverslip borders; (E) sealed sample, then incubated at 37°C.

Drug-experiment (inhibition of polymerization by voxelotor): Voxelotor was dissolved in 100% DMSO for a concentration of 10µM (working solution). RBCs with 85% HbS were used for the experiments. Previous work describes the use of a 1:1000 dilution of RBCs and a voxelotor concentration of 30µM (101). A final dilution of RBCs of 1:200 was used by adding 10µL of blood to a tube with a total of 2mL of either: (i) 190µL of a 20% glucose solution added to 1800 µL PBS and 10µL of the voxelotor working solution (final concentration: 50µM voxelotor), or (ii) 20 µL of 20% glucose only added to 1800µL PBS (control). The tubes were incubated for 30 min at 37°C. After centrifugation at 800g for 5 minutes the supernatant was discarded, and the RBC resuspended in 20mL homologous EDTA plasma. This suspension was then used to perform the sickle test as described. The samples were examined by microscopy after 3h incubation at 37°C.

Microscopic observation and image acquisition: The sickle cell test was observed under bright-field conditions using a 40x objective to assess the quality of the test (to exclude extensive lysis, for example). Then they were observed using a 100x oil-immersion objective. Ten random microscopic fields were photographed using bright-field and crossed polarizers for each field. Settings for the image acquisition were set before (saved) and applied for all image acquisitions (figure 23).

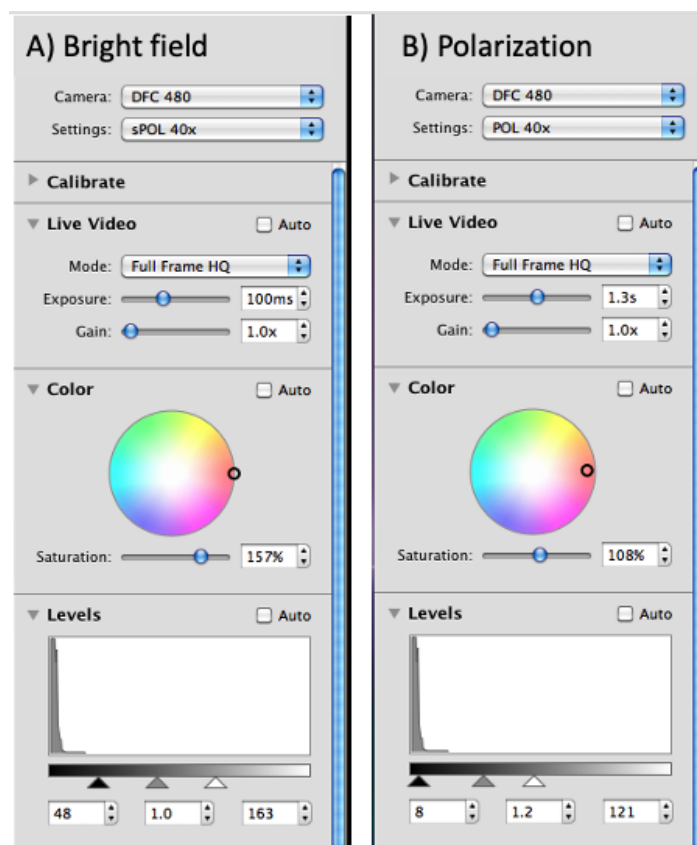


Figure 23: Settings for image acquisitions (bright-field and crossed polarizers).

Panel (A) shows the settings for bright-field microscopy while panel (B) shows the settings for crossed polarizers. Note that all settings were manual and thus constant.

3.4. Image analysis

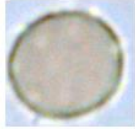
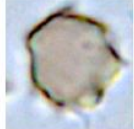



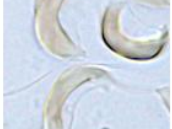
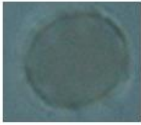
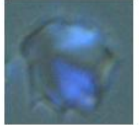


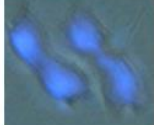
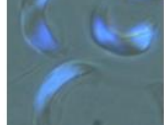
Manual image analysis: From each sample 1-3 images were systematically analyzed to acquire a total cell counting of at least 100. The number of RBCs in each respective category as shown in table 6 were manually counted in each bright-field and crossed-polarizer image. Examples of each cell category are presented in table 7. To avoid mistakes (double counting/omission), counting was performed using the program Image J where clicking the cursor on each RBCs produces a numbered, colored dot. Each category had an attributed code number in the program (table 6). To assure these categories lead to consistent counts, some images (n=5) were recounted blindly.

Table 6: Categories for the different cell shapes with respective code number.

Number	Category / Cell description	Microscopy technique	Depolarization properties
0	Normal round RBC	Polarized (POL)	Bright
1	Normal round RBC	Polarized	Dark
2	Granular round RBC	Polarized	Bright
3	Granular round RBC	Polarized	Dark
4	Spiculated RBC	Polarized	Bright
5	Spiculated RBC	Polarized	Dark
6	Flattened RBC	Polarized	Bright
7	Flattened RBC	Polarized	Dark
8	Elongated RBC	Polarized	Bright
9	Elongated RBC	Polarized	Dark
10	Sickled RBC	Polarized	Bright
11	Sickled RBC	Polarized	Dark
12	Normal round RBC	Optical (OP)	Bright
13	Normal round RBC	Optical	Dark
14	Granular round RBC	Optical	Bright
15	Granular round RBC	Optical	Dark
16	Spiculated RBC	Optical	Bright
17	Spiculated RBC	Optical	Dark
18	Flattened RBC	Optical	Bright
19	Flattened RBC	Optical	Dark
20	Elongated RBC	Optical	Bright
21	Elongated RBC	Optical	Dark
22	Sickle RBC	Optical	Bright
23	Sickle RBC	Optical	Dark

Note that all even numbers correspond to depolarizing cells (bright cells), whereas all odd numbers correspond to non-depolarizing cells (dark cells). Although no bright cells were expected to be found using optical microscopy, categories 12, 14, 16, 18, 20 and 22 were still created to serve as control. See table 7 for representative images of each category.

Table 7: Representative images of RBC for classification.

Normal round RBC	Granular round RBC	Spiculated RBC	Flattened RBC	Elongated RBC	Sickle RBC
					
					

Top panel shows images of typical RBCs used for classifying them in optical microscopy. Bottom panel shows images of typical RBCs used for classifying them in polarized light microscopy. Note that each category in optical microscopy may or may not depolarize.

Automatic image analysis using Fiji/ImageJ2: Images obtained with crossed polarizers (showing depolarizing HbS polymers) were analyzed with the Fiji/ImageJ2 open-source software (version: 2.9.0/1.53t) (<https://imagej.net/software/fiji/downloads>). The obtained photographic images were in JPEG format, with 2560 x 1920 pixels (72 pixels / inch), in RGB (red, green blue, https://en.wikipedia.org/wiki/RGB_color_model). RGB pixels are converted to brightness values using the formula $V=(R+G+B)/3$ (<https://imagej.nih.gov/ij/docs/menus/analyze.html#sum>).

The settings in the respective pop-up windows in Fiji/ImageJ2 are shown in figure 24. The analysis included five major steps (figure 24 – A, B, C, D).

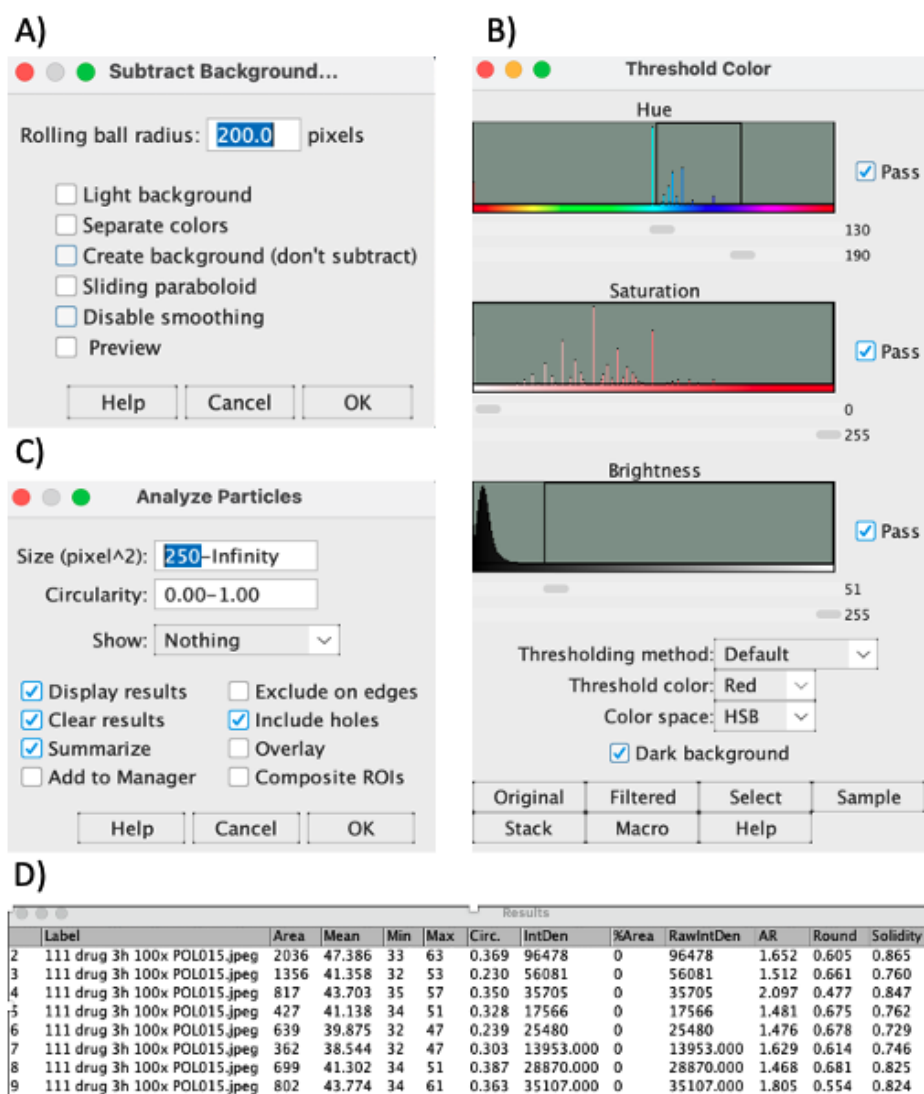


Figure 24: Steps and settings in Fiji/ImageJ for automatic analysis.

The image was opened in Fiji/ImageJ2. The background was subtracted by using from the menu: Process>Subtract Background. In the pop-up window a rolling ball radius 200 pixels was chosen (A). Then from the menu Image>Adjust>Color Threshold was selected. In the pop-up window the flowing parameters were selected. Hue: only blue from 130 – 190, Saturation: from 0-255, Brightness: from 51 – 255 (B). Then from the menu Analyze>Analyze Particles was selected. In the pop-up window the flowing parameters were selected. Size (pixel): 250-infinity, Circularity: 0-1, Show: Overlay Masks (C). Finally, the analysis produced a list mode (D) which was exported to Excel (Microsoft) where summary, descriptive statistics were calculated, and histograms created using the analysis ToolPak.

3.5. Data analysis and statistics

Data was first analyzed with standard descriptive statistics (mean, standard deviation, median, percentiles, skewness). Scatter plots were created to analyze the distribution pattern and as a basis for correlation analysis. Correlations were analyzed by calculating Pearson's correlation coefficients and respective P-values using the online programs below:

- <https://www.socscistatistics.com/tests/pearson/default2.aspx>
- <https://www.socscistatistics.com/pvalues/pearsondistribution.aspx>
(accessed on 30/04/2023)

Results from the automated image analysis of the drug-experiment were analyzed using the Mann-Whitney U Test for non-normally distributed samples.

3.6. Ethics

This research project was approved by the ethics committee of the CAML/CHULN (Nº 1153/13). All samples were processed only after they had been anonymized in the hospital laboratory and the investigators had no access to any patient information. The study did not produce any relevant novel information of any clinical value. All investigators were trained in handling blood under Category 2 Laboratory Safety standards.

4. Results

4.1. Sample characteristics

A total of 51 samples were obtained for this study. Figure 25 shows the frequency of HbS distribution of the samples, with intervals (bins) of 5%. The minimum percentage of HbS was 26,9% whereas the maximum was 93%.

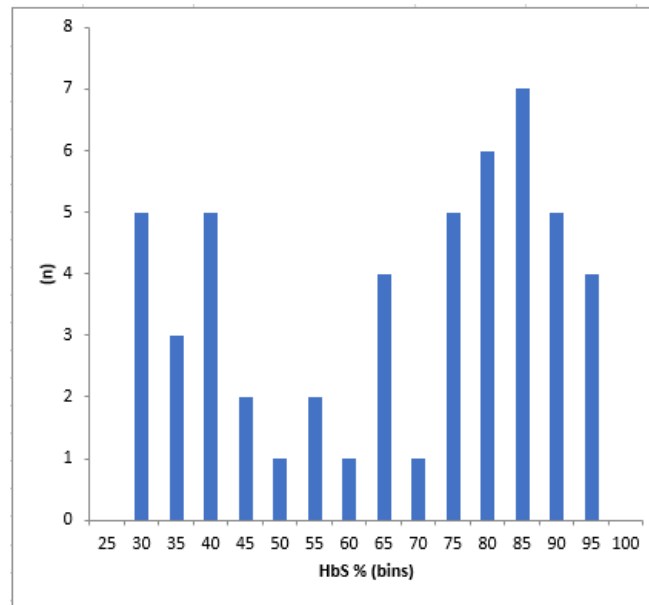


Figure 25: Distribution of the percentage of HbS in each sample (HbS %).

The samples could not be processed immediately after collection and were prepared for analysis at different time intervals after blood collection (figure 26). The maximum of this interval was 17 days for n=3 samples.

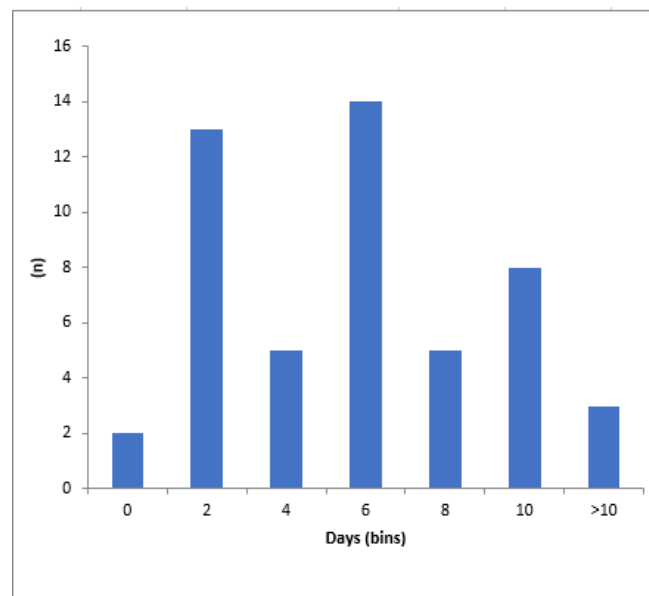


Figure 26: Distribution of time-intervals (days) from collection to processing.

4.2. Sickling and depolarization at two different time points (1h and 24h)

Six samples, used to investigate the time effects of the sickle cell test, show comparable results for depolarization after 1h and 24h of incubation (figure 27, red areas).

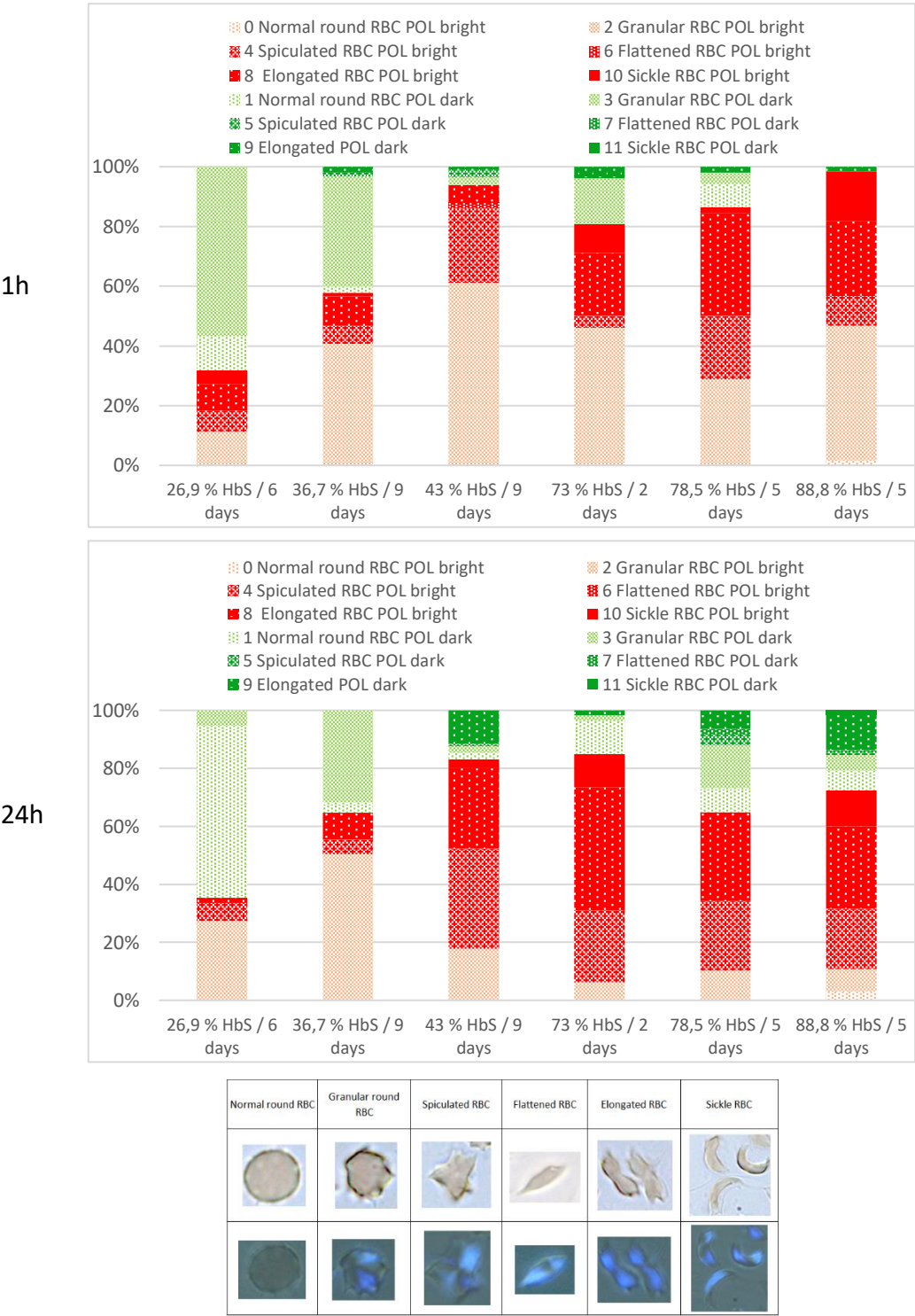


Figure 27: Sickle cell test after 1h (top) and 24h (bottom) of incubation. Cells were classified according to table 7 (shown below graph for reference). Green are non-polarizing RBCs (top part of table), and red are polarizing RBCs (bottom part of table). Note variation in the shape of the RBCs.

4.3. Optical microscopy observations

The 51 samples were observed with an optical microscope, allowing the determination of the different cell categories (table 7) and the proportion (%) in each sample is shown in figure 28.

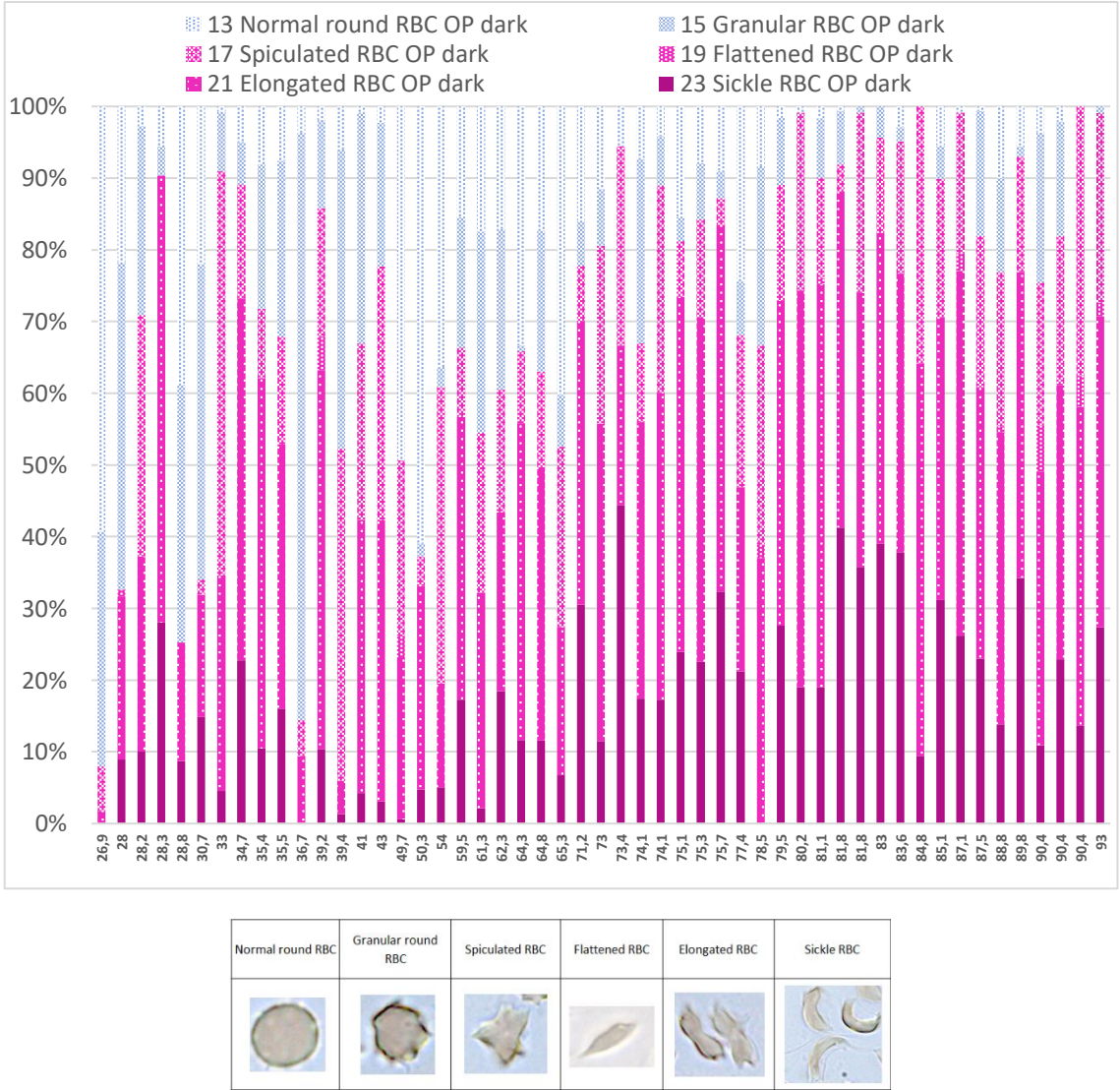
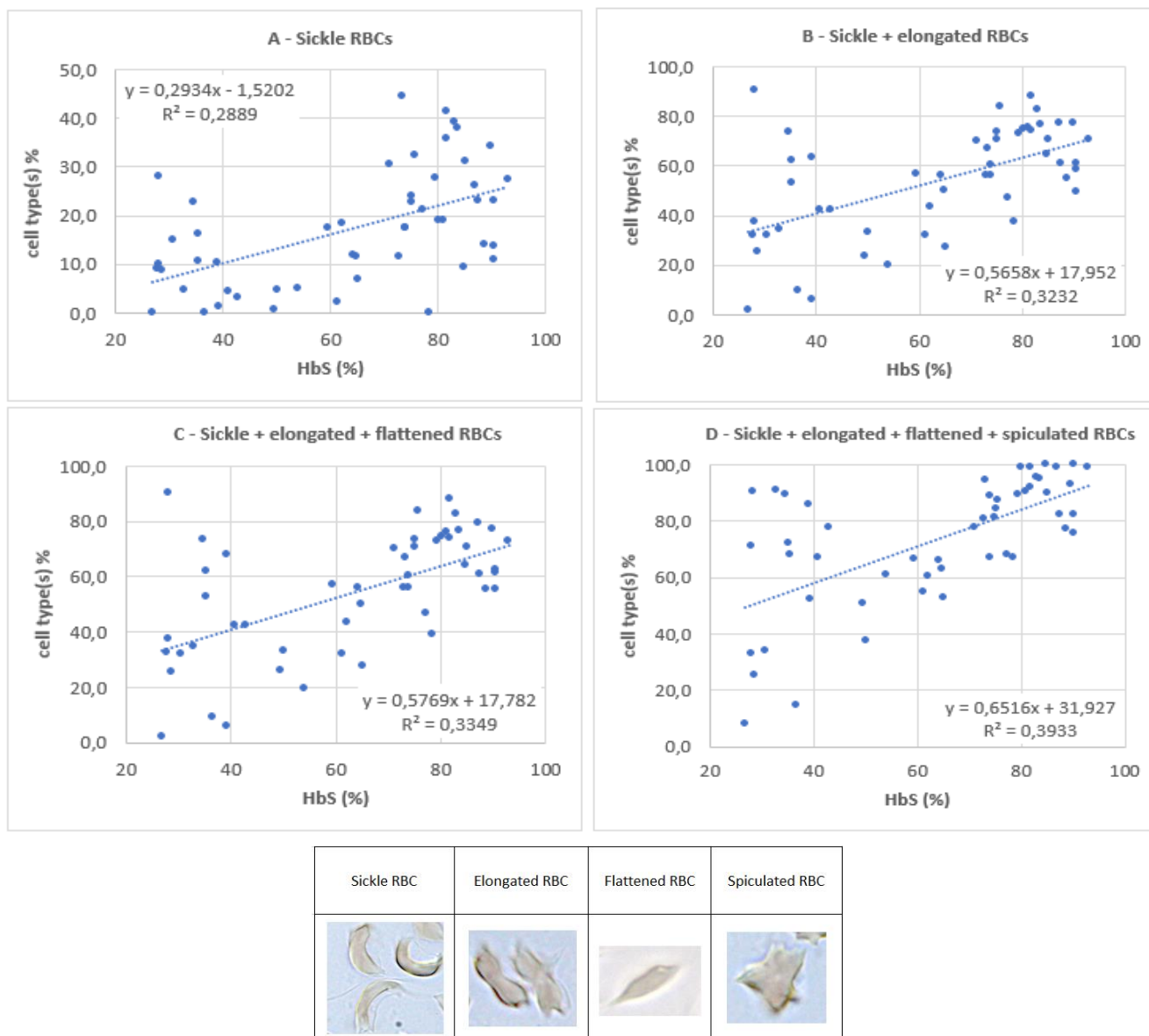


Figure 28: Cell types observed with optical microscopy. Percentage of each cell type (top part of table 7 with cell types shown below graph for reference) per sample. OP: optical microscopy, dark: no depolarization. X-axis: HbS in %.

The distribution of the different cell categories was plotted versus the percentage of HbS (%) and a correlation was calculated (figure 29). Four different distributions were analyzed with increasing number of deformed cells: (i) only sickle RBCs (figure 29, A), (ii) both, sickle RBCs and elongated RBCs (figure 29, B), adding flattened RBCs (figure 29, C), and finally adding spiculated RBCs (figure 29, D).



Cell types	R ²	R	p-value
A – HbS (%) and sickle RBCs (%)	0,29	0,54	<0,001
B – HbS (%) and sickle + elongated RBCs (%)	0,32	0,57	<0,001
C – HbS (%) and sickle + elongated + flattened RBCs (%)	0,33	0,58	<0,001
D – HbS (%) and sickle + elongated + flattened + spiculated RBCs (%)	0,39	0,63	<0,001

Figure 29: Correlation between HbS (%) and deformed RBCs in optical microscopy.

Plots of HbS (%) versus increasing types of deformed RBCs and respective correlation (R^2 and R). All combinations show a moderate correlation (R) – see text for details. RBC images from table 7 for reference below graph.

R^2 : Coefficient of determination - proportion of the variation in the dependent variable (cell types) that is predictable from the independent variable (HbS).

R : Pearson correlation coefficient - measure of linear correlation with respective P-value.

Interpretation of Pearson's correlation coefficient (R): 0-0.1: none, 0.1-0.39: weak, 0.4-0.69: moderate, 0.7-0.89: strong, 0.9-1: very strong. Adapted from (102).

All combinations in figure 29 show a moderate correlation (R). Squaring the Pearson’s coefficient produces the “coefficient of determination” (R^2) which can vary between 0 and 1 and provides information about the amount of variance shared by the correlated variables. In figure 29, the Pearson’s coefficient (R) gradually augments until it reaches a moderate correlation of 0.63 between HbS (%) and all four deformed cells (sickled RBCs + elongated RBCs + flattened RBCs + spiculated RBCs) (%). These were the categories selected for the analysis presented below when referring to deformed RBCs.

4.4. Polarization microscopy observations

The different cell categories observed with polarization microscopy, are shown in figure 30.

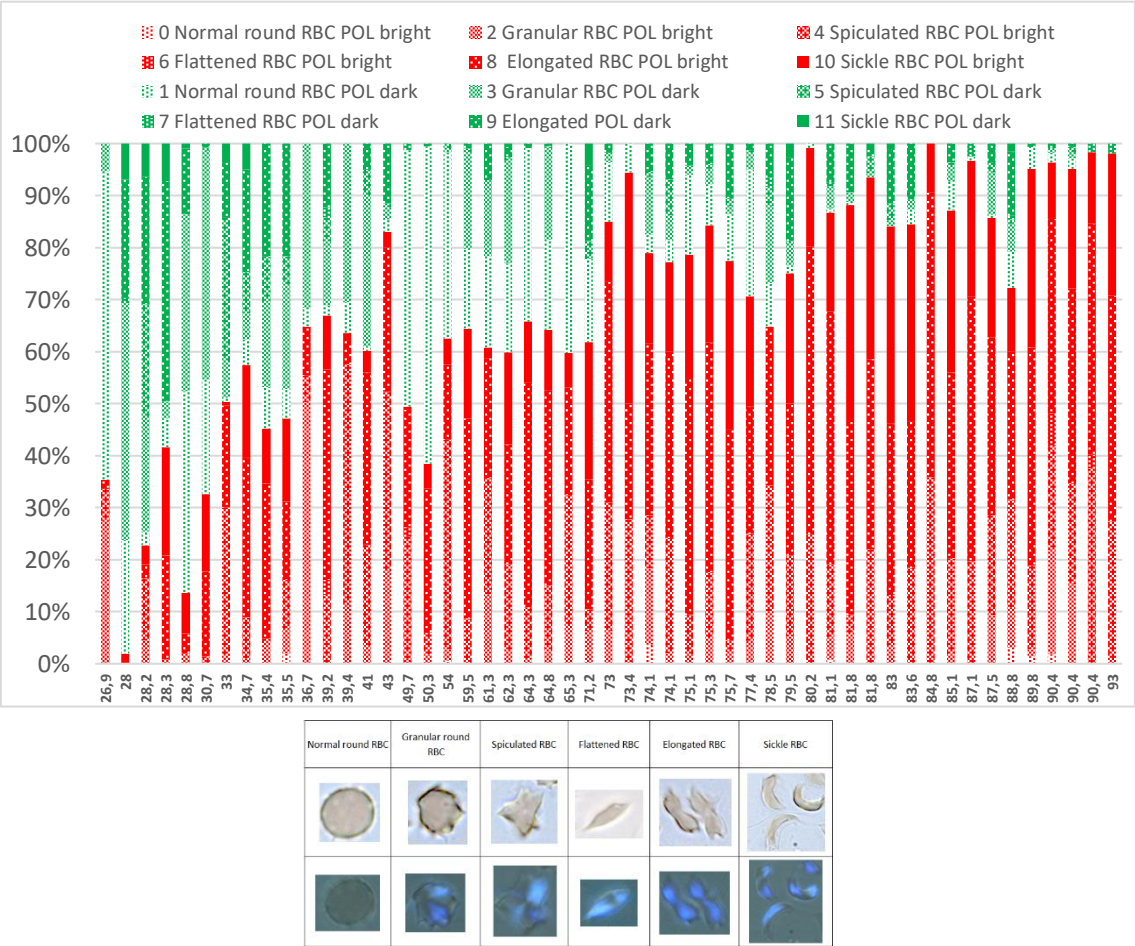


Figure 30: Representation of all cell categories identified in each sample with polarizing microscopy.
 Green bars represent non-depolarizing (dark) cells while red bars represent depolarizing (bright) cells. X-axis shows HbS (%). Note that not only sickled RBCs show depolarization. Cell types from table 7 for reference.

Figure 30 shows a strong variation of different cell types, both in the non-depolarizing (dark) and depolarizing (bright) groups. Overall, the percentage of depolarizing (bright) events seems to increase with higher amounts of HbS, although differently shaped cell types may account for this.

4.4.1. Correlation of polarizing events *versus* deformed RBCs

A first analysis of all depolarizing events shows that they are much more frequent than the number of sickle cells or even all deformed cells as observed in optical microscopy (figure 31), as evidenced by the fact that the trend lines cross the zero value on the x-axis at 53,1 (see also formula - figure 31 top) and 23,9 (see also formula - figure 31 bottom).

However, the Pearson's correlation is only moderate for sickle cells, although it shows a strong correlation for all deformed events.

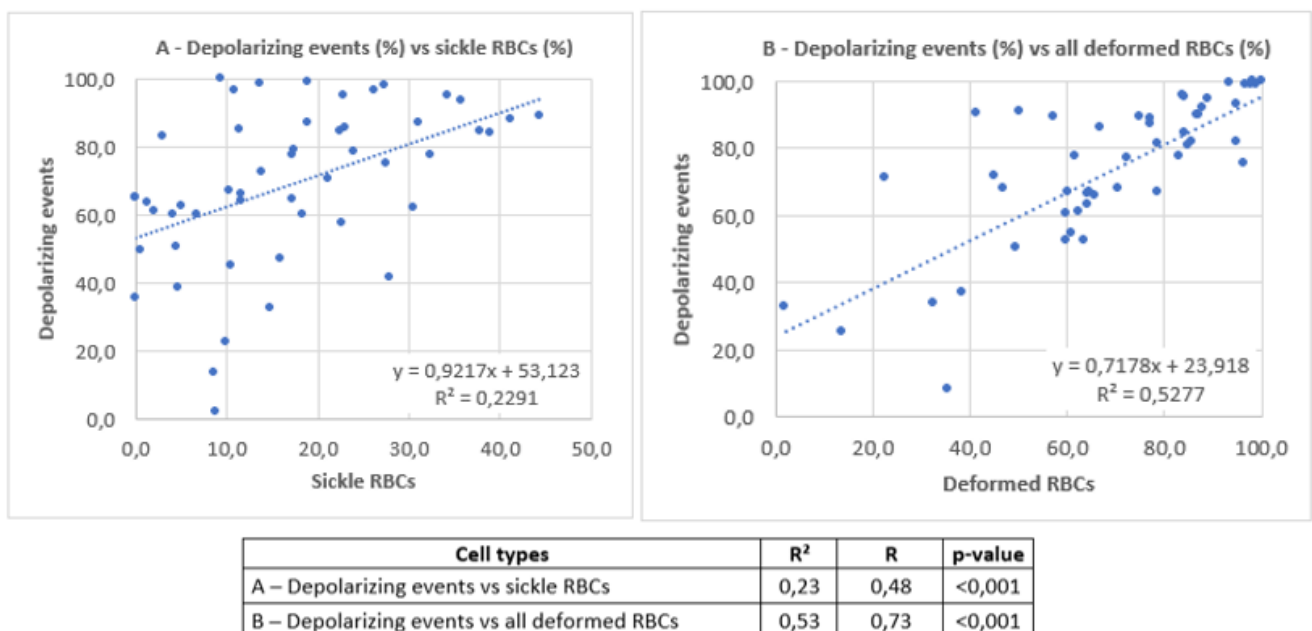
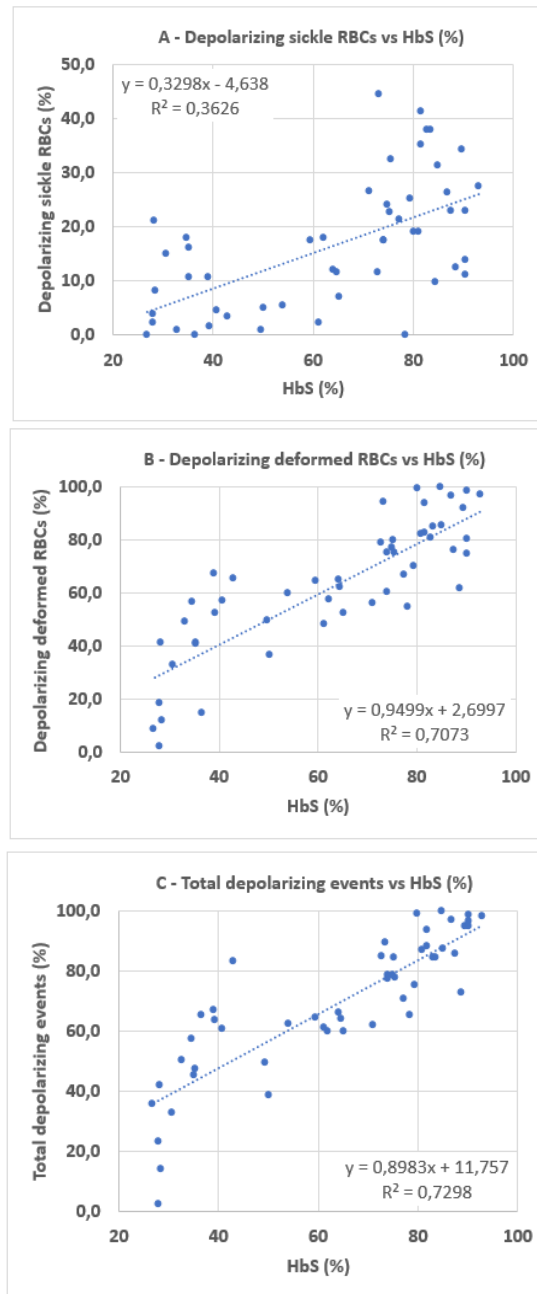


Figure 31: Correlation between depolarizing events versus deformed RBCs.

Plots of all depolarizing events observed with polarizing microscopy versus sickle RBCs (top) and all deformed RBC (bottom) as observed in optical microscopy. Cell types according to table 7. **R²**: coefficient of determination - proportion of the variation in the dependent variable (cell types) that is predictable from the independent variable (HbS). **R**: Pearson correlation coefficient - measure of linear correlation with respective P-value. Interpretation of Pearson's correlation coefficient (R): 0-0.1: none, 0.1-0.39: weak, 0.4-0.69: moderate, 0.7-0.89: strong, 0.9-1: very strong. Adapted from (102).

4.4.2. Correlation of polarizing events versus HbS levels (%)



Cell types	R ²	R	p-value
A – Depolarizing sickle RBCs (%) vs HbS (%)	0,36	0,60	<0,001
B – Depolarizing deformed RBCs (%) vs HbS (%)	0,71	0,84	<0,001
C – Total depolarizing events (%) vs HbS (%)	0,73	0,85	<0,001

Figure 32: Correlation between HbS (%) and different depolarizing events (%).

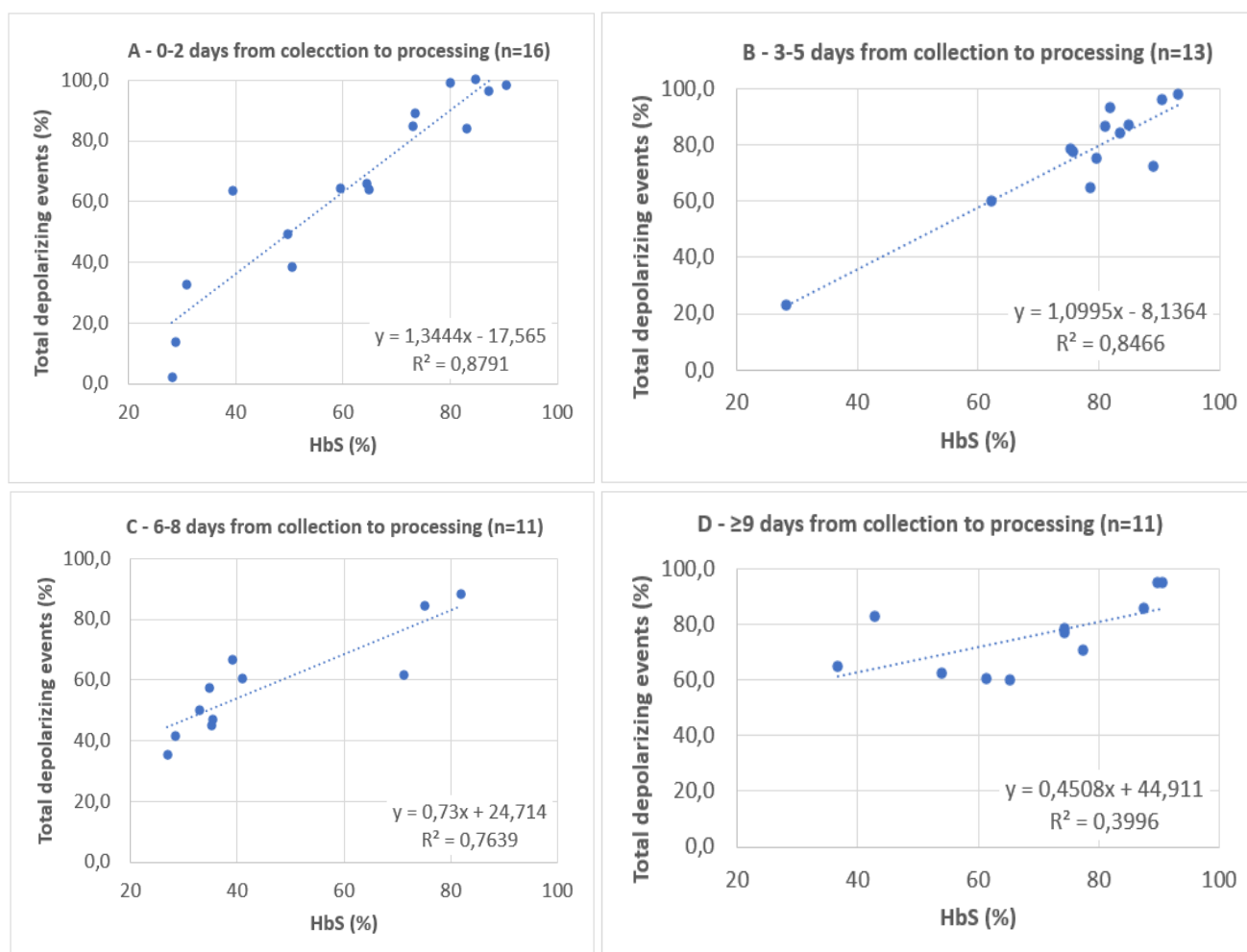
Plots of different depolarizing events vs HbS in %. Note increasing correlation with inclusion of more cell types. Total depolarizing events (bottom) includes non-deformed cells. Cell types according to table 7. **R²**: coefficient of determination - proportion of the variation in the dependent variable (cell types) that is predictable from the independent variable (HbS). **R**: Pearson correlation coefficient - measure of linear correlation with respective P-value. Interpretation of Pearson's correlation coefficient (R): 0-0.1: none, 0.1-0.39: weak, 0.4-0.69: moderate, 0.7-0.89: strong, 0.9-1: very strong. Adapted from (102).

Analyzing the correlation between HbS levels (in %) and depolarizing events (figure 32) it was noted that the correlation was lowest when only typical shaped sickle cells were considered (figure 32, top). Including all deformed cells increased the correlation substantially with Pearson's R rising from 0,6 to 0,84. Interestingly, some non-deformed RBCs (see table 7 for representative images) also showed depolarization. When these cells were also included the best correlation results reached 0,85 (figure 32, bottom).

4.4.3. Possible effect of delayed sample processing

Since it was not possible to process the samples immediately after collection and some samples were only analyzed with a delay of several days, the possible effect of this delay on the results was analyzed in more detail.

Plots of all depolarizing events versus HbS levels (in %) were created as in figure 32 (bottom, C). The plots and the respective correlation were analyzed by creating several plots for different time intervals (age) of the sample from collection to processing, with the following time intervals: (i) 0-2 days, (ii) 3-5 days, (iii) 6-8 days, and finally (iv) older than 8 days. As expected, the correlation decreased with older samples, dropping from $R = 0,94$ on the first 2 days to $R = 0,63$ for samples older than 8 days (figure 33).



Correlation graphic (respective figure number and title)	R ²	R	p-value
A – 0-2 days from collection to processing (n=16)	0,88	0,94	<0,001
B – 3-5 days from collection to processing (n=13)	0,85	0,92	<0,001
C – 6-8 days from collection to processing (n=11)	0,76	0,87	<0,001
D – ≥9 days from collection to processing (n=11)	0,40	0,63	<0,05

Figure 33: Influence of delayed sample processing on correlation of HbS – depolarizing events.

Plots of total depolarizing events vs HbS in % for 4 different time intervals: (i) 0-2 days, (ii) 3-5 days, (iii) 6-8 days, and finally (iv) older than 8 days. **R²**: coefficient of determination - proportion of the variation in the dependent variable (cell types) that is predictable from the independent variable (HbS). **R**: Pearson correlation coefficient - measure of linear correlation with respective P-value. Interpretation of Pearson's correlation coefficient (R): 0-0.1: none, 0.1-0.39: weak, 0.4-0.69: moderate, 0.7-0.89: strong, 0.9-1: very strong. Adapted from (102).

4.5. Drug (voxelotor) experiment

The experimental conditions were difficult to set up because the solvent (DMSO) for the drug tended to lyse RBCs, especially sickled cells, after prolonged incubation (>3-5h). The RBCs from a patient with 85% HbS showed marked sickling during the sickle cell test after 3h of incubation (figure 34, A). Two photographic images (1000x amplification) were analyzed and had similar numbers of RBCs when counted manually.

The number of typical sickle cells counted manually (in figure 34, A - top panel) was n=44 (53%) while in the voxelotor treated samples no completely sickled cells were observed (in figure 34, B - top panel). However, several RBCs (n=33) showed some irregularities or deformities (42%).

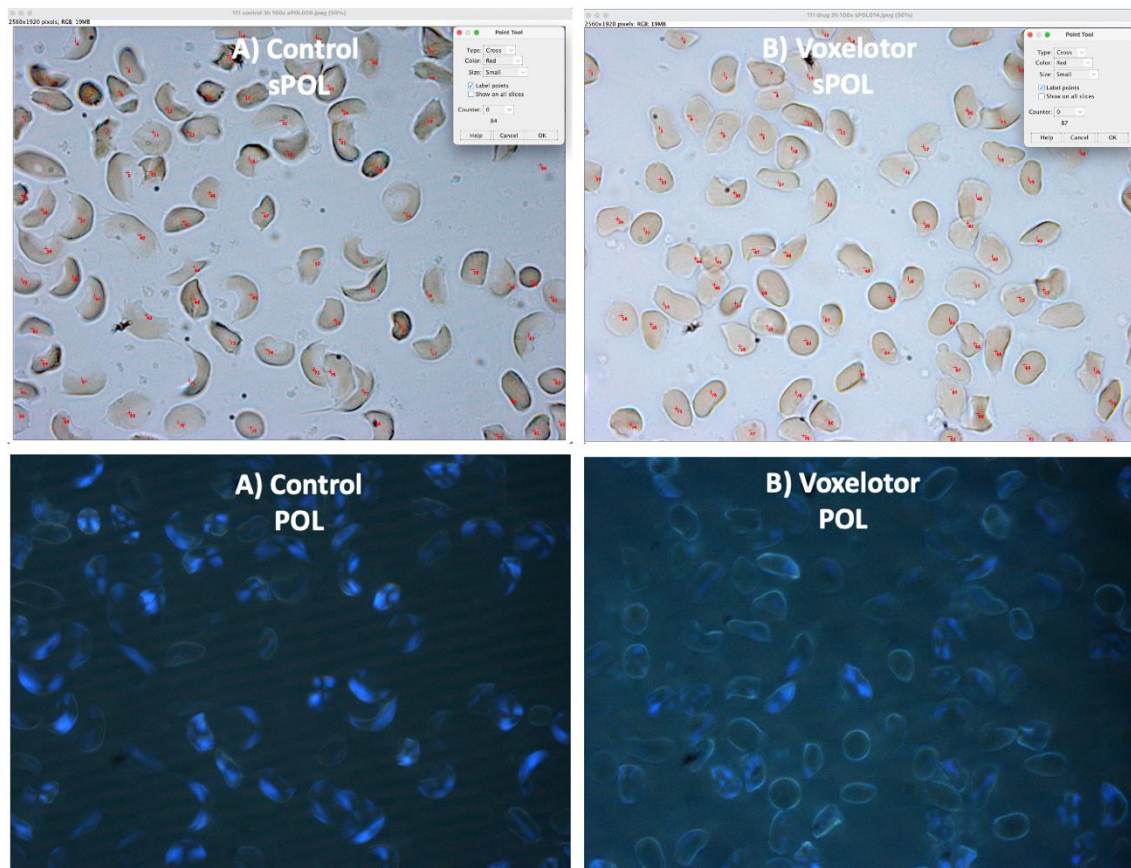


Figure 34: Images of brightfield and depolarizing RBCs after voxelotor treatment.

Untreated RBCs (A) and voxelotor treated RBCs (B) observed with brightfield (top panels) and under crossed polarizers (bottom panels). Manual counting (numbered red dots in top panels) showed 84 RBCs in the control condition and 87 RBCs in the drug-treated condition. Of note all RBC were counted, also those at the edge, because the program analysis all polarizing events. The control showed 53% of typical sickled cells (A, top panel) while the drug-treated sample showed only some deformed cells (B, top panel). Image size: 2650 x 1920 = 5,167,500 pixels, color: RGB.

4.5.1. Automated analysis of images of control and drug-treated RBCs

Using four steps in the Fiji/ImageJ2 program allowed to automatically determine the depolarizing areas and the respective brightness (intensity) caused by the polymerized Hb (Figure 35).

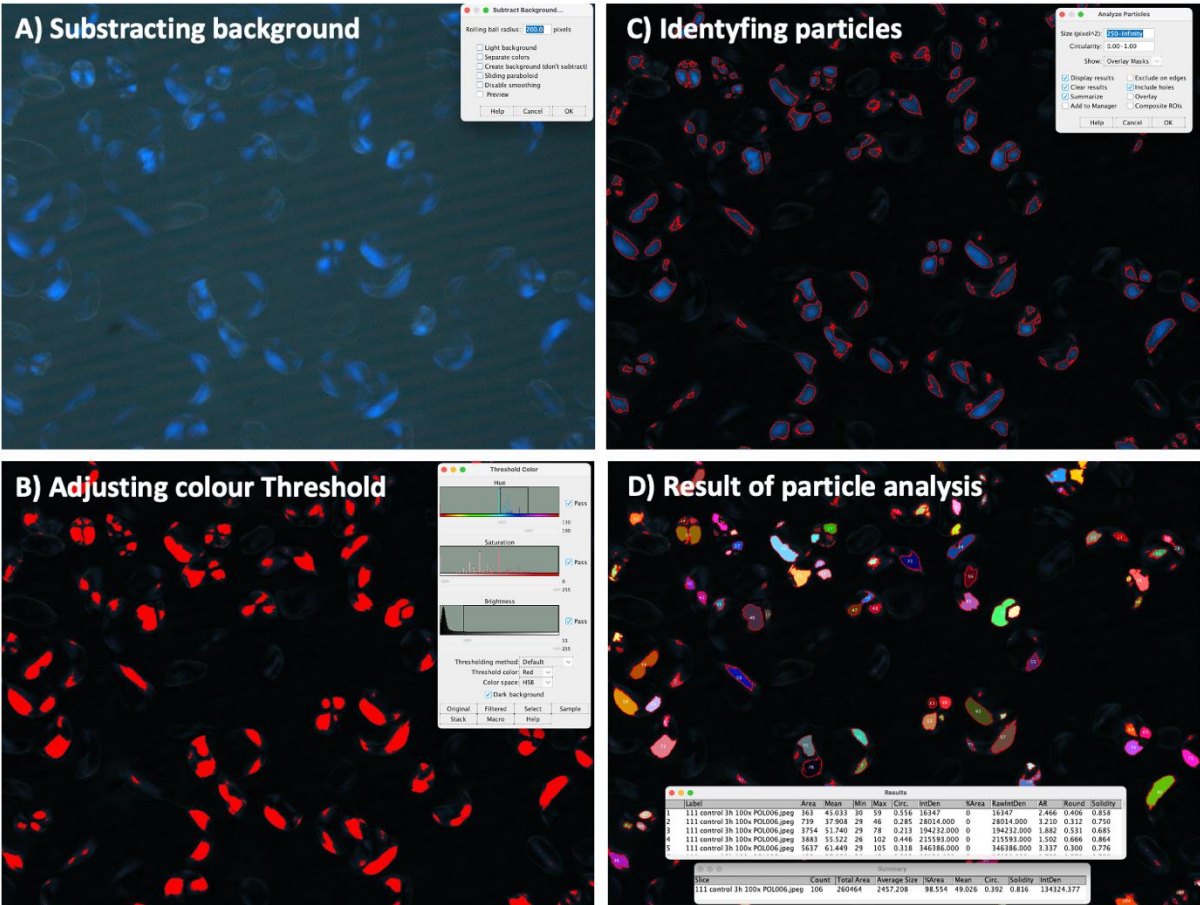


Figure 35: Automated analysis of depolarizing images.

Representative schema of the automated analysis which consisted of 4 steps. The image was opened in Fiji/ImageJ2 (A). The dark background was subtracted to increase the contrast (settings in insert). The resultant image was subjected to a color thresholding (B) (settings in insert); only pixels within the blue color spectrum were included with a brightness >50 (B). This produced analyzable particles of various sizes (C). Background noise was eliminated by only analyzing particles of a size >250 pixels. This value was determined before by manually measuring the pixel sizes of several of the smallest intra-erythrocytic depolarizing areas (C). The analysis step confers each particle a different color and number (D). This produces data on each particle (list-mode data) with several parameters and summary statistic (D, inserts).

4.5.2. Statistical analysis of image data comparing control to drug treated sample

The list-mode data was imported into Excel and analyzed. Interestingly, the drug treated control had significantly smaller depolarizing areas (in pixels) than the control (figure 36, A). The same was observed for the brightness (intensity) of the depolarization which was significantly reduced in the drug-treated sample as well (figure 36, B).

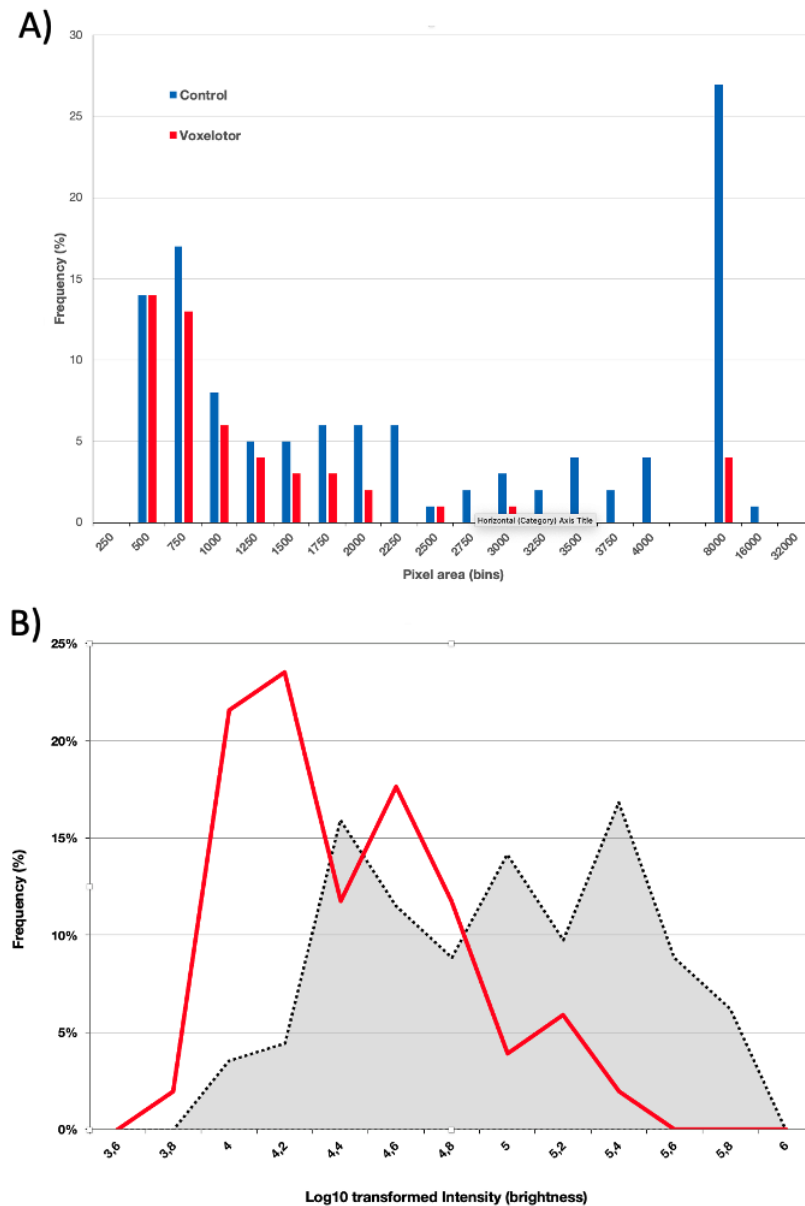


Figure 36: Difference in distribution of area and brightness between control and drug. The pixel size is significantly smaller in drug treated RBCs as compared to the control (A). Histogram using bins of 250 (up to 4000), then using bins with doubling value (8000, 16000, 32000). The brightness (intensity) is also reduced in the drug treated condition (red line) as compared to the control (dotted black line/grey area) (B). The brightness values were \log_{10} transformed as they spanned 3 decades (table 8) which was difficult to show in a histogram. Percentage of observations (drug, n= 51, control, n=113) in each condition.

The differences between both samples are significantly different but show only a medium effect size (table 8).

Table 8: Summary of parameters comparing control to drug treated sample.

AREA ¹	particles (n)	Mean (SD)	Min./Max.	Median	Skew.	P-value ²	Effect size ³
Control	113	2536 (2130)	264/8234	1869	0,9	<0,001	0,34 (medium)
Voxelotor	51	1162 (1245)	255/6684	717	2,6		
INTENSITY ⁴	particles (n)	Mean (SD)	Min./Max.	Median	Skew.	P-value ²	Effect size ⁵
Control	113	126900 (125755)	9093/474954	78090	1,3	<0,001	0,47 (medium)
Voxelotor	51	33680 (40396)	5865/233273	18580	3,1		

¹ Area in pixels

² Mann-Whitney U Test for non-normally distributed samples.

³ Standard effect size (common language effect size: $U_1/(n_1n_2)$, is 0.29, this is the probability that a random value from Group1 is greater than a random value from Group2.).

⁴ Intensity of pixels in RGB as calculated by the program Fiji/ImageJ2 (see methods).

⁵ Standard effect size (common language effect size: $U_1/(n_1n_2)$, is 0.21, this is the probability that a random value from Group1 is greater than a random value from Group2.).

SD: standard deviation, Min.: minimum, Max.: maximum, Skew.: Skewness (0 = normally distributed)
Analysis performed online (https://www.statskingdom.com/170median_mann_whitney.html, on 6/3/2023)

5. Discussion

General aspects

This project investigated whether the observation of depolarization, reported to occur with polymerized HbS (47), could be a useful indicator for the detection of HbS in the traditional metabisulfite sickling test. The overall results seem to indicate that this novel method could be a simple and easy way to establish the diagnosis of SCD but may also be a promising new way to assess the amount of HbS (semi-quantitatively).

Sickle cell disease is caused by the intracellular polymerization of HbS which is directly dependent on the intracellular HbS concentration (47,48). Most laboratory methods do support only the diagnosis (i.e. sickling test, etc.) (83), might confirm the diagnosis (i.e., alkaline electrophoresis) (35) or are used to monitor the concentration of HbS (i.e., electrophoresis, HPLC) (35). The later methods (i.e., HPLC) can determine the percentage of HbS in a sample with high accuracy, although the results report to the proportion of HbS in the total hemolysate. However, HbS (and HbF) is not homogenously distributed in RBCs (61) and the type of distribution in each individual RBC determines the predisposition to sickle (37). Current routine laboratory tests give no information on the distribution of polymerized HbS in each RBCs, which might potentially be useful to assess disease severity, and even might serve as a predictor of the occurrence of vaso-occlusive crisis for instance. Using the observation of depolarization of polymerized HbS shows different patterns within RBCs (103) and it seems possible that this might provide additional information.

This study confirms that not only typical sickled RBCs, but also many other types of deformed RBCs show depolarization, and even non-deformed RBCs might exhibit depolarization (figure 30). It also shows that this novel method provides a very strong correlation with the HbS concentration (in %) (figure 32). However, for the interpretation of the results, two possible major limitations should be noted: (i) the delayed sample processing after blood collection, which ranged up to 17 days, and (ii) the fact that the sickling test was only read after 24h of incubation.

Optical microscopy

The classical method of optical microscopy to assess samples using the metabisulfite sickling test, depends on the detection of RBC abnormalities (deformations) to diagnose SCD (83). Usually, the sample is observed for the presence of typical sickle RBC, because other deformations could have other underlying causes (43), and thus, there is a possibility to misdiagnose samples with few typical sickle cells. The number of typical sickle shaped RBCs can be rather low, even in cases with very high concentrations of HbS, as illustrated by two representative samples (table 9). Certainly, the presence of many deformed cells should trigger further laboratory tests, which eventually would confirm the diagnosis of SCD. However, it should be noted that the studied method almost showed a universal depolarization in all RBCs, indicating its potential superior usefulness for detection of polymerized HbS (table 9).

Table 9: Low proportion of sickled RBC in two studied samples.

HbS (%)	Days: collection to processing	Normal round RBCs	Granular RBCs	Spiculated RBCs	Elongated RBCs	Flattened RBCs	Sickle RBCs	Total cell count	% Total depolarizing events	% Total Sickle RBCs
84,8	1	0	0	38	58	0	10	106	100,0	9,4
90,4	5	4	23	22	42	7	12	110	96,4	10,9

Two representative samples to illustrate low percentage of sickled RBCs. However, deformed RBCs categories show elevated levels while almost all RBC showed depolarization. Categories of cells as in table 7, page 65)

A systematic analysis of the results shows the high variability of all different deformed RBCs in the 51 investigated samples (figure 28, page 70), while only a moderate degree of correlation was observed with the HbS concentration (figure 29, page 71). In fact, sickle RBCs show the lowest correlation with HbS ($R=0,54$). However, when considering all the deformed cell categories the correlation with HbS improves ($R=0,63$). Apparently, optical microscopic observation of the metabisulfite sickling test, while simple and rapid (35), would benefit from improvement.

Polarization microscopy – Deformed RBCs and types of depolarization patterns

By using an optical microscopy equipped with crossed polarizers, it is possible to observe the depolarization properties of the polymerized HbS inside the RBCs. Interestingly, not only typically shaped sickle RBCs depolarize light (figure 30, page 72), but also other deformed RBCs, with various morphologies. Additionally, the depolarization pattern and the abnormal morphologies of the RBCs seems to vary between samples with different percentage of HbS (figure 37).

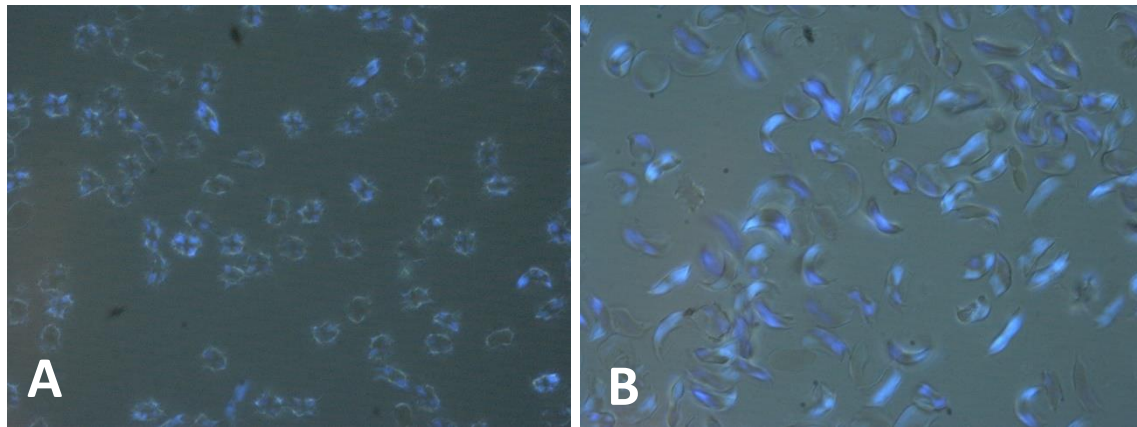


Figure 37: Representative images of two samples using polarizing microscopy.

Two samples (2 days old) of a metabisulfite sickling test (Panel A: 39,4% HbS, Panel B: 83% HbS) after 24h incubation. Note polarization pattern which is not restricted to typically shaped sickle RBC and the percentage of depolarizing events seems higher with higher amounts of HbS. Images acquired with polarization microscopy, 1000x.

Different types of deformed RBCs and polarization patterns have been reported (103,104) which were also the basis for the classification (table 7, page 65) of this study. During the 1990s several studies investigated the pathophysiology of the sickling process and used polarizing microscopy to study this (103). Several ideas were proposed to explain the different shapes, including speed of deoxygenation (50), as well as the amounts and distribution of HbS/HbF inside individual RBCs (61). In fact, recent studies have shown convincingly that individual RBCs contain varying amounts of HbS/HbF which determines their propensity to sickle (37). Interestingly, this raises the question if counting these different RBCs may produce a parameter which might correlate with the clinical situation (i.e., the predisposition to have a sickle cell crisis). In this study a wide variation of these different types of cells was observed in the 51 samples (figure 30), without any apparent pattern. Unfortunately, the delay of sample processing makes any meaningful interpretation of this data difficult.

Polarization microscopy – An easy and clinically useful way to monitor HbS

The most interesting results of this pilot study is the observation that depolarizing deformed cells seem to increase with increasing amounts of HbS (in %) (figure 30). A formal analysis of this possible association with Pearson's correlation coefficient, showed a strong effect which was highly statistically significant ($P < 0,001$) (figure 32, page 74).

When considering all depolarizing events, regardless of any specific RBC morphology (table 7), the best correlation with HbS (in %) was ($R = 0,85$, $P < 0,001$) (figure 32, C). However, it should be noted that the percentage of depolarizing events is not directly equal to the percentage of HbS, as the correlation formula indicates ($y = 0,9 * x + 11,8$): for each given value of HbS it would be necessary to add the constant of 11,8 (figure 32, C). Interestingly, the observation of deformed depolarizing RBCs gives a more directly equal result of HbS ($y = 0,95 * x + 2,7$), with a constant of only 2,7 (figure 32, B).

The coefficient of determination (R^2 value) is defined as the proportion of the variation in the dependent variable (here depolarizing events) that can be predicted from the independent variable (here HbS in %) (102). The R^2 of 0,73 (figure 32) between the total depolarizing events (%) and the HbS (%) means that 73% of the variability of the total (%) depolarizing events is explained by the variability (concentration) of the HbS (in %), while the remaining 27% must be explained by other factors.

Indeed, the factors (i) speed and duration of hemoglobin deoxygenation (50), and (ii) the intracellular HbF concentration (in individual RBCs) (58) have been described to influence the rate of HbS polymerization. These variables were not considered in this investigation. As mentioned before, the "age" of the sample (delay in processing) (figure 26, page 68) may be the most relevant factor, confirmed to have influenced the results. It is also possible that the used categories (table 7) to define a deformed RBCs may not be the ideal ones, possibly as they were based on investigations into the pathophysiology of sickling (103,104), rather than their correlation with HbS (in %). Perhaps, creating new categories might also lead to better results.

Still, this novel method seems capable to provide a reliable approximation of the percentage of HbS and might allow the clinical monitoring of SCD patients. In fact, it appears that some patients may have been given a blood transfusion, as indicated by very low levels of HbS (for a SCD patient) and the presence of a population of RBCs without anisocytosis and poikilocytosis (figure 38). In this case the depolarizing events (49,4%) almost equaled perfectly the HbS level (49,7%)

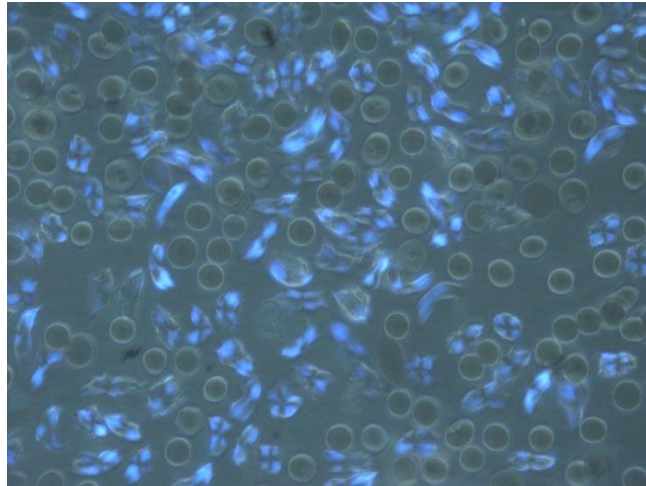


Figure 38: Sample of SCD patient that possibly undergone a blood transfusion.

Sample (49,7% HbS), two days old, observed under crossed polarizers (1000x) after 24h incubation (metabisulfite sickling test). Note the presence of two cell populations: (i) deformed and depolarizing RBCs (49,4%) but also (ii) normal RBCs without any polarization, likely indicating the presence of HbA RBC from blood transfusion.

Other aspects

This studied method may also have other potential applications, such as in the field of investigation of emerging therapies or as a predictor of outcome in drug testing experiments, as the preliminary results with the drug voxelotor illustrate (section 4.5). Screening for drugs which interfere with sickling has been done with rather high-tech and complex methods (70,101). Certainly, manual counting of images acquired with optical microscopy may reveal a reduction in the typical sickled cells but is cumbersome, while image analysis is still fraught with difficulties.

Contrary to this, polarization microscopy may allow a simpler determination of a decline of depolarizing events, as shown in this study. In fact, it was possible to use a simple, automated image analysis (figure 35, page 78), which demonstrated smaller depolarizing areas as well as a significant decrease in the brightness (intensity) of depolarization in the drug-treated sample (figure 36, page 79).

This suggests that this method may not only be a simpler way to screen for novel compounds, but also indicates the possibility of complete automation using image analysis. Moreover, automated image analysis may enable to objectively measure the brightness (intensity) of depolarization, eventually refining the assessment of HbS polymerization within the RBC.

The growth and alignment of HbS polymers inside the RBC leads to variable stress in the cell membrane, thus producing heterogeneous cell shapes (104). Consequently, the distribution and degree of depolarization may vary between the different RBC morphologies (figure 39), which automated image analysis could measure easily, open the possibility to investigate if counting different cell categories could have any clinical value.

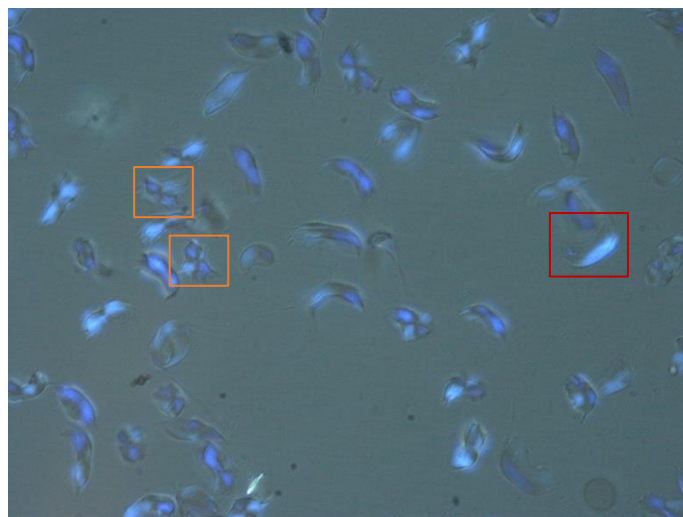


Figure 39: Different types of depolarization patterns in sickled RBCs.

Sample, 3 days old, with 93% HbS (after 4h incubation, metabisulfite sickling test). Note how independent polymer domains result in a spiculated morphology (orange square), whereas a single fiber domain growing in one general direction (aligned polymers) lead to the typical sickled RBC (red square).

Limitations and future work

As mentioned before, a major limitation of this investigation was the impossibility of processing the samples immediately after blood collection, leading to the necessity of storing the samples in the fridge until processing for several days (figure 26). This delay appeared to have a significant impact, as evidenced by the fact that the correlation between depolarizing events and HbS (in %) was strongest in samples processed within 2 days ($R=0,94$) and decreased with longer delays (figure 33, page 76). Most likely, it may be related to RBC lysis, which could have affected some cell types more than others.

Another limitation, also related to delays, was the realization of the metabisulfite sickling test. Two time points were assessed (1h and 24h) to establish if meaningful results could be obtained at 24h. The expectation was to observe a general increase in sickling and depolarization, as maximum deoxygenation occurred during incubation. Indeed, an increase in the total number of deformed cells was observed at 24h, however, it seemed that the total of depolarizing and sickling events was slightly higher at 1h of incubation (figure 27, page 69). The observation that only samples with 2 days showed an increase in both sickling and depolarization further supports the relevancy of the “age” variable. Once again, it may be related to RBC lysis which affected some cell types more than others.

Other limitations include the manual counting method, which ideally should have been executed blindly (not knowing the percentage of HbS) and performed by at least two independent observers.

Future work should clarify the limitations of the method and investigate this novel method with freshly collected blood and a minimum of incubation time, established after carefully producing a time-curve.

Further aspects may include:

- (i) Evaluation of other Hb variants as well as sickle cell trait.
- (ii) Eventually validation with some blood from newborns due to their high HbF levels.
- (iii) Correlation with clinical information, and eventual testing of blood during sickle cell crisis.

6. Conclusions

The results of this pilot study indicate that this novel method could be a simple and easy way to establish the diagnosis of SCD. All samples showed many easily observable depolarizing events, based on the presence of polymerized HbS.

More importantly, it may also be a promising new way to assess the amount of HbS (semi-quantitatively) and use this to monitor SCD patients. In fact, total depolarizing events or depolarizing deformed RBCs correlated very strongly with the concentration of HbS (in %).

The results seem to have been negatively influenced by the age of the sample, and (perhaps) the prolonged incubation time (24h) during the sickling test. Using only fresh samples (and shorter incubation times) might produce a correlation very close to 1,0. In fact, analyzing only samples with <2 days already produced a correlation coefficient of 0,94.

This novel method is simple and low-cost, based on the detection of depolarizing RBCs using standard microscopy equipped with crosses polarizers (and eventually a camera), and requires only a few, economic reagents, and equipment. Possible use of smartphone (with a camera) and eventually, automated image analysis would provide a practical portable platform for point-of-care settings. It might be adjusted for use in resource-limited areas as a same-day POC-test.

7. References:

1. Grace RF, Ware RE. Pediatric Hematology. Hematol Oncol Clin North Am [Internet]. 2019;33(3):xiii–xiv. Available from: <https://doi.org/10.1016/j.hoc.2019.02.001>
2. Roberts DJ, Weatherall DJ. Introduction: The Complexity and Challenge of Preventing, Treating, and Managing Blood Diseases in the Developing Countries. Hematol Oncol Clin North Am [Internet]. 2016 Apr;30(2):233–46. Available from: <https://linkinghub.elsevier.com/retrieve/pii/S0889858815001884>
3. Ochocinski D, Dalal M, Black LV, Carr S, Lew J, Sullivan K, et al. Life-Threatening Infectious Complications in Sickle Cell Disease: A Concise Narrative Review. Front Pediatr [Internet]. 2020 Feb 20;8(February). Available from: <https://www.frontiersin.org/article/10.3389/fped.2020.00038/full>
4. Chaparro CM, Suchdev PS. Anemia epidemiology, pathophysiology, and etiology in low- and middle-income countries. Ann N Y Acad Sci [Internet]. 2019 Apr 22;1450(1):nyas.14092. Available from: <https://onlinelibrary.wiley.com/doi/10.1111/nyas.14092>
5. McPherson, Richard and Pincus MR. Henry's Clinical Diagnosis and Management by Laboratory Methods. Nineteenth. W.B. Saunders Company, editor. Philadelphia, Pennsylvania; 2017.
6. Weatherall DJ, Clegg JB. Inherited haemoglobin disorders: An increasing global health problem. Bull World Health Organ. 2001;79(8):704–12.
7. Ross, H. M, Pawlina W. Histology. In: Wilkins LW&, editor. 6th ed. Philadelphia; 2011. p. 268–309.
8. Siems WG, Sommerburg O GT. Erythrocyte free radical and energy metabolism. Clin Nephrol 53(1 Suppl), S9–S17. 2000;
9. Silva JAM. Biopatologia vascular e sanguínea - Função respiratória do sangue [Internet]. 2005. Available from: <http://hdl.handle.net/10451/1123>
10. Barcellini W, Fattizzo B. Clinical Applications of Hemolytic Markers in the Differential Diagnosis and Management of Hemolytic Anemia. Dis Markers [Internet]. 2015;2015:1–7. Available from: <http://www.hindawi.com/journals/dm/2015/635670/>
11. Vasković J. Erythrocytes [Internet]. Available from: <https://www.kenhub.com/en/library/anatomy/erythrocytes>
12. Shiga T, Maeda N, Kon K. Erythrocyte rheology. Crit Rev Oncol Hematol [Internet]. 1990 Jan;10(1):9–48. Available from: <https://linkinghub.elsevier.com/retrieve/pii/104084289090020S>
13. Junqueira L, Carneiro J. Histologia básica. In: Grupo Editorial Nacional GK, editor. 12th ed. Rio de Janeiro; 2013. p. 217–32.
14. Eastlund T. The histo-blood group ABO system and tissue transplantation. Transfusion [Internet]. 2003 Feb 27;38(10):975–88. Available from: <http://doi.wiley.com/10.1046/j.1537-2995.1998.381098440863.x>

15. Faghih MM, Sharp MK. Modeling and prediction of flow-induced hemolysis: a review. *Biomech Model Mechanobiol* [Internet]. 2019;18(4):845–81. Available from: <https://doi.org/10.1007/s10237-019-01137-1>
16. Puchkov EO. Intracellular viscosity: Methods of measurement and role in metabolism. *Biochem Suppl Ser A Membr Cell Biol* [Internet]. 2013;7(4):270–9. Available from: <https://doi.org/10.1134/S1990747813050140>
17. Jameson, Fauci, Kasper, Hauser, Longo L. *Harrisons's Principles of Internal Medicine*. 20th ed. Education MGH, editor. 2018. 690–698 p.
18. CDC. Hemoglobinopathies: Current Practices for Screening, Confirmation and Follow-up. *Assoc Public Heal Lab*. 2015;(December):5–57.
19. Dame C, Juul SE. The Switch from fetal to adult erythropoiesis. *Clin Perinatol* [Internet]. 2000 Sep;27(3):507–26. Available from: <https://linkinghub.elsevier.com/retrieve/pii/S0095510805700361>
20. Manning LR, Russell JE, Padovan JC, Chait BT, Popowicz A, Manning RS, et al. Human embryonic, fetal, and adult hemoglobins have different subunit interface strengths. Correlation with lifespan in the red cell. *Protein Sci* [Internet]. 2007 Aug;16(8):1641–58. Available from: <http://doi.wiley.com/10.1110/ps.072891007>
21. Hoeger U, Robin J, Editors H. *Vertebrate and Invertebrate Respiratory Proteins, Lipoproteins and other Body Fluid Proteins* [Internet]. Hoeger U, Harris JR, editors. *Subcellular Biochemistry* 94. Cham: Springer International Publishing; 2020. 465–497 p. (*Subcellular Biochemistry*; vol. 94). Available from: <http://www.springer.com/series/6515>
22. Yoshida T, Prudent M, D'Alessandro A. Red blood cell storage lesion: Causes and potential clinical consequences. *Blood Transfus*. 2019;17(1):27–52.
23. Vutturi A vardhan. Hemoglobin & Myoglobin [Internet]. [cited 2023 Jan 23]. Available from: <http://www.adichemistry.com/inorganic/bioinorganic/hemoglobin/hemoglobin.html>
24. ANTONINI E. History and theory of the oxyhemoglobin dissociation curve. *Crit Care Med* [Internet]. 1979 Sep;7(9):360–7. Available from: <http://journals.lww.com/00003246-197909000-00003>
25. Clark KD. *Vertebrate and Invertebrate Respiratory Proteins, Lipoproteins and other Body Fluid Proteins* [Internet]. Hoeger U, Harris JR, editors. Cham: Springer International Publishing; 2020. 123–163 p. (*Subcellular Biochemistry*; vol. 94). Available from: <http://link.springer.com/10.1007/978-3-030-41769-7>
26. Jorge SE, Ribeiro DM, Santos MNN, de Fátima Sonati M. Hemoglobin: Structure, Synthesis and Oxygen Transport. In: *Sickle Cell Anemia* [Internet]. Cham: Springer International Publishing; 2016. p. 1–22. Available from: http://link.springer.com/10.1007/978-3-319-06713-1_1

27. Marengo-Rowe AJ. Structure-Function Relations of Human Hemoglobins. *Baylor Univ Med Cent Proc* [Internet]. 2006 Jul 11;19(3):239–45. Available from: <https://www.tandfonline.com/doi/full/10.1080/08998280.2006.11928171>
28. Kumar R. Oxyhemoglobin Dissociation Curve [Internet]. [cited 2023 Jan 23]. Available from: <https://rk.md/2017/oxyhemoglobin-dissociation-curve/>
29. Dua. ABAKPKSA. Physiology, Bohr Effect. NCBI [Internet]. 2022; Available from: <https://www.ncbi.nlm.nih.gov/books/NBK526028/>
30. Collins JA, Rudenski A, Gibson J, Howard L, O'Driscoll R. Relating oxygen partial pressure, saturation and content: The haemoglobin–oxygen dissociation curve. *Breathe*. 2015;11(3):194–201.
31. Semedo MSSDCCN. Mioglobina e hemoglobina. 2007;115.
32. Kohne E. Hemoglobinopathies. *Dtsch Arztebl Int* [Internet]. 2011 Aug 8;108(31–32):532–40. Available from: <https://www.aerzteblatt.de/10.3238/arztebl.2011.0532>
33. Angastiniotis M, Lobitz S. Thalassemias: An Overview. *Int J Neonatal Screen* [Internet]. 2019 Mar 20;5(1):16. Available from: <https://www.mdpi.com/2409-515X/5/1/16>
34. Thom CS, Dickson CF, Gell DA, Weiss MJ. Hemoglobin Variants: Biochemical Properties and Clinical Correlates. *Cold Spring Harb Perspect Med*. 2013;3(3):1–22.
35. Arishi WA, Alhadrami HA, Zourob M. Techniques for the Detection of Sick Cell Disease: A Review. *Micromachines* [Internet]. 2021 May 5;12(5):519. Available from: <https://www.mdpi.com/2072-666X/12/5/519>
36. Ashley-Koch A, Yang Q, Olney RS. Sick Cell Hemoglobin (Hb S) Allele and Sick Cell Disease: A HuGE Review. *Am J Epidemiol* [Internet]. 2000 May 1;151(9):839–45. Available from: <https://academic.oup.com/aje/article-lookup/doi/10.1093/oxfordjournals.aje.a010288>
37. Steinberg MH. Overview of Sick Cell Anemia Pathophysiology. In: *Sick Cell Anemia* [Internet]. Cham: Springer International Publishing; 2016. p. 49–73. Available from: http://link.springer.com/10.1007/978-3-319-06713-1_3
38. Gardner K, Thein SL. Genetic Factors Modifying Sick Cell Disease Severity. In: *Sick Cell Anemia* [Internet]. Cham: Springer International Publishing; 2016. p. 371–97. Available from: http://link.springer.com/10.1007/978-3-319-06713-1_15
39. Piel FB, Patil AP, Howes RE, Nyangiri OA, Gething PW, Williams TN, et al. Global distribution of the sickle cell gene and geographical confirmation of the malaria hypothesis. *Nat Commun* [Internet]. 2010 Nov 2;1(1):104. Available from: <https://www.nature.com/articles/ncomms1104>
40. Adekile A, Makani J. Sick Cell Disease in Africa and the Arabian Peninsula: Current Management and Challenges. In: *Sick Cell Anemia* [Internet]. Cham: Springer International Publishing; 2016. p. 339–70. Available from: http://link.springer.com/10.1007/978-3-319-06713-1_14

41. Platt OS. Sickie Syndromes. In: Blood - Principles and practice of hematology. Second edi. Lippincott Williams & Wilkins; p. 1650–96.
42. World Health Assembly; 59. (2006). Sickie-cell anaemia: report by the Secretariat. World Health Organization.
43. Randolph TR. Hemoglobinopathies (Structural defects in hemoglobin). In: Saunders E, editor. Rodak's Hematology: Clinical Principles and Applications. 5th editio. p. 426–53.
44. Piel FB, Williams TN. Sickie Cell Anemia: History and Epidemiology. In: Sickie Cell Anemia [Internet]. Cham: Springer International Publishing; 2016. p. 23–47. Available from: http://link.springer.com/10.1007/978-3-319-06713-1_10
45. Goldsmith JC, Bonham VL, Joiner CH, Kato GJ, Noonan AS, Steinberg MH. Framing the research agenda for sickie cell trait: Building on the current understanding of clinical events and their potential implications. *Am J Hematol*. 2012;87(3):340–6.
46. Brittenham GM, Schechter AN, Tom Noguchi C. Hemoglobin S polymerization: Primary determinant of the hemolytic and clinical severity of the sickling syndromes. *Blood*. 1985;65(1):183–9.
47. Christoph GW, Hofrichter J, Eaton WA. Understanding the shape of sickled red cells. *Biophys J*. 2005;88(2):1371–6.
48. Rees DC, Williams TN, Gladwin MT. Sickie-cell disease. *Lancet* [Internet]. 2010;376(9757):2018–31. Available from: [http://dx.doi.org/10.1016/S0140-6736\(10\)61029-X](http://dx.doi.org/10.1016/S0140-6736(10)61029-X)
49. Eaton WA, Hofrichter J. Sickie Cell Hemoglobin Polymerization. *Adv Protein Chem*. 1990;40(C):63–279.
50. Kaul DK, Xue H. Rate of deoxygenation and rheologic behavior of blood in sickie cell anemia. *Blood*. 1991;77(6):1353–61.
51. Coates DR, Chin JM, Chung STL. Therapeutic Strategies to Alter Oxygen Affinity of Sickie Hemoglobin. *Bone*. 2011;23(1):1–7.
52. Briehl RW. Nucleation, fiber growth and melting, and domain formation and structure in sickie cell hemoglobin gels. *J Mol Biol*. 1995;245(5):710–23.
53. Nader E, Skinner S, Romana M, Fort R, Lemonne N, Guillot N, et al. Blood rheology: Key parameters, impact on blood flow, role in sickie cell disease and effects of exercise. *Front Physiol*. 2019;10(OCT):1–14.
54. Pecker LH, Ackerman HC. Cardiovascular Adaptations to Anemia and the Vascular Endothelium in Sickie Cell Disease Pathophysiology. In: Costa FF, Conran N, editors. Sickie Cell Anemia [Internet]. Cham: Springer International Publishing; 2016. p. 129–76. Available from: <http://link.springer.com/10.1007/978-3-319-06713-1>
55. Zhang D, Frenette PS. Leukocytes in the Vaso-Occlusive Process. In: Sickie Cell Anemia [Internet]. Cham: Springer International Publishing; 2016. p. 91–107. Available from: http://link.springer.com/10.1007/978-3-319-06713-1_5

56. Colella MP, de Paula EV, Ozelo MC, Traina F. Hypercoagulability and Sick Cell Disease. In: Sick Cell Anemia [Internet]. Cham: Springer International Publishing; 2016. p. 109–27. Available from: http://link.springer.com/10.1007/978-3-319-06713-1_6
57. Wandersee NJ, Hillery CA. Red Blood Cells and the Vaso-Occlusive Process. In: Sick Cell Anemia [Internet]. Cham: Springer International Publishing; 2016. p. 75–90. Available from: http://link.springer.com/10.1007/978-3-319-06713-1_4
58. Hebert N, Rakotoson MG, Bodivit G, Audureau E, Bencheikh L, Kiger L, et al. Individual red blood cell fetal hemoglobin quantification allows to determine protective thresholds in sickle cell disease. *Am J Hematol*. 2020;95(11):1235–45.
59. Steinberg MH. Fetal Hemoglobin in Sick Hemoglobinopathies: High HbF Genotypes and Phenotypes. *J Clin Med* [Internet]. 2020 Nov 23;9(11):3782. Available from: <https://www.mdpi.com/2077-0383/9/11/3782>
60. Sebastiani P, Steinberg MH. Fetal hemoglobin per erythrocyte (<scp>HbF</scp> /F-cell) after gene therapy for sickle cell anemia. *Am J Hematol* [Internet]. 2023 Feb;98(2):E32–4. Available from: <https://onlinelibrary.wiley.com/doi/10.1002/ajh.26791>
61. Steinberg MH, Chui DHK, Dover GJ, Sebastiani P, Alsultan A. Fetal hemoglobin in sickle cell anemia: A glass half full? *Blood*. 2014;123(4):481–5.
62. Costa FF, Fertrin KY. Clinical Manifestations and Treatment of Adult Sick Cell Disease. In: Sick Cell Anemia [Internet]. Cham: Springer International Publishing; 2016. p. 285–318. Available from: http://link.springer.com/10.1007/978-3-319-06713-1_12
63. Pinto VM, Balocco M, Quintino S, Forni GL. Sick cell disease: a review for the internist. *Intern Emerg Med* [Internet]. 2019;14(7):1051–64. Available from: <https://doi.org/10.1007/s11739-019-02160-x>
64. Nickel RS, Hsu LL. Clinical Manifestations of Sick Cell Anemia: Infants and Children. In: Sick Cell Anemia [Internet]. Cham: Springer International Publishing; 2016. p. 213–29. Available from: http://link.springer.com/10.1007/978-3-319-06713-1_9
65. Abdenmour R, Abboud MR. Treatment of Childhood Sick Cell Disease. In: Costa FF, Conran N, editors. Sick Cell Anemia [Internet]. Cham: Springer International Publishing; 2016. p. 231–67. Available from: <http://link.springer.com/10.1007/978-3-319-06713-1>
66. Brandow AM, Liem RI. Advances in the diagnosis and treatment of sickle cell disease. *J Hematol Oncol* [Internet]. 2022;15(1):1–13. Available from: <https://doi.org/10.1186/s13045-022-01237-z>
67. Ware RE, de Montalembert M, Tshilolo L, Abboud MR. Sick cell disease. *Lancet* [Internet]. 2017;390(10091):311–23. Available from: [http://dx.doi.org/10.1016/S0140-6736\(17\)30193-9](http://dx.doi.org/10.1016/S0140-6736(17)30193-9)

68. Abdenmour R, Abboud MR. Treatment of Childhood Sickle Cell Disease. In: Sickle Cell Anemia [Internet]. Cham: Springer International Publishing; 2016. p. 231–67. Available from: http://link.springer.com/10.1007/978-3-319-06713-1_10
69. Jafri F, Seong G, Jang T, Cimpeanu E, Poplawska M, Dutta D, et al. L-glutamine for sickle cell disease: more than reducing redox. *Ann Hematol* [Internet]. 2022;101(8):1645–54. Available from: <https://doi.org/10.1007/s00277-022-04867-y>
70. Oksenberg D, Dufu K, Patel MP, Chuang C, Li Z, Xu Q, et al. GBT440 increases haemoglobin oxygen affinity, reduces sickling and prolongs RBC half-life in a murine model of sickle cell disease. *Br J Haematol*. 2016;175(1):141–53.
71. Raghupathy R, Billett H. Promising Therapies in Sickle Cell Disease. *Cardiovasc Hematol Disord Targets*. 2009;9(1):1–8.
72. Nottage K, Estep J, Hankins J. Future Perspectives for the Treatment of Sickle Cell Anemia. In: Sickle Cell Anemia [Internet]. Cham: Springer International Publishing; 2016. p. 399–429. Available from: http://link.springer.com/10.1007/978-3-319-06713-1_16
73. Moutouh-de Parseval LA, Verhelle D, Glezer E, Jensen-Pergakes K, Ferguson GD, Corral LG, et al. Pomalidomide and lenalidomide regulate erythropoiesis and fetal hemoglobin production in human CD34+ cells. *J Clin Invest*. 2008 Jan;118(1):248–58.
74. Alapan Y, Fraiwan A, Kucukal E, Hasan MN, Ung R, Kim M, et al. Emerging point-of-care technologies for sickle cell disease screening and monitoring. *Expert Rev Med Devices* [Internet]. 2016 Dec 1;13(12):1073–93. Available from: <https://doi.org/10.1080/17434440.2016.1254038>
75. Direcção-Geral da Saúde. Circular Normativa N^o: 18/DSMIA: Prevenção das formas graves de Hemoglobinopatia. 2004;4.
76. Dhaliwal G, Cornett PA, Tierney LMJ. Hemolytic anemia. *Am Fam Physician*. 2004 Jun;69(11):2599–606.
77. Phillips J, Henderson AC. Hemolytic Anemia: Evaluation and Differential Diagnosis. *Am Fam Physician*. 2018 Sep;98(6):354–61.
78. BJ B. The peripheral blood smear. In: Goldman L, Schafer AI, eds *Goldman-Cecil Medicine* 25th ed Philadelphia, PA: Elsevier Saunders. 2016. p. chap 157.
79. Scafidi JM, Amraei R, Gupta V. Histology, Howell Jolly Bodies [Internet]. StatPearls. Treasure Island (FL); 2023. Available from: <http://www.ncbi.nlm.nih.gov/pubmed/21946828>
80. Broadway-Duren JB, Klaassen H. Anemias. *Crit Care Nurs Clin North Am*. 2013;25(4):411–26.
81. Bain BJ. Haemoglobinopathy diagnosis: Algorithms, lessons and pitfalls. *Blood Rev* [Internet]. 2011;25(5):205–13. Available from: <http://dx.doi.org/10.1016/j.blre.2011.04.001>

82. Alli NA, Loonat SB. Solubility tests and the peripheral blood method for screening for sickle-cell disease. Vol. 100, South African medical journal = Suid-Afrikaanse tydskrif vir geneeskunde. South Africa; 2010. p. 616; author reply 616, 618.
83. Old J, Hartevelt CL, Traeger-Synodinos J et al. Prevention of Thalassaemias and Other Haemoglobin Disorders: Volume 2: Laboratory Protocols HAEMATOLOGICAL METHODS. Available from: <https://www.ncbi.nlm.nih.gov/books/NBK190583/?report=classic#ch02-S014>
84. Piety NZ, Yang X, Lezzar D, George A, Shevkoplyas SS. A rapid paper-based test for quantifying sickle hemoglobin in blood samples from patients with sickle cell disease. *Am J Hematol*. 2015 Jun;90(6):478–82.
85. Kumar AA, Patton MR, Hennek JW, Lee SYR, D'Alesio-Spina G, Yang X, et al. Density-based separation in multiphase systems provides a simple method to identify sickle cell disease. *Proc Natl Acad Sci U S A*. 2014 Oct;111(41):14864–9.
86. Segbena AY, Guindo A, Buono R, Kueviakoe I, Diallo DA, Guernec G, et al. Diagnostic accuracy in field conditions of the sickle SCAN® rapid test for sickle cell disease among children and adults in two West African settings: the DREPATEST study. *BMC Hematol*. 2018;18:26.
87. Masilamani V, Devanesan S, AlQathani F, AlShebly M, Daban HH, Canatan D, et al. A Novel Technique of Spectral Discrimination of Variants of Sickle Cell Anemia. *Dis Markers*. 2018;2018:5942368.
88. Masilamani V, Al Salhi MS, Devanesan S, Algahtani FH, Abu-Salah KM, Ahamad I, et al. Spectral detection of sickle cell anemia and thalassemia. *Photodiagnosis Photodyn Ther*. 2013 Dec;10(4):429–33.
89. Bhatnagar N. Dacie and Lewis Practical Haematology (12th edition) By B. J.Bain, I.Bates and M. A.Laffan, Elsevier, London, 2017. Elsevier, editor. *Br J Haematol* [Internet]. twelfth ed. 2017 Aug;178(4):652–652. Available from: <https://www.sciencedirect.com/book/9780702066962/dacie-and-lewis-practical-haematology#book-info>
90. Cotton F, Malaviolle X, Vertongen F, Gulbis B. Evaluation of an automated capillary electrophoresis system in the screening for hemoglobinopathies. *Clin Lab*. 2009;55(5–6):217–21.
91. Kumar R, Derbigny WA. Cellulose Acetate Electrophoresis of Hemoglobin. *Methods Mol Biol*. 2019;1855:81–5.
92. Wild BJ, Stephens AD. The use of automated HPLC to detect and quantitate haemoglobins. *Science* (80-). 1997;171–6.
93. Hempe JM, Craver RD. Quantification of hemoglobin variants by capillary isoelectric focusing. *Clin Chem*. 1994 Dec;40(12):2288–95.
94. Frömmel C. Newborn screening for sickle cell disease and other hemoglobinopathies: A short review on classical laboratory methods — Isoelectric focusing, HPLC, and capillary electrophoresis. *Int J Neonatal Screen*. 2018;4(4).

95. INSA. (2022, February 2). Instituto Ricardo Jorge alarga estudo piloto para o rastreio neonatal da drepanocitose. SNS. <https://www.insa.min-saude.pt/instituto-ricardo-jorge-alargaestudo-piloto-para-o-rastreio-neonatal-da-drepanocitose/>.
96. Campbell M, Henthorn JS, Davies SC. Evaluation of cation-exchange HPLC compared with isoelectric focusing for neonatal hemoglobinopathy screening. *Clin Chem*. 1999;45(7):969–75.
97. richard oliver (dalam Zeithml. dkk 2018). Cord blood screening for Hb abnormalities by thin layer isoelectric focusing. *Angew Chemie Int Ed* 6(11), 951–952. 2021;56(6):2013–5.
98. Hänscheid T, Valadas E, Grobusch MP. Automated malaria diagnosis using pigment detection. *Parasitol Today*. 2000 Dec;16(12):549–51.
99. Lawrence C, Olson JA. Birefringent hemozoin identifies malaria. *Am J Clin Pathol*. 1986 Sep;86(3):360–3.
100. Hárosi FI, von Herbing IH, Van Keuren JR. Sickling of anoxic red blood cells in fish. *Biol Bull*. 1998 Aug;195(1):5–11.
101. Nakagawa A, Cooper MK, Kost-Alimova M, Berstler J, Yu B, Berra L, et al. High-Throughput Assay to Screen Small Molecules for Their Ability to Prevent Sickling of Red Blood Cells. *ACS Omega*. 2022;7(16):14009–16.
102. Schober P, Boer C, Schwarte LA. Correlation Coefficients: Appropriate Use and Interpretation. *Anesth Analg*. 2018 May;126(5):1763–8.
103. Corbett, J. D., Mickols, W. E., & Maestre MF. Effect of Hemoglobin Concentration on Nucleation and Polymer Formation in Sick Red Blood Cells. *ournal Biol Chem* 270(6), 2708–2715.
104. Lei H, Karniadakis GE. Predicting the morphology of sickle red blood cells using coarse-grained models of intracellular aligned hemoglobin polymers. *Soft Matter*. 2012;8(16):4507–16.